Assessment of Climate Change Impacts on the Hydrology of Upper Guder Catchment, Upper Blue Nile

By

Fikru Fentaw Abera

Addis Ababa University

June, 2011

Addis Ababa University
School of Graduate Studies
Institute of Technology

Assessment of Climate Change Impacts on the Hydrology of Upper Guder Catchment, Upper Blue Nile

A thesis submitted and presented to the School of Graduate Studies of Addis Ababa University in Partial fulfillment of the Degree of Masters of Science in Civil Engineering under Hydraulics Engineering

By

Fikru Fentaw Abera

Advisor

Dr.-Ing. Dereje Hailu

Addis Ababa,
Ethiopia
June, 2011

Addis Ababa University
School of Graduate Studies
Institute of Technology

Assessment of Climate Change Impacts on the Hydrology of Upper Guder Catchment, Upper Blue Nile

A thesis submitted and presented to the School of Graduate Studies of Addis Ababa University in partial fulfillment of the Degree of Masters of Science in Civil Engineering under Hydraulics Engineering

By

Fikru Fentaw Abera

Approval by Board of Examiners

Dr.-Ing. Dereje Hailu ---------------- Signature
Advisor

Dr. Ing. Melesse Temesgen ---------------- Signature
Internal Examiner

Dr. Semu A ---------------- Signature
External Examiner

Dereje Tadesse ---------------- Signature
Chairman (Department of graduate committee)

CERTIFICATION

The undersigned certify that he has read the thesis entitled**: Assessment of Climate Change Impacts on the Hydrology of Upper Catchment, Upper Blue Nile** and hereby recommend for acceptance by the Addis Ababa University in partial fulfillment of the requirements for the degree of Master of Science.

____

Dr.-Ing. Dereje Hailu
(Supervisor)

____

Date

DECLARATION AND COPY RIGHT

Fikru Fentaw Abera

fikrufentaw@gmail.com

Signature ____________________

Dedicated to the Memory of my Mother Asrebeb Aragie

Mom, you are the main reason for being what I am.

Abstract

Climate changes alter regional hydrologic conditions and results in a variety of impacts on water resource systems. Such hydrologic changes will affect almost every aspect of human well-being. The goal of this thesis is to assess the impact of climate change on the hydrology of Upper Guder catchment located in Northwest of Ethiopia. The GCM derived scenarios (HadCM3 A2a & B2a SRES emission scenarios) experiments were used for the climate projection. The statistical Downscaling Model (SDSM) was used to generate future possible local meteorological variables in the study area. The down-scaled data were then used as input to the Soil and Water Assessment Tool (SWAT) model to simulate the corresponding future stream flow regime in Upper Guder catchment of the Abbay River Basin. A semi distributed hydrological model, SWAT was developed and Generalized Likelihood Uncertainty Estimation (GLUE) was utilized for uncertainty analysis. GLUE is linked with SWAT in the Calibration and Uncertainty Program known as SWAT-CUP.

Three benchmark periods simulated for this study were 2020s, 2050s and 2080s. The time series generated by GCM of HadCM3 A2a and B2a and Statistical Downscaling Model (SDSM) indicate a significant increasing trend in maximum and minimum temperature values and a slight increasing trend in precipitation for both A2a and B2a emission scenarios in both Gedo and Tikur Inch stations for all three bench mark periods. The hydrologic impact analysis made with the downscaled temperature and precipitation time series as input to the hydrological model SWAT suggested for both A2a and B2a emission scenarios. The model output shows that there may be an annual increase in flow volume up to 35% for both emission scenarios in three benchmark periods in the future. All seasons show an increase in flow volume for both A2a and B2a emission scenarios for all time horizons. Potential evapotranspiration in the catchment also will increase annually on average 3 - 15% for the 2020s and 7-25% for the 2050s and 2080s for both A2a and B2a emissions scenarios.

Key words: Climate Change; Guder Sub-Basin; GCM; SDSM; SWAT; SWAT-CUP; GLUE

Acknowledgment

First of all my thank to Above all, creator and governor of the two worlds, the almighty GOD, Jesus Christ, his mother Saint Marry, all his Angels and Saints for his priceless and miracle gifts to me.

I wish to express my utmost gratitude to Dr.-Ing Dereje Hailu, for his precious advice, encouragement and decisive comment during the research period. His critical comments and valuable advices helped me to take this research in the right direction.

I would like also to thank Ministry of Water & Energy and National Meteorological Service Agency for their cooperation in availing the necessary data.

I would like to express my appreciation to all my friends and course mates for their support and wonderful social atmosphere.

Back to home, I wish to express my deep gratitude to all my family members, their prayers for me when the main sources of inspiration, motivation and encouragement to continue this work. Especially, I would like to give my special thanks to my brother, Ato Berhanu Alemu and my father, Ato Fentaw Abera whose patient love encouraged me to complete this work.

Last of all, thanks to everyone who helped me and I wish all of you wonderful happy life.

Fikru Fentaw Abera

fikrufentaw@gmail.com

June, 2011

Table of Contents

List of Figures

List of Tables

List of Acronyms

A2-storyline is referred as the medium-high emissions scenario

AOGCM-Atmospheric Ocean General Circulation Models

Arc SWAT-SWAT Integrated with Arc GIS

B2-storyline is referred as the medium-low emissions scenario

GCM-General Circulation Model

GHG-Greenhouse Gases

GIS-Geographic Information Systems

GLUE-Generalized Likelihood Uncertainty Estimation

HadCM3A2a-Hadley Centre Coupled Model, version 3, for the A2a emission scenario

HadCM3B2a-Hadley Centre Coupled Model, version 3, for the B2a emission scenario

HRU-Hydrological Response Unit

IPCC-Intergovernmental Panel on Climate Change

Masl-Meters above sea level

MoWR-Ministry of Water Resources, Ethiopian

NCEP-National Centre for Environmental Prediction

NMSA-National Metrological Services Agency, Ethiopian

RCM-Regional Climate Models

SCS-Soil Conservation Service

SDSM-Statistical Downscaling Model

SRES-Special Report on Emission Scenarios

SWAT_CUP-SWAT Calibration and Uncertainty Programs

SWAT-Soil and Water Assessment Tool

TGICA-Task Group on Data and Scenario Support for Impacts and Climate Analysis

WHAT-Web Based Hydrograph Analysis Tool

WMO-World Metrological Organization

1. INTRODUCTION

1.1 Back Ground

Climate is the average behavior of the atmosphere over long periods of time. Despite the annual periodicity in weather patterns, the climate is subject to changes. During the past few decades, it has become apparent that human activities such as fossil fuel burning and land-use change (e.g. deforestation) have considerably increased the atmospheric concentrations of greenhouse gases (GHGs). As a result, changes in climate have started and are expected to continue for centuries/millennia until GHGs concentrations stabilize (if at all possible). Scientists agreed that climate change have adverse impacts on socio-economic development of all nations. But the degree of the impact will vary across nations. It is expected that changes in the earth's climate will hit developing countries like Ethiopia first and hardest because their economies are strongly dependent on crude forms of natural resources and their economic structure is less flexible to adjust to such drastic changes (NMSA, 2001). According to the Intergovernmental Panel on Climate Change (IPCC, 2001a) report, by 2100 global average temperature would raise between 1.4 and 5.8°C and precipitation would vary up to ±20% from the 1990 level.

Climate changes have had visible impacts on the natural systems. Climate change is expected to aggravate current stresses on water resources availability from population growth, urbanization and land-use change. A major effect of climate change is likely to be alterations in hydrologic cycles and changes in water availability. Increased evaporation, combined with changes in precipitation, has the potential to affect runoff, the frequency and intensity of floods and droughts, soil moisture and available water for irrigation and hydroelectric power generation. In addition, watershed hydrology is affected by vegetation types, soil properties, geology, terrain land use practices, and the spatial pattern of interactions among these factors and with climate.

Upper Blue Nile Basin is one of the largest basins in Ethiopia with high population pressure, degradation of land and highly dependent on agricultural economy and sensitive to climatic variations (Conway, 2005). The increase in population growth, economical development and climate change have been proven by IPCC, 2007 to cause rise in water demand, necessity of improving flood protection system and drought (water scarcity). Guder Sub-basin is one of the primary sub-basin of Upper Blue Nile Basin which experiences severe famine due to recurrent drought and the lack of advanced water infrastructure to use the full potential of available water resources. Therefore, this study is used to assess the future variability of hydrologic regimes and water resources of the Upper Guder Catchment under climate change, and to assess the potential impacts on the study area which may be used for the planners, decision makers and any concerned person to understand the consequences of climate change on the hydrological variables.

In climate change impact studies, hydrologic models are required to simulate sub-grid scale phenomena, and such hydrologic models require input data at a similar scale. These data are generally provided by converting the GCM outputs into a reliable regional hydrologic time series at the selected watershed scale. The methods used to convert GCM outputs into local meteorological variables are usually referred to as 'downscaling' techniques (Dibike and Coulibaly, 2005). In this study, the statistically downscaled GCM output and the atmospheric Circulation variables derived from the HadCM3 model SRES A2 and B2 emissions scenarios were used to down-scale daily precipitation and temperature series for the Upper Guder Catchment of the Abbay River Basin. The climate scenarios generated were then used to drive the distributed Soil and Water Assessment Tool (SWAT) model. Changes in the modeled daily flow regime between current and future climate scenarios were compared and analyzed.

1.2 Statement of the Problem

Water is the most important natural resource required for the survival of all living species. Since the available amount of water is limited, scarce, and not spatially distributed in relation to the population needs, proper management of water resources is essential to satisfy the current demands as well as to maintain sustainability. Water resources planning and management in the 21st century is becoming difficult due to the conflicting demands from various stakeholder groups, increasing population, rapid urbanization, climate change producing shifts in hydrologic cycles, the use of high-yielding but toxic chemicals in various land use activities and the increasing incidences of natural disasters. Therefore, the impacts of climate change on water resources are the most crucial research agenda in worldwide level (IPCC, 2007).

The Upper Blue Nile (Abbay River Basin) is critically important to Ethiopia, in view of the combination of large population, huge development potential and massive natural resource. The large population growth in Ethiopia will increase the demand for natural resources, mainly water among each region. Ethiopia is also under great pressure on economic expansion, deforestation, urbanization and climate change. For the Guder sub-basin, human activities in the catchments have increased over the past century and expected to grow even more rapidly in the future; hence, water management will become even more important with a changing climate.

Management of water resources of the Abbay basin is one of the biggest challenges even if the Ministry of Water Resources (MoWR) work with its overall goal to “enhance and promote all national efforts towards the efficient, equitable and optimum utilization of the available Water Resources of Ethiopia for significant socioeconomic development on a sustainable basis” (MoWR, 2002) . If the water of the Abbay River Basin is managed properly, it could offer great potential as a lever for development. It has been currently shown that the demand for agricultural production and hydropower in the region has increased. There are also numerous development investment projects underway in the Abbay River Basin. Yet, with all this huge development potential of the basin and all these investment projects in progress Awulachew et al (2008a) state that “Currently, the Abbay is one of the least planned and managed sub-basins of the Nile.”

The Intergovernmental Panel on Climate Change's (IPCC, 2007) findings suggests that developing countries like Ethiopia will be more vulnerable to climate change due to their economic, climatic and geographic settings. Climate change can affect multiple features of water resources (e.g., quantity and quality, high and low flow extremes, timing of events, water temperature, etc). All these aspects affect livelihoods in the Abbay basin but have not received attention in planning for future water allocation and design of water infrastructures yet (Kim *et al.*, 2008).

The Blue Nile River basin is one of the most sensitive basins to changing climate and water resources variability in the region (Kim and Kaluarachchi, 2009). But the effects of climate change on water availability (with respect to water resources analysis, management and policy formulation in the country) in the Guder Sub-Basin have not been adequately addressed. Hence it is necessary to improve our understanding of the problems involved due to the changing climate.

Having the above mentioned and other related problems, it is imperative to understand the impact of future climate change on hydrometeorology and the subsequent impact on the lives of people and water resources. Model evaluation is also need to be carried out using observed data to verify accuracy. High resolution GCMs (HadCM3) with two SRES emissions scenarios A2a and B2a, Statistical Downscaling Model (SDSM) and hydrological model Soil and Water Assessment tool (SWAT) with SWAT-CUP linked GLUE uncertainty analysis has been utilized in this study to evaluate climate changes impacts on the hydrology of Guder sub-basin, Ethiopia.

1.3 Objective of the Research

General objective: - the overall objective of the research is to assess the impact of climate change on the hydrology of Upper Guder Catchment, Upper Blue Nile.

Specific objectives:

i. To develop and evaluate climate scenario data for maximum temperature, minimum temperature and precipitation based on GCM and SDSM for the Catchment.
ii. To downscale the climate variables for the Catchment.
iii. To develop hydrologic SWAT model and assess the quality of available data.
iv. To quantify possible effects of climate change on the hydrology of the catchment based on the down scale climate scenario data using hydrological model (SWAT).

In order to meet the above objectives the research questions for this study are:

i. What are the potentials of a selected General Circulation Model and Downscaling Models for the hydrological assessment at the catchment scale?
ii. What are general trends of maximum temperature, minimum temperature and precipitation scenario in the future compared to the present condition and how this is reflected on hydrology of the Upper Guder Catchment?
iii. What is the effect of change in rainfall and temperature for the future (increase/decrease) on run-off in the Catchment?

1.4 Limitation of the Research

World Meteorological Organization (WMO) recommends a baseline period of at least 30 years against which future climate projection can be done. However due to data availability this study considered 1980 to 2000 as a baseline period. In this study the impact of climate change was assessed assuming the land cover will remain the same. However, in real world the land cover is dynamic due to natural and human influences. It is also assumed that the socio-economic condition in the area will remain the same.

1.5 Thesis Outline

This thesis contains six chapters organized as follows. Chapter one gives a general introduction to the study with its objective and research questions. Chapter two describes the reviewed literature related to the study. Chapter three gives a brief description of the study area and data availability. Chapter four deals with the methodology adopted for the study. In Chapter five the results are shown and discussed. In chapter six conclusion and recommendation are presented.

2 LITERATURE REVIEW

2.1 Climate Change Science

Climate change refers to any long-term significant change in the expected patterns of average weather of a specific region or area or zone over an appropriately significant period of time. It is a long-term change in the statistical distribution of weather patterns over period of time that range from decades to millions of years. Climate change may be limited to a specific region, or may occur across the whole Earth. The factors that determine the climate at a location are the rainfall, sunshine, wind, humidity and temperature. Climate change may result from events such as changes in the Earth's orbit around the sun, earth’s tilt, burning fossil fuels, Greenhouse effect, deforestation, urbanization, desertification, volcanic eruption, flood, forest fire, storms etc.

Evidence indicates that the Earth’s climate is warming. So warming of the climate system in recent decades is obvious, as is now evident from observations of increases in global average air and ocean temperatures, widespread melting of snow and ice, and rising global sea level. Among the different assessment that are carried out by the IPCC, the recent one which published in 2001, states the projected global surface warming by 2100 using the SRES scenarios as input, current models estimate global temperature to increase by 1.4ºC to 5.8ºC and precipitation would vary up to ±20% from the1990 level (IPCC, 2001a).

2.1.1 Climate Change and Water Resources

Climate variability and change are expected to alter regional hydrologic conditions and results in a variety of impacts on water resource systems throughout the world. Potential impacts may include changes in hydrological processes such as Evapotranspiration, soil moisture, water temperature, stream flow volume, timing and magnitude of runoff, and frequency and severity of floods, all of which would cause changes in other environmental variables such as plant growth and sediment and nutrient fluxes in to water bodies. Such hydrologic changes will affect almost every aspect of human well-being, from agricultural productivity and energy use to flood control, municipal and industrial water supplies, and fish and wild life management (Xu, 2000).

Since hydrologic conditions vary from region to region, the influence of climate change on local hydrological processes will likely differ between localities, even under the same climate scenarios. Studies in recent years have been shown important regional water resource vulnerabilities to changes in both temperature and precipitation patterns (Lahmer et al., 2001). It is primarily at the regional and local scales that policy and technical measures could be taken to avoid or reduce the negative effect of climate change on the natural environment and society.

2.1.2 Climate Models

The Earth's climate is governed by the interaction between many processes in the atmosphere, ocean, land surface and cryosphere (glaciers and ice sheets). These climate processes can be represented in mathematical terms based on physical laws such as the conservation of mass, momentum and energy.
The mathematical formulation is therefore implemented in a computer program, which is referred to as a model. If the model includes enough of the components of the climate system to be useful for simulating the climate, it is commonly called a climate model (IPCC, 1997). The current state of climate modeling science is accomplished with general circulation models (GCMs), which integrate complex interactions of atmosphere-land-ocean-ice systems that simulate the Earth's climate and projections of its future change on timescales of seasonal forecasts to decades and centuries. Climate change scenarios developed from General Circulation Models (GCMs) are the initial source of information for estimating plausible future climate. Most GCMs have a horizontal resolution of between 250 and 600 km, and 10 to 20 vertical layers in the atmosphere (IPCC, 2001). The spatial resolution of GCMs is too coarse to resolve regional scale effect therefore downscaling is required.

In order to assess the implications of future changes in the environment, society and economy on an exposure unit, it is first necessary to have information about the present day or recent conditions as a reference point or baseline. In order to characterize the present day climate in a region, good quality observed climatological data are required for a given baseline period. Issues to consider in selecting the climatological baseline include the types of data required, duration of the baseline period, sources of the data and how they can be applied in an impact assessment.

A popular climatological baseline period is a 30-year "normal" period as defined by the World Meteorological Organization (WMO). The current WMO normal period is 1961-1990. It represents the recent climate, to which many present day human or natural systems are likely to have become reasonably well adapted (though there are exceptions, such as vegetation zones or groundwater levels that can have a response lag of many decades or more relative to the ambient climate). Climatological data from the 1990s will certainly be required for the calibration and testing of many impact models. Moreover, 1961-1990 will be superseded by 1971-2000 as a new standard 30-year averaging period.

Baseline climatological data are obtained from a number of alternative sources that can be applied in impact assessments. The most common source of observed climatological data applied in impact assessments is the national meteorological agencies. These agencies usually have responsibility for the day-to-day operation and maintenance of national meteorological observational networks for purposes of weather forecasting and other public services. The second one is supranational and global data sets include observations of surface variables at a monthly time step over land and ocean, surface and upper air observations at a daily time step from sites across certain regions and for recent decades, satellite observations. The third one is from stochastic weather generators a computer models that generate synthetic series of daily or sub-daily resolution weather at a site conditional on the statistical features of the historically observed climate. The last one is obtaining the baseline climatological data from Climate model outputs of reanalysis data and outputs from GCM control simulations.

Reanalysis data are fine resolution gridded data which combine observations with simulated data from numerical models. Through a process known as data assimilation, the observations (available only sparsely and irregularly over the globe), along with data from satellites and information from a previous model forecast, are input into a short-range weather forecast model. This is integrated forward by one time step and combined with observational data for the corresponding period. The result is a comprehensive and dynamically consistent three-dimensional gridded data set (the "analysis") which represents the best estimate of the state of the atmosphere at that time. The assimilation process fills data voids with model predictions and provides a suite of constrained estimates of unobserved quantities such as vertical motion, radiative fluxes and precipitation.

Outputs from GCM control simulations are model-based source of information on the present-day climate is multi-century control simulations from Atmospheric Ocean General circulation Models (AOGCMs). These simulations attempt to represent the dynamics of the global climate system unforced by anthropogenic changes in atmospheric composition. Since observations with a reasonable global coverage barely extend beyond one century in duration, model control simulations offer an alternative source of data enabling impact analysts to investigate the impact of multi-decadal variations in climate.

2.1.3 Climate Scenario

A climate scenario is a plausible representation of future climate conditions (temperature, precipitation and other climatological phenomena) that has been constructed for explicit use in investigating the potential impacts of anthropogenic climate change (IPCC, 2001). Climate change scenarios are developed to give coherent, internally consistent and plausible descriptions of future state of the world (IPCC, 1999). The climate change scenarios should be assessed according to consistency with global projections, physical plausibility, applicability in impact assessments and representativity.

Climate change scenarios for impact assessment can be developed in three major techniques; analogue, synthetic and GCM-based climate change scenarios. Analogue scenarios are constructed by identifying a recorded climate regime which may resemble the future climate anticipated for a particular site or region. These recorded climates may be identified in the long observational record at a site (temporal analogues) or be from other geographical locations (spatial analogues). Synthetic, or arbitrary, scenarios are the simplest climate scenarios available. They are used mainly for defining the sensitivity of an exposure unit to a plausible range of climatic variations, but they rarely present a future climate that is realistic and physically plausible. Synthetic scenarios describe techniques where particular climatic (or related) elements are changed by a realistic but arbitrary amount, often according to a qualitative interpretation of climate model simulations for a region. For example, adjustments of baseline temperatures by +1, 2, 3 and 4°C and baseline precipitation by ±5, 10, 15 and 20 percent could represent various magnitudes of future change.

Scenarios from general circulation model outputs are the most common method of developing climate scenarios for quantitative impact assessment. These are numerical models representing physical processes in the atmosphere, ocean, cryosphere and land surface and considered as the most advanced tools currently available for simulating the response of the global climate system to increasing greenhouse gas concentrations. GCMs depict the climate using a three dimensional grid over the globe, typically having a horizontal resolution of between 250 and 600 km, 10 to 20 vertical layers in the atmosphere and sometimes as many as 30 layers. Of the above techniques, Scenarios from general circulation model outputs were the most precisely specified and the most widely used.

Regardless of whether or not the climate changes in the future, there is no doubt that changes in socio-economic and environmental conditions will occur. The major underlying cause of rapid changes in atmospheric composition is human economic activity, in particular emissions of greenhouse gases and aerosols, and changing land cover and land use. IPCC-TGICA (2007) indicates that carbon dioxide concentration increase for the future as in 2000 is 367ppm, for SRES A2 emission scenario is 536ppm in 2050 and 857ppm in 2100 and for SRES B2 emission scenario is 478ppm in 2050 and 615ppm in 2100.

A set of scenarios was published by the IPCC with a projection period out to 2100. The Special Report on Emissions Scenarios (SRES) has been constructed to explore future developments in the global environment with special reference to the production of greenhouse gases and aerosol precursor emissions. The approach has been to develop a set of four "scenario families". The Special Report on Emission Scenario (SRES) team defined four narrative storylines, labeled A1, A2, B1 and B2, describing the relationships between the forces driving greenhouse gas and aerosol emissions and their evolution during the 21st century for large world regions and globally. Each storyline represents different demographic, social, economic, technological and environmental developments that diverge in increasingly irreversible ways. The storylines are summarized as follows:

A1 storyline and scenario family: globalization, emphasis on human wealth Globalized, intensive (market forces). The A1 storyline and scenario family describes a future world of very rapid economic growth, global population that peaks in mid-century and declines thereafter, and the rapid introduction of new and more efficient technologies. Major underlying themes are convergence among regions, capacity building, and increased cultural and social interactions, with a substantial reduction in regional differences in per capita income.

A2 storyline and scenario family: regionalization, emphasis on human wealth Regional, intensive (clash of civilizations). The A2 storyline and scenario family describes a very heterogeneous world. The underlying theme is self-reliance and preservation of local identities. Fertility patterns across regions converge very slowly, which results in continuously increasing global population. Economic development is primarily regionally oriented and per capita economic growth and technological changes are more fragmented.

B1 storyline and scenario family: globalization, emphasis on sustainability and equity Globalized, extensive (sustainable development). The B1 storyline and scenario family describes a convergent world with the same global population that peaks in mid-century and declines thereafter, as in the A1 storyline, but with rapid changes in economic structures toward a service and information economy, with reductions in material intensity, and the introduction of clean and resource-efficient technologies. The emphasis is on global solutions to economic, social and environmental sustainability, including improved equity, but without additional climate initiatives and slower than in other storylines.

B2 storyline and scenario family: regionalization, emphasis on sustainability and equity Regional, extensive (mixed green bag). The B2 storyline and scenario family describes a world in which the emphasis is on local solutions to economic, social and environmental sustainability. It is a world with continuously increasing global population at a rate lower than A2, intermediate levels of economic development, and less rapid and more diverse technological change than in the B1 and A1 storylines. While the scenario is also oriented toward environmental protection and social equity, it focuses on local and regional levels.

2.2 Downscaling Methods and Tools

Studies on the impact of global warming on the hydrological cycles and water resources in the future usually rely on climate change scenarios projected by General Circulation Models (GCMs). However, the coarse scaled GCM projections cannot be applied directly in hydrologic studies at regional or basin scales. To derive local or station-based climate change scenarios from GCM output, a procedure called downscaling has been developed. As a consequence, two sets of techniques have emerged as a means of deriving local scale surface weather from regional scale atmospheric predictor variables. These are statistical downscaling and dynamical downscaling.

Dynamical downscaling involves the use of higher resolution regional climate models (RCMs) that use GCM output as the input or boundary conditions and simulates the climate over a smaller region. The use of a RCM in dynamical downscaling requires substantial computational effort and cost and typically limits the length of the simulation period to about 10 years. Dynamical downscaling is most useful for diagnostic studies to understand local climate. The major drawback of dynamic downscaling, which restricts its use in climate change impact studies is its complicated design and high computational cost. Moreover, it is inflexible in the sense that expanding the region or moving to a slightly different region requires redoing the entire experiment.

Statistical downscaling is based on the view that the regional climate is conditioned by two factors: the large scale climatic state and local physiographic features (example: topography, land-sea distribution and land use). From this perspective, regional or local climate information is derived first by determining a statistical model which relates large-scale climate variables (predictors) to regional and local variables (predictands). So statistical downscaling involves developing quantitative relationships between large-scale atmospheric variables (predictors) and local surface variables (predictands). The most common form has the predictand as a function of the predictor(s). The large scale output of a GCM simulation is fed in to this statistical model to estimate the corresponding local and regional climate characteristics. Statistical downscaling methodologies have several practical advantages over dynamical downscaling approaches. In situations where low–cost, rapid assessments of localized climate change impacts are required, statistical downscaling (currently) represents the more promising option.

2.3 Hydrological Models

Hydrological models are simplified, conceptual representations of the hydrologic cycle. They are primarily used for hydrologic prediction and understanding of hydrologic processes. Hydrological models are also considered to be mathematical formulations to simulate natural hydrologic phenomena. Hydrological models have been developed for various reasons and therefore have different forms. According to Chow (1964), they are generally designed to meet one of the two fundamental purposes: scientific inquiry or resource management. As a tool of scientific enquiry, hydrologic models can be used to gain a better understanding of the hydrologic processes and how changes affect these processes. In the context of resource management, the hydrologic model can be used as a planning tool to guide decision making for management practices of both land and water resources.

2.3.1 Classification of Hydrological Models

There are many classification schemes of hydrologic models such as: short term versus long term; deterministic versus stochastic; lumped versus distributed and etc. Classifications are generally based on the method of representation of the hydrological cycle or a component of the hydrological cycle. In detailed physically-based models, the relation between model input and output is described by a large number of equations, each representing a physical process. A more macroscopic description of the processes is found in a conceptual model. “Macroscopic description means that the processes are represented in the way they are observed and that an abstraction is made of the several microscopic processes that underlie the observation” (Willems, 2000). They are also further explained with their physical-based level as it is shown in Figure 1.

The stochastic versus deterministic classification of models depends on the behavior of the results obtained. If one or more of the variables in a mathematical model are regarded as random variables having distributions in probability, then the model is stochastic. If all the variables are considered to be free from a random variation, the model is deterministic. Using long data series, deterministic models can compute a higher number of calculations required to describe the complexity of a system. They can provide reliable information on the behavior of the system (Cunderlik, 2003).

MODELLING TYPES			
Increasing level of physically-based modelling ↑	Detailed physically-based models Partly physically-based models	White box	Most model parameters can be measured
	Conceptual models	Grey box	Model parameters need calibration (e.g. using measurements for model output variables)
	Empirical models Black-box models	Black box	Also the model-structure building depends on the measurements for the model output variables

Figure 1 Schematic Overview of different model types (Willems, 2000)

Chow (1964) expressed the difference between stochastic and deterministic models in the sense of using probability laws. It is explained that the conventional routing of flood flow through reservoirs is a deterministic process. However, if the probability of the flow is taken in to account in the probability of routing, the model employed is considered to be stochastic. Deterministic hydrologic models further classified into three main categories (Cunderlik, 2003):

Lumped Models: parameters of lumped models do not vary spatially within the basin and thus, basin response is evaluated only at the outlet, without explicitly counting for the response of individual sub-basins. Parameters of lumped models often do not represent physical features of hydrologic processes. The impact of spatial variability on the model parameters is evaluated by using certain procedures for calculating effective values for the entire basin.

Semi-distributed Models: parameters of semi-distributed models are partially allowed to vary in space by dividing the basin into a number of smaller sub-basins. The main advantage of semi-distributed models is their more physically based structure than that of lumped models, and the lesser amount of input data than fully distributed models. SWAT is in the domain of semi-distributed hydrological models.

Distributed Models: parameters of distributed models are allowed to vary in space at a resolution usually chosen by the user. Distributed modeling approach attempts to incorporate data concerning the spatial distribution of parameter variations together with computational algorithms. Distributed models generally require large amounts of data for parameterization.

2.3.2 Hydrological Model Selection Criteria

There are a number of criteria which can be used for choosing the right hydrologic model. These criteria are mainly dependent on the use of the model. Furthermore, some criteria are also user dependent such as: personal preference; computer operation system; input/output management and structure etc. Cunderlik (2003) suggested four criteria for the selection of hydrological models. These are: (1) required model outputs for the needed purpose, (2) different hydrological processes that are required to be modeled for the desired purpose, (3) availability of input data and (4) Price-does the investment appear to be worthwhile within the objectives?

Depending upon the above selection criteria for this research Soil and Water Assessment Tool (SWAT) and GLUE linked in SWAT-CUP is selected.

2.3.3 The Soil and Water Assessment Tool (SWAT)

SWAT- Soil and Water Assessment Tool is a physically based, continuous time and computationally efficient hydrological/water quality model, which uses readily available inputs. As a physically-based model, SWAT use hydrologic response units (HRUs) to describe spatial heterogeneity in terms of land cover, soil type and slope within the watershed. The SWAT system is embedded within a geographic information system (GIS) that can integrate various spatial environmental data including soil, land cover, climate and topographic features. It was developed to predict the impact of land management practices on water, sediment and agricultural chemical yields in large complex watersheds with varying soils, land use and management conditions (Neitsch et al., 2005). It enables users to study long term impacts and hence is being used extensively in the U.S. and other parts of the world to assess the impact of global climate change and water quality (Neitsch et al., 2005).

Hydrological Component of SWAT

For any types of problems studied with SWAT, water balance is the driving force behind everything that happens in the watershed. The simulation of the hydrology of a watershed is done in two separate divisions (Neitsch et al., 2005). The first is the land phase process of the hydrological cycle that controls the fluxes of water, sediment, nutrient and pesticide loadings to the main channel in each sub-basin. Hydrological components which are simulated in this process include: precipitation, canopy storage, infiltration, Evapotranspiration, lateral flow, surface runoff and return flow. The second division is the water or routing phase of the hydrological cycle which is the movement of water, nutrients, sediment and pesticides through the channel network of the watershed into the outlet.

Land phase Processes

In the land phase process of the hydrological cycle, SWAT simulates the hydrological cycle based on the water balance of the soil profile (Equation 1).

$$SW_t = SW_o + \sum_{i=1}^{t} \left[R_{day} - Q_{surf} - E_a - W_{seep} - Q_{wg} \right] \text{.............................} Eqn1$$

Where: SW_t is the final soil water content (mm/day); SW_o is the initial soil water content on day i (mm/day); t is the time in days; R_{day} is the amount of precipitation on day i (mm/day); Q_{surf} is the amount of runoff on day i (mm/day); E_a is the amount of Evapotranspiration on day i (mm/day); W_{seep} is the amount of water entering the vadose zone from the soil profile on day i (mm/day) and Q_{gw} is the amount of return flow on day i (mm/day).

Surface runoff occurs whenever the rate of precipitation exceeds the rate of infiltration. SWAT offers the Soil Conservation Service (SCS), curve number equation and the Green & Ampt infiltration methods to estimate the surface runoff volume (Neitsch et al., 2005). For this study the SCS curve number procedure was preferred over the Green & Ampt infiltration method. The Green & Ampt infiltration method assumes that there will be excess water at the surface at all times which was invalid assumption in the study area and also this method requires sub-daily precipitation data which was the other limitation to use this method.

SCS curve number method estimates the amount of runoff based on land use, soil type and antecedent moisture condition. Therefore, the SCS curve number method is simple, widely used and efficient for determining the approximate amount of runoff from a rainfall event under a varying land use and soil types (Neitsch et al., 2005). The 1972 SCS curve number equation (Equation 2) is used in SWAT model.

$$Q_{surf} = \frac{\left(R_{day} - I_a\right)^2}{\left(R_{day} - I_a + S\right)} \text{..............................} Eqn2$$

Where Q_{surf} is the accumulated rainfall excess (mm/day); R_{day} is the rainfall depth for the day (mm/day); I_a is the initial abstraction which includes surface storage, infiltration and infiltration prior to runoff (mm/day) and S is the retention parameter (mm/day).

The retention parameter varies spatially due to changes in soils, land use, management and slope, and temporarily due to changes in the soil water content. The retention parameter is defined as in (Equation 3).

$$S = 25.4\left(\frac{1000}{CN} - 10\right) \text{..............................} Eqn3$$

Where, CN is the curve number for the day. The curve number is based on the areas, hydrologic soil group, land use and hydrologic condition. The initial abstractions, I_a, is commonly approximated as 0.2S and Equation 2 becomes:

$$Q_{surf} = \frac{\left(R_{day} - 0.2S\right)^2}{\left(R_{day} + 0.8S\right)} \text{..............................} Eqn4$$

Runoff will occur when $R_{day} > I_a$.

Most of the water in the earth's surface is removed by Evapotranspiration. Roughly 62% of the precipitation that falls on the continents is evapotranspired (Neitsch et al., 2005). Hence accurate estimation of Evapotranspiration is vital in the assessment of water resources and the impact of climate and land use on these resources. Three methods for estimating potential Evapotranspiration (PET) are provided in SWAT. These are: Priestly-Taylor, Penman-Monteith and Hargreaves methods. These methods have different input data requirements. The Penman-Monteith method requires solar radiation, air temperature, relative humidity and wind speed; Priestley-Taylor method requires solar radiation, air temperature and relative humidity; whereas Hargreaves method requires only air temperature. For this study due to availability of only temperature data, the Hargreaves method was used for the determination of the potential Evapotranspiration.

The Hargreaves method was developed in 1975 but several improvements were made to the original equation. The form used in SWAT (Equation 5) was published in 1985 (Neitsch et al., 2005).

$$\lambda E_O = 0.0023 * H_O * (T_{mx} - T_{mn})^{0.5} \left(T_{av} + 17.8 \right) .... Eqn5$$

Where: λ is the latent heat of vaporization (MJ kg^{-1}); E_o is the potential Evapotranspiration (mmd^{-1}); H_o is the extraterrestrial radiation ($MJm^{-2}d^{-1}$); T_{mx} is the maximum air temperature for a given day (^oC); T_{mn} is the minimum air temperature for a given day (^oC) and T_{av} is the mean air temperature for a given day (^oC).

SWAT assumes two aquifers to address ground water: the shallow and the deep aquifers. Ground water movement in the shallow aquifer is represented by three processes: upward migration, seepage to the deep aquifer and ground water flow to the stream (Neitsch et al., 2005). In the model, the volume of water available in the shallow aquifer is governed by: the recharge from the top soil profile (recharge); the flow into the main stream channels or reach (base flow); the water movement into the overlying unsaturated zone or through deep rooted plants (revap); and the flow to the deep aquifer (deep percolation).

Routing phase

The second phase of the SWAT hydrologic simulation, the routing phase, consists of the movement of water, sediment and other constituents (e.g. nutrients, pesticides) in the stream network. As an optional process, the change in channel dimensions with time due to down cutting and widening is also included. Similar to the case for the overland flow, the rate and velocity of flow is calculated by using the Manning's equation. The main channels or reaches are assumed to have a trapezoidal shape by the model. Two options are available to route the flow in the channel networks: the variable storage and Muskingum methods. Both are variations of the kinematic wave model. While calculating the water balance in the channel flow, the transmission and evaporation are also well considered by the model.

The variable storage method uses a simple continuity equation in routing the storage volume, whereas the Muskingum routing method models the storage volume in a channel length as a combination of wedge and prism storages.

For this study, the variable storage method was adopted. The method was developed by (Williams, 1969). Storage routing is based on the continuity equation:

$$\nabla V_{stored} = V_{in} - V_{out} \text{ .... } .Eqn\ 6$$

Where: V_{in} is the volume of inflow during the time step (m^3/day), V_{out} is the volume of outflow during the time step (m^3/day), and $\blacktriangledown V_{stored}$ is the change in volume of storage during the time step (m^3/day). Detail of the equation was given in SWAT theoretical documentation manual.

2.3.4 SWAT Calibration and Uncertainty Procedures (SWAT-CUP)

Distributed watershed models are increasingly being used to support decisions about alternative management strategies in the areas of land use change, climate change, and pollution control and water allocation. For this reason it is important that these models pass through a careful calibration and uncertainty analysis. Furthermore, as calibration model parameters are always conditional in nature the meaning of a calibrated model, its domain of use, and its uncertainty should be clear to both the analyst and the decision maker. Large-scale distributed models are particularly difficult to calibrate and to interpret the calibration because of large model uncertainty, input uncertainty and parameter non uniqueness. To perform calibration and uncertainty analysis, in recent years many procedures have become available. For this study the hydrologic simulator SWAT under the same platform, SWAT-CUP (SWAT Calibration Uncertainty Procedures) used.

SWAT-CUP is a public domain program and it is an interface that was developed for SWAT. Using this generic interface, any calibration, uncertainty or sensitivity program can easily be linked to SWAT. The program links Generalized Likelihood Uncertainty Estimation (GLUE), Parameter Solution (ParaSol), Sequential Uncertainty Fitting (SUFI2) and Markov Chain Monte Carlo (MCMC) procedures to SWAT (Abbaspour, et al., 2007). It enables sensitivity analysis, calibration, validation and uncertainty analysis of SWAT models. For this study GLUE is used. GLUE was introduced partly to allow for the possible non-uniqueness (equifinality or ambiguity). Zheng and Keller (2007) highlighted on some advantages of GLUE which include; i) GLUE accounts for all sources of uncertainty, either explicitly or implicitly; ii) GLUE is conceptually simple, and requires no restricted error assumptions if a goodness-of-fit measure is used as its likelihood function; iii) GLUE is less vulnerable to model discontinuity since no optimum searching is necessary; iv) compared to multi-objective approaches, GLUE's uncertainty bounds are more likely to reflect the real magnitude of uncertainty, since GLUE identifies many non-optimal simulations that yet conform to the observations to certain degree.

3.3 Review of Previous Studies

There are limited climate change impact studies in Blue Nile basin. Some of the previous research results are shown below.

The study of Kim and Kaluarachchi (2008) is a step towards integrating climate change and hydrology of the Upper Blue Nile River Basin to assess the changes to water resources and the impacts due to potential dam operation policies in the 2050s. The study was conducted with limited hydrological data and hence used simple, yet reliable, modeling approaches to simulate various impacts of climate change scenarios on hydrology and water resources of the basin. The major findings of the study include: a generally increasing trend in both precipitation and runoff in the northern part of the study area, is identified under the weighted scenario (combination of six GCMs outputs of CCSR/NIES, CGCM2, CSIRO, ECHAM4, GFDL-R30 and HADCM3) for the 2050s. It is, therefore, possible to suggest that water availability will most likely improve in this area.

Muluneh B. (2008) used HBV hydrological model to understand the spatial variability of climate change impact in 10 selected Blue Nile Basin based on hypothetical climate change scenario. In terms of spatial variability of climate changes, he ordered the 10 catchments from the most sensitive to least sensitive as Chacha, Birr, Sechi, Guder, Teme, Gilgel Belese, Muger, Koga, Little Anger and Neshi. He also concludes that the result obtained for all catchments indicate that any future perturbation in the climate, significantly affects all catchments in the Upper Nile Basin.

The study of Elshamy (2009) discuss as the Nile Basin spans different hydro-climatic zones ranging from tropical wet climate to semi-arid and arid climate. Climate change impacts on the Nile flows will thus vary depending on the location of the studied sub-basin. In this study, the sensitivity to climatic changes of three different sub-catchments, namely, the Upper Kagera in Lake Victoria Basin, Gilgel Abbay in the Blue Nile Basin, and the Atbara, is studied in terms of flow response to uniform changes in rainfall and potential Evapotranspiration using the HBV hydrological model. Results show that runoff is more sensitive to precipitation changes than to potential Evapotranspiration changes and that the sensitivity increases with the aridity of the catchment.

Thesis of Yihun D. (2009) objective is to assess the impact of climate change on Gilgel Abbay River by using GCM (HadCM3) and A2a and B2a emissions scenarios; the coarse GCM downscale using Statistical Downscaling Model (SDSM) and using physically based hydrological model (SWAT) for run off generation. His result shows that the mean annual precipitation may decrease in the 2020s and increase in the 2050s and 2080s, the maximum and minimum temperature indicated an increasing trend for all time horizon. And also his result show that there may be a net annual increase in flow volume in Gilgel Abbay River due to climate change.

The study of Elshamy (2010) was conducted on Upper Blue Nile of Ethiopian high land area using three GCMs (CGCM2 (The Canadian Climate Modeling Centre), ECHAM4 (Max Planck Institute for Meteorology, Hamburg) and HadCM3 (UK Hadley Centre) with two emission scenarios SRES A2 and B2 and then downscaled using statistical downscaling approaches coupled with hydrological modeling the Nile Forecast System (NFS).It is evident that despite advances in climate modeling over the years, there still appears to be disagreement amongst GCMs in simulating future precipitation for a given region. In the case of the Blue Nile, results reported in this study indicate a drier future according to one GCM (CGCM2) whilst two others indicate wetter futures. Better consistency is observed in temperature changes, which leads to more consistent potential Evapotranspiration changes and these are expected to be very large by the 2080s. Based on work reviewed by the (IPCC, 2007), East Africa has experienced an increasingly wetter climate and is likely to become wetter in future according to the majority of climate model simulations. However, it should be noted that the lack of good rain gauge coverage prevents conclusive rainfall trend detection.

3 STUDY AREA AND DATA AVAILABILTY

3.1 Study Area Description

3.1.1 Location

Guder sub-basin which has a drainage area of 7011square kilometers is situated in the Northwest of Ethiopia; in the Southeastern part of the Blue Nile Basin approximately between 7^{o}30' to 9º30' N latitude and 37º00' to 39º00'E longitude. The Guder River originates from the mountainous area of south of the towns of Ambo and Guder at an elevation of 3000masl. The river flows from the south to the north and has its outlet to the Abbay River. The Guder sub-basin borders with the Muger sub-basin to the east, the Awash Basin to the south and the Fincha sub-Basin to the west.

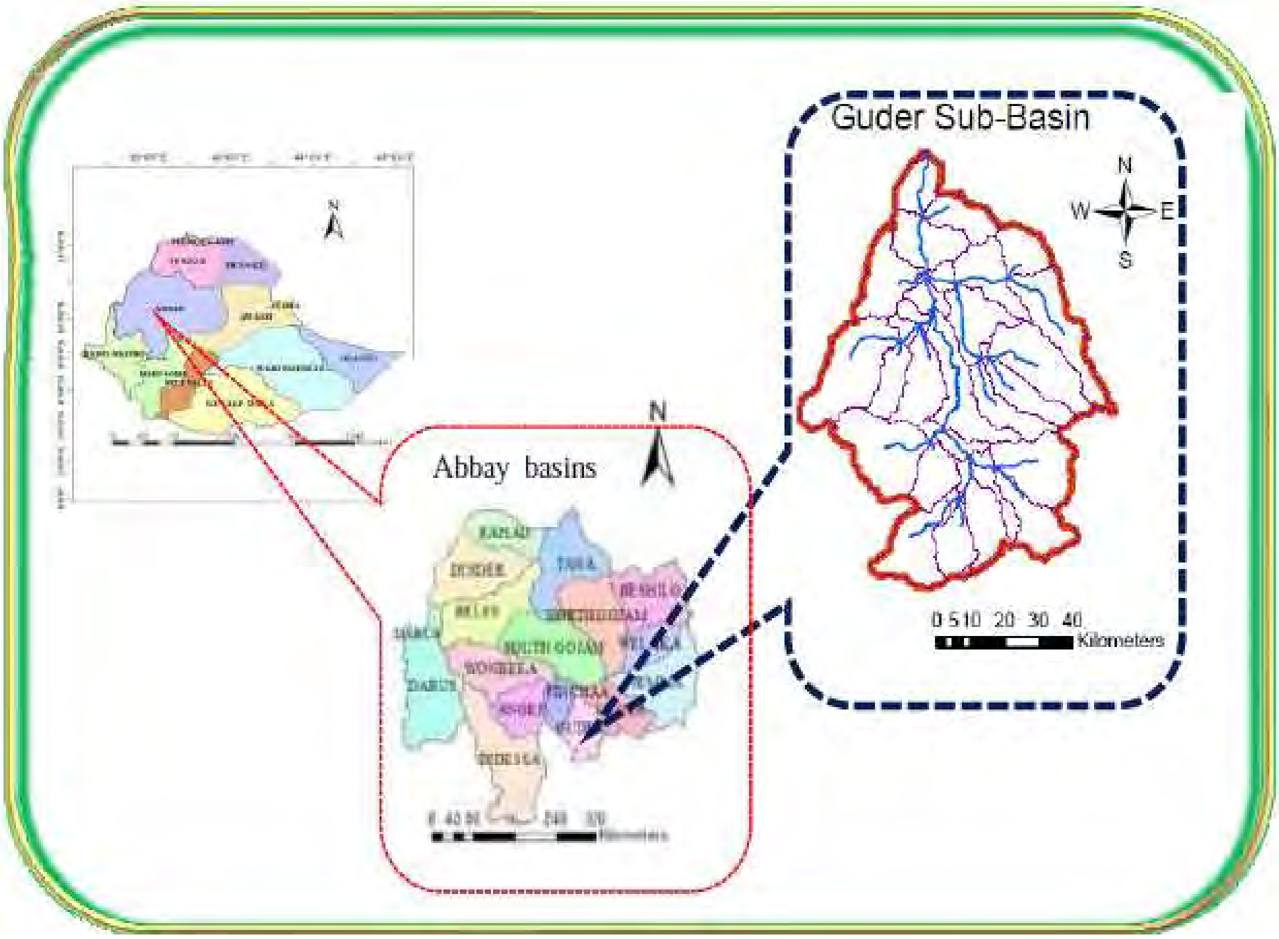

Figure 2 Location of Guder sub-basin

3.1.2 Topography

The elevation of Guder sub-basin varies from 1500 to 3000masl. The higher elevation ranges are located on the mountainous area at the South of the town of Ambo and Guder.

3.1.3 Climate

Guder sub-basin, in spite of being near the equator, has a comparatively mild climate because of its high elevation (1500-3000masl).

The annual climate may be divided in a rainy and dry season. The rainy season may be divided in to a major rainy season (Kiremt) and minor rainy seasons (Belg & Tsedey). During Kiremt season from June through August above 75% of total rainfall occurs and in Belg season from March to May small rainfall occur. The dry seasons (Bega) occurs in December to February and Tsedey covers from September through November. The long term mean annual rainfall of Guder sub-basin at different station is shown in Figure 3.

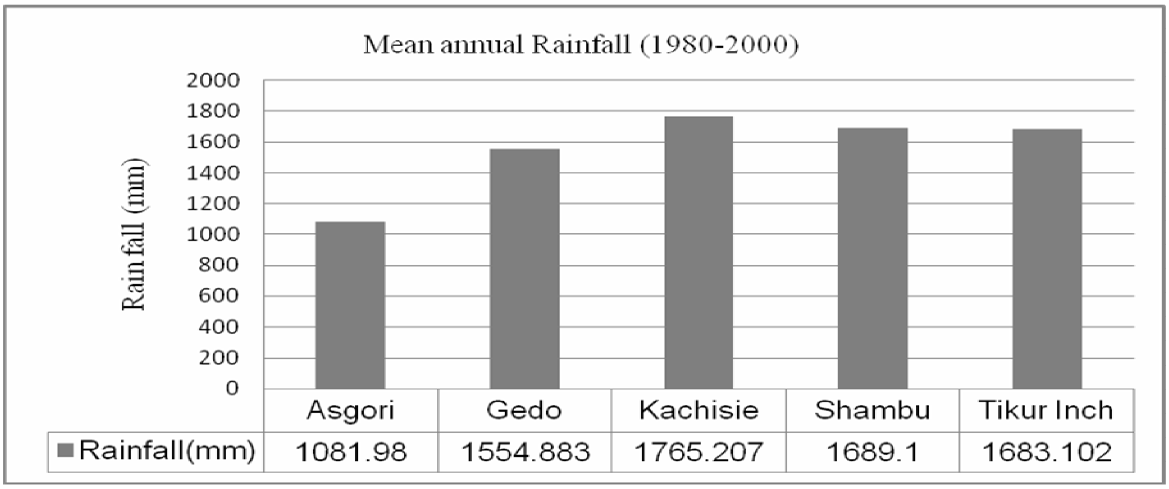

Figure 3 Mean annual rainfall of various stations

There is high diurnal variation in temperature. The annual average daily maximum and minimum temperature of each station is shown in Figure 4.

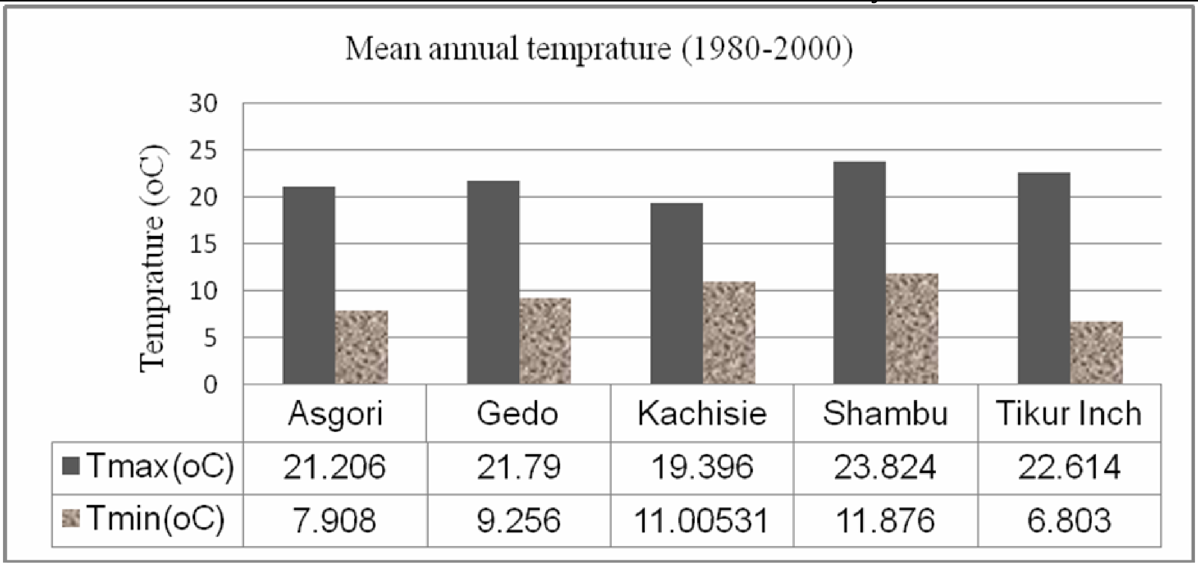

Figure 4 Mean annual Tmax and Tmin of various stations

3.1.4 Land Cover and Land Use

The land cover of the Guder sub-basin essentially follows the divide between highland and lowland. The high land around the Ambo and Guder mountainous areas were once dominantly covered with forests. However, these sub-humid tropical forests have been reduced to remnants, having been converted to cultivation and grazing. Almost the entire highland area is now under farm land (BCEOM, 1998).

3.1.5 Geology and Soil

Guder Sub-Basin lies in a large structural basin surrounded by volcanic mountains composed mostly of Quaternary volcanic rocks on the mountainous area of south of the towns of Ambo and Guder and Mesozoic sedimentary rock on the lower part of the river.

Corresponding to the variation in landscape and other soil forming factors such as climate and vegetation, the soils of the Guder sub-basin are also highly variable. The major soil types in the area includes: Chromic Luvisols, Eutric Cambisols, Eutric Fluvisols, Eutric Leptosols, Eutric Regosols, Eeutric Vertisols, Haplic Luvisols, Haplic Alisols and Haplic Nitisols. Apparently, these soils have various productivity limiting characteristics such as acidity, depth and permeability.

3.2 Data Availability

3.2.1 Meteorological Data

Meteorological data was required for two purposes in this study. First the data was used for down scaling the GCM data using Statistical Downscaling Model (SDSM). Second the data was used as input to the SWAT model in hydrological model development. Based on these objectives, the meteorological data required for this study were collected from the Ethiopian National Meteorological Services Agency (NMSA) at Addis Ababa office. The meteorological variables collected vary from station to station depending on the class of the stations. The daily meteorological data collected were precipitation, maximum and minimum temperature, relative humidity, wind speed and sunshine hours.

Table 1 List of station name, location and meteorological variables

No	Station name	Latitude (degree)	Longitude (degree)	Elevation (m)	Rainfall	Max Temp.	Min Temp.	Start year	End year
1	Kachisie	9.35	37.2	2520	√	√	√	1986	2000
2	Asgori	8.966	38	2500	√	**X**	√	1980	2000
3	Gedo	9.05	37.4333	2500	√	√	√	1980	2000
4	Shambu	9.56	37.1	2430	√	√	√	1980	2000
5	Tikur inch	8.7833	37.633	2480	√	√	√	1980	2000

The only station which has data for relative humidity, sunshine hours and wind speed is Kachisie with short period of record. All stations listed above contain daily rainfall and temperature data for at least ten years. Therefore all stations were used for hydrological model development. However, for deriving statistical relationships between the predictand and predictor long period of records are required. Hence downscaling experiments have been executed based on Gedo and Tikur Inch meteorological data which fulfill all input requirements for SDSM.

3.2.2 Hydrological Data

The hydrological data was required for performing sensitivity analysis, calibration and validation of the Hydrological model. In the Guder Sub-Basin there are some flow gauging stations located on upper Guder relatively small tributaries and/or near the head waters of the main river that have relatively long record of daily stream flow data. These stream flow data from 1990-2005 collected at the four gauging stations from the Ethiopian Ministry of Water and Energy hydrology department at Addis Ababa office(Table 2).

Table 2 Hydrological gauging stations of Guder River

S.No	Station Name	Location	
		Latitude(degree)	Longitude(degree)
1	Guder @ Guder	8.95	37.083
2	Fatto near Guder	8.8667	37.1667
3	Debis near Guder	9.01667	37.6667
4	Indris near Guder	8.9333	37.75

Figure 5 Hydrological and Meteorological stations of Guder sub-basin

2.2.3 Remote Sensing Data

The SWAT model can be applied as a spatially distributed model; hence it can analyze both small and large watersheds by subdividing the area into homogenous parts. As a physically-based model, SWAT use hydrologic response units (HRUs) to describe spatial heterogeneity in terms of land cover, soil type and slope within a watershed. Based on this, a Digital Elevation Model (DEM, 90mx90m), soil data, land use and stream network data as a shape file are collected from Ministry of water and Energy GIS department at Addis Ababa office.

3.2.4 Climate Scenario Data

The climate scenario data used for statistical downscaling model (SDSM) was obtained from the Canadian Institute for climate studies website (http://www.cics.uvic.ca/scenarios/sdsm/select.cgi) for model output of HadCM3 of two SRES scenarios A2 and B2 produced by greenhouse gas, sulphate aerosol, and solar forcing and NCEP reanalysis data. The predictor variables are supplied on a grid by grid basis so that the data was downloaded from the nearest grid box (in African window 7.5^{o}N latitude and 37.5^{o}E longitude) as a zipped file to the study area.

4 METHODOLOGY

Investigation of climate change effect on the hydrological regimes consists of the following three steps:

1. Use of General Circulation Models (GCMs) to provide future global climate scenarios under the effect of increasing greenhouse gases,
2. Downscaling techniques for downscaling the GCMs output to the scales compatible with hydrological models, and
3. Use of hydrological models to simulate the effects of climate change on hydrological regimes at various scales (Xu et al., 2005).

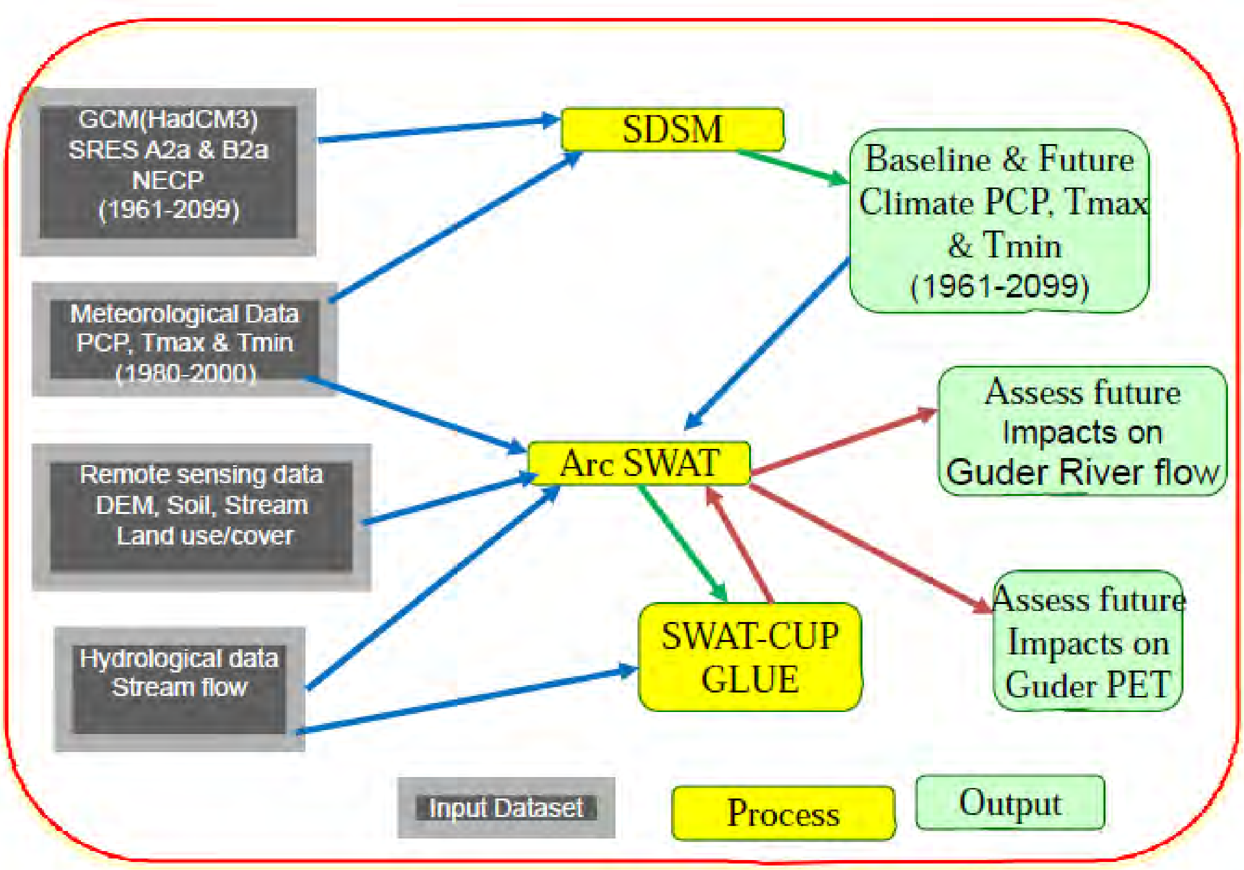

Figure 6 General methodology flow chart used in the study

4.1 General Circulation Model (GCM)

The climate model is a mathematical description of the Earth's climate system, broken into a number of grid boxes and levels in the atmosphere, ocean and land. At each of these grid points equations are solved which describe the large-scale balances of the momentum, heat and moisture. Based on this, a wide range of climate models are developed as listed in Appendix B. The modeling approach and the resolution of the model vary from model to model.

The relative performance of GCMs can depend on the size of the region (i.e. small regions at sub-grid scale are less likely to be well described than large regions at continental scale), on its location (i.e. the level of agreement between GCM outputs varies a lot from region to region) and on the variables being analyzed (for instance, regional precipitation is more variable and more difficult to model than regional temperature) (Carter, 2007). For this study the model output of HadCM3 was employed for the A2 (Medium-High Emissions) and B2 (Medium-Low Emissions) SRES Emission Scenarios.

HadCM3 is a coupled atmospheric-ocean GCM developed at Hadley Centre for Climate Prediction, detection, attribution and other climate sensitivity studies & Research, UK. The atmospheric part of HadCM3 has a horizontal resolution of 2.5º latitude x 3.75º longitude, (228kmx417km) and has 19 vertical levels. The ocean component of the model has 20 vertical levels with horizontal resolution of 1.25º latitude x 1.25º longitude. HadCM3 is applied in this study because the model is widely applied in many climate change impact studies, it is a public domain model and the model provides daily predictor variables which can be used for the Statistical Downscaling Model. The predictor variables used for the SDSM model input can be downloaded from the Canadian Institute for climate studies website (http://www.cics.uvic.ca/scenarios/sdsm/select.cgi) for model output of HadCM3. The predictor variables are supplied on a grid basis so that after selecting the Africa window and the location of Guder sub-basin (at 37.5^{o}E longitude and 7.5^{o}N latitude) on the grids, the zip file will be available. When the downloaded zip file is unpacked, it gives the following three directories:

NCEP_1961-2001: This directory contains 41 years of daily observed predictor data, derived from the NCEP reanalysis', normalized (with respect to the mean and standard deviation) over the complete 1961-1990 period. These data were interpolated to the same grid as HadCM3 (2.5° latitude x 3.75° longitude) before the normalization was implemented.

H3A2a_1961-2099: This directory contains 139 years of daily GCM predictor data, derived from the HadCM3 A2 (a) experiment, normalized over the 1961-1990 period.

H3B2a_1961-2099: This directory contains 139 years of daily GCM predictor data, derived from the HadCM3 B2 (a) experiment, normalized over the 1961-1990 period.

NCEP data are re-analysis sets from the National Centre for Environmental Prediction (NECP) which was re- girded to match with the grid system of the HadCM3. These are the data used for SDSM model calibration. Both the NCEP and HadCM3 data have daily predictors. The predictor variables which are available for both NCEP and HadCM3 are shown in Appendix D. The Predictand (maximum temperature, minimum temperature and precipitation) for a specific site can be prepared in the same format as predictor with single column text file to use as input for the SDSM downscaling model.

4.2 Statistical Downscaling Model

4.2.1 General Description of the Model

Statistical Downscaling Model (SDSM) is a Windows–based decision support tool for the rapid development of single–site, ensemble scenarios of daily weather variables under present and future regional climate forcing. The SDSM Version 4.2 software used in this study reduces the task of statistically downscaling daily weather series into seven discrete steps (Dawson & Wilby, 2007), namely: quality control of input data; screening of candidate predictor variables; model calibration; synthesis of present weather data; generation of future climate scenarios; basic statistical and time series analyses and graphing results. SDSM provides a robust and parsimonious technique of scenario construction that complements other methods (e.g., direct use of climate model output, dynamical downscaling, sensitivity analysis, etc.). SDSM permits the spatial downscaling of daily predictor-Predictand relationships using multiple linear regression techniques. The predictor variables provide daily information concerning the large scale state of the atmosphere, while the Predictand describes conditions at the site scale.

4.2.2 SDSM Model Setup

Predictor and Predictand file

Statistical downscaling involves developing quantitative relationship between the predictor and the Predictand. The predictor represents large-scale atmospheric variables as shown in Appendix C; whereas the Predictand represents local surface variables such as temperature and precipitation.

Setting of the model parameter

The normal calendar year (366) which allows 29 days in February every fourth year (i.e. leap year) is used whenever dealing with Predictand and NCEP predictor whereas the year length of 360 days is used in the scenario generation part as using HadCM3. The event threshold is set to zero for temperature and 0.1 mm/day for precipitation to treat trace rain days as dry days. Missing data identifier is the code assigned to missing data in all input with the code (-999) the value will be skipped (e.g., during model calibration, or calculation of summary statistics). Negative values also allowed by unconditional processes in the downscaling model (e.g., for minimum temperature).

Model Transformation is applied to the Predictand in conditional models with fourth root transformation in the case of daily precipitation and the default none used whenever the predictand is normally distributed (as in the case of daily temperature). Bias correction compensates for any tendency to over or under estimates the mean of the conditional process by the downscaling model. This parameter is set to1 (default value) for maximum and minimum temperature since the process is unconditional whereas for precipitation this parameter can be adjusted in order to match the mean of the conditional process.

Screening the downscaling predictor variables

The choice of predictor variables is one of the most influential steps in the development of statistical downscaling procedure. Identifying empirical relationships between girded predictors and single site predictands is central to all statistical downscaling. The screen variable option in SDSM assists the choice of appropriate downscaling predictor variables through seasonal correlation analysis, partial correlation analysis and scatter plots. One of the approaches is to choose all predictors and run the explained variance on a group of eight or nine at a time.

Out of the groups, those predictors which have high explained variance are selected. Then partial correlation analysis is done for selected predictors to see the level of correlation with each other. There could be a predictor with a high explained variance but it might be very highly correlated with another predictor. This means that it is difficult to tell that this predictor will add information to the process and therefore it will be dropped from the list.

SDSM Model Calibration

The calibration model process constructs downscaling models based on multiple regression equations, given daily weather data (the predictand) and regional-scale, atmospheric (predictor) variables. The model structure for calibration can be specified by selecting the process either unconditional or conditional. In unconditional models a direct link is assumed between the predictors and predictand. In conditional models, there is an intermediate process between the regional forcing and local weather (e.g., local precipitation amounts depend on wet-/-dry-day occurrence, which in turn depend on regional-scale predictors such as humidity and atmospheric pressure). The model structure is set to unconditional for maximum and minimum temperature and conditional for precipitation. The model type determines whether individual downscaling models will be calibrated for each calendar months, climatological season or entire year. The model is structured as a monthly model for both precipitation and temperature downscaling, in which case, twelve regression equations are derived for twelve months using different regression parameters for each month equation. Finally the data period should be set in order to specify the start and end date of the analysis.

Weather and Scenario Generator

The Weather Generator operation produces ensembles of synthetic daily weather series given observed (or NCEP re–analysis) atmospheric predictor variables and regression model weights produced by the Calibrate Model operation. It enables the verification of calibrated models (assuming the availability of independent data) as well as the synthesis of artificial time series representative of present climate conditions. It can also be used to reconstruct predictands or to infill missing data. The Scenario Generator operation produces ensembles of synthetic daily weather series given the regression weight produced during the calibration process and the daily atmospheric predictor supplied by a GCM (either under the present or future greenhouse gas forcing). Twenty ensembles of synthetic daily time series were produced for the two emission scenarios (HadCM3 A2a & B2a) for a period of 139 years (1961 to 2099). Finally the mean of twenty ensembles for the specified period is produced for the maximum & minimum temperature and precipitation.

Analysis of Observed and Downscaled Data

Statistical analyses of observed and downscaled weather data are handled in slightly different ways by SDSM but both are performed in the Summary Statistics screen. Common diagnostic tests are available for both observed and synthetic data. These statistics include the variable mean, maximum, minimum, variance, peaks above/below thresholds, percentiles, etc computed on a calendar month, seasonal or annual basis.

4.3 Hydrological Modeling with SWAT

Soil and Water Assessment tool (SWAT) was selected as the best modeling tool owing to many reasons. (1) SWAT is one of the promising and applicable rainfall-runoff models for developing countries which do not have enough data for fully distributed hydrological models. (2) It is also computationally efficient to operate on large basins in a reasonable time (being semi-distributed) and capable of simulating long periods. (3) Moreover, SWAT is public domain software.

SWAT is a river basin scale, a continuous time, a spatially distributed model developed to predict the impact of land management practices on water, sediment and agricultural chemical yields in large complex watersheds with varying soils, land use and management conditions over long periods of time (Neitsch et al., 2005) and it is computationally efficient, uses readily available inputs and enables users to study long-term impacts. Currently SWAT is imbedded in Arc GIS interface called Arc SWAT and for this study ArcSWAT2005 is used.

SWAT requires daily values of precipitation, maximum and minimum temperature, solar radiation, relative humidity and wind speed. They can be given to the model as a user defined measured time series or can be generated within SWAT from a monthly data and its statistics summarized over a number of years. A weather generator WXGEN model is included in SWAT which can generate the above stated data or fill in gaps for measured records. The inside model is based on the contiguous U.S. condition. However, it can be brought to local conditions by providing a user defined database (userwgn.dbf) (Neitsch et al., 2005).

4.3.1 Arc SWAT Model Setup

Watershed Delineation

Arc SWAT uses digital elevation model (DEM) data to automatically delineate the watershed into several hydrological connected sub-watersheds. The first step in the watershed delineation was loading the properly projected DEM. To reduce the processing time of the GIS functions, a mask was created over the DEM around the study area. Then a polyline stream network dataset was burnt-in to force SWAT sub-basin reaches to follow known stream reaches. Burning-in a stream network improves hydrological segmentation, and sub-watershed delineation. After the DEM grid was loaded and the stream networks superimposed, the DEM map grid was processed to remove the non draining zones.

The initial stream network and sub-basin outlets were defined based on drainage area threshold approach. The interface lists a minimum, maximum and suggested threshold area. The smaller the threshold area, the more detailed the drainage network delineated by the interface but the slower the processing time and the larger memory space required. In this study, defining of the threshold drainage area was done by successive re-run of the stream and outlet definition routine from the suggested to the minimum area until known smaller streams were created. Besides those sub-basin outlets created by the interface, outlets were also manually added at the three hydro gauging stations where sensitivity analysis, calibration and validation tasks were later performed. The watershed delineation activity was finalized by calculating the geomorphic sub-basin parameter.

Hydrologic Response Unit Analysis

Hydrologic response units (HRUs) are lumped land areas within the sub-basin that are comprised of unique land cover, soil and management combinations. HRUs enable the model to reflect differences in Evapotranspiration and other hydrologic conditions for different land covers and soils. The runoff is estimated separately for each HRU and routed to obtain the total runoff for the watershed. This increases the accuracy in flow prediction and provides a much better physical description of the water balance.

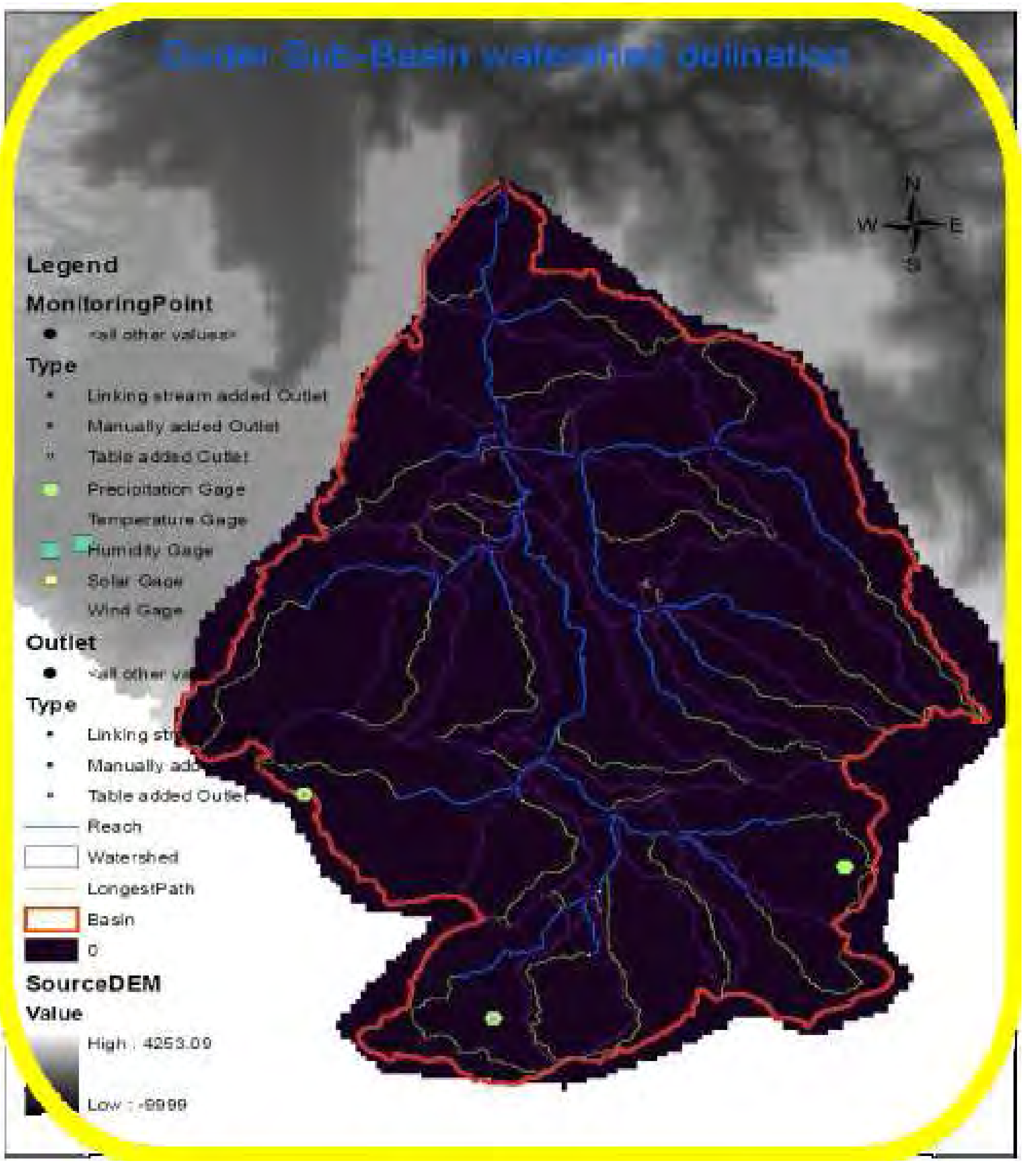

Figure 7 *Delineated watershed of Guder sub-basin*

The land use and the soil data in a projected shape file format were loaded into the Arc SWAT interface to determine the area and hydrologic parameters of each land-soil category simulated within each sub-watershed. The land cover/land use classes were defined using the look up table that identifies the 4-letter SWAT code for the different categories of land cover/land use so as to relate the grid values to SWAT land cover/land use classes. After the land use SWAT code assigned to all map categories, calculation of the area covered by each land use and reclassification were done. The land slope classes were also integrated in defining the hydrologic response units. The DEM data used during the watershed delineation was also used for slope classification.

The multiple slope discretization operation was preferred over the single slope discretization as the sub-basins have a wide range of slopes between them. Based on the suggested min, max, mean and median slope statistics of the watershed, four slope classes (0-5, 5-10, 10-15 and >15%) were applied and slope grids reclassified. After the reclassification of the land use, soil and slope grids overlay operation was performed.

In last step HRU definition was performed. In this study the HRU distribution was determined by assigning multiple HRU in order to eliminate minor land uses, soils or slope classes in each sub-basin which is less than the threshold level. After the elimination process, the area of the remaining land use, soil, or slope class was reapportioned so that 100% of the land area in the sub-basin is modeled. In the SWAT user manual it is suggested that it is better to use a larger number of sub-basins than larger number of HRUs in a sub-basin; a maximum of 10 HRUs in a sub-basin is recommended. Hence, taking the recommendations in to consideration, 15%, 10%, and 5% threshold levels for the land use, soil and slope classes were applied, respectively so as to encompass most of spatial details.

In this study the overall watershed delineation and HRU definition simulation gave a watershed area of 7011km^2 which resulted in 34 sub-basins and 358 HRUs. The watershed delineation of the area gave minimum, maximum and mean elevations in the basin of 1042, 3265, and 2123masl respectively. Figure 7 above shows delineated watershed and sub-basins.

Each HRU is composed of land use, soil, and slope parameters. The land use for this analysis consists of 11 land use types described in Table 3 with the Moderately cultivated and dominantly cultivated Agricultural land use (like Wheat, Teff, Maize, Barley etc…) covering about 90% of the area.

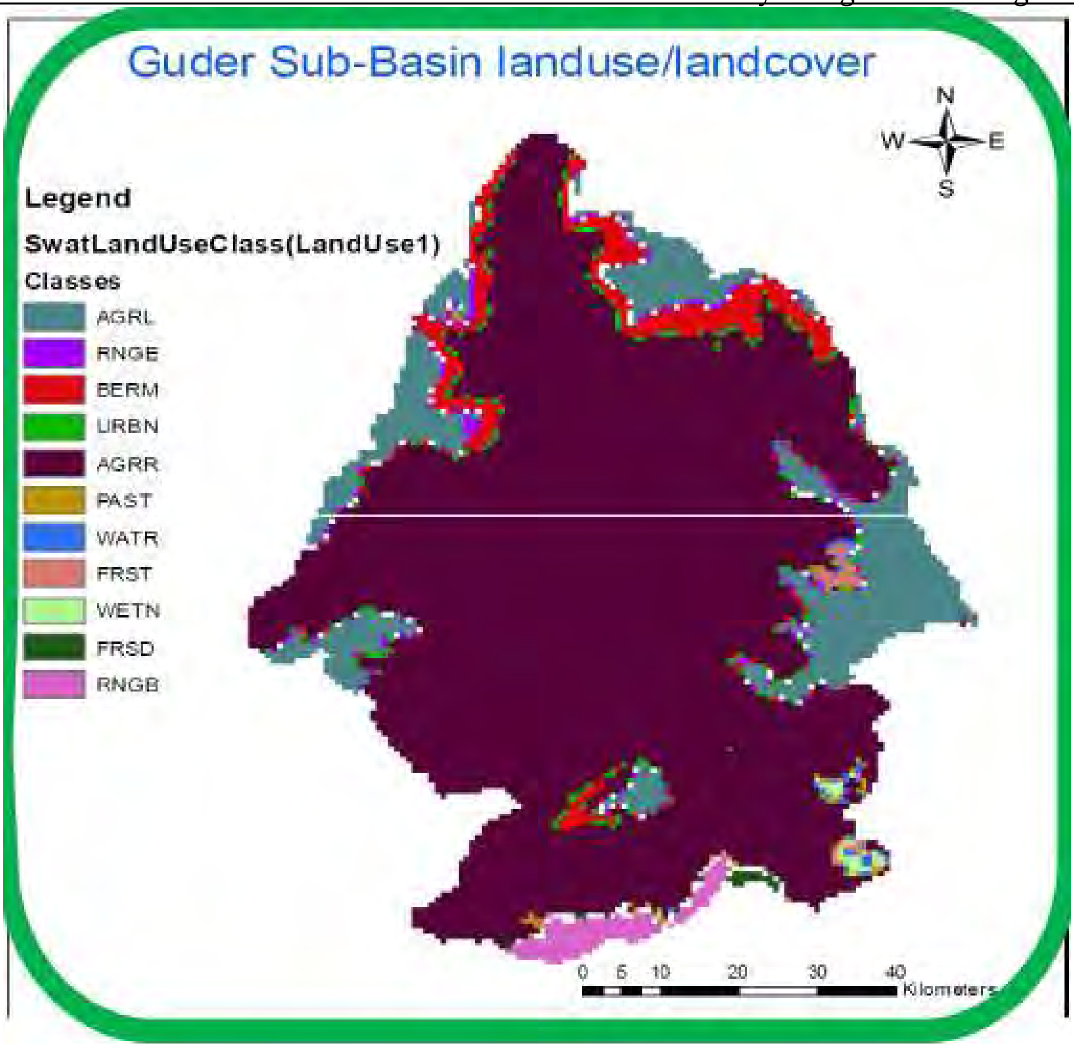

Figure 8 *Land Use/Land Cover of Guder sub-basin*

Table 3 Land use/land cover types and their areal coverage in Guder sub-basin

Land Use/land Cover	SWAT Code	Area (km^2)	% of total area
Dominantly cultivated Agriculture	AGRL	943.6806	13.46
Ranged Grasses	RNGE	2.804	0.04
Grass land	BERM	363.87	5.19
Residential	URBN	2.804	0.04
Moderately Cultivated Agriculture	AGRR	5500.13	78.45
Pasture	PAST	2.103	0.03
Water	WATR	6.31	0.09
Forest ever green	FRST	31.55	0.45
Wetlands-Non forested	WETN	32.25	0.46
Forest Deciduous	FRSD	11.02	0.17
Range Brush	RNGB	112.88	1.61

The second components of HRU was soil type, the sub-basin covers 15 different soil types. The soil type with detailed total area coverage is given in the Table 4.

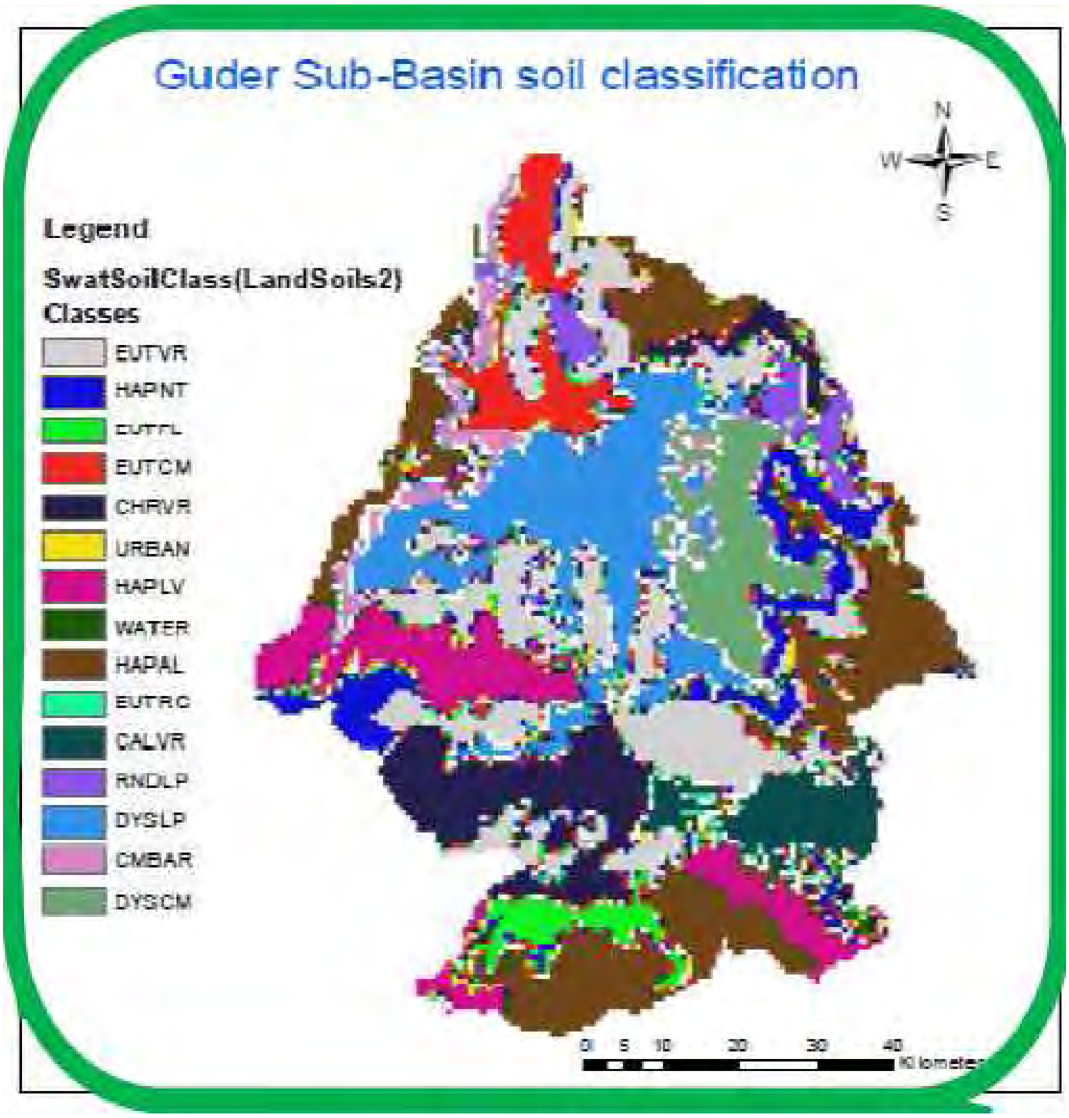

Figure 9 *Soil Map of Guder sub-basin*

SWAT slope computation using the DEM data indicated that three-fourth of the Catchment has a slope of less than 15%. The slope classes and their areal coverage are shown in Table 4.

Table 4 Soil types/ slope classes and their areal coverage in Guder sub-basin

	Soil type/slope classes	SWAT Code	Area (km^2)	% of total area
Soil type	Eutric Vertisols	EUTVR	1425.336	20.33
	Haplic Nitisols	HAPNT	436.084	6.22
	Eutric Fluvisols	EUTFL	178.7805	2.55
	Eutric Cambisols	EUTCM	356.860	5.09
	Chromic Vertisols	CHRVR	609.256	8.69
	Urban	URBAN	10.516	0.15
	Haplic Luvisols	HAPLV	611.359	8.72
	Water	WATER	10.516	0.15
	Haplic Alisols	HAPAL	1121.059	15.99
	Eutric Regosols	EUTRG	12.62	0.18
	Calcic Vertisols	CALVR	307.08	4.38
	Rendzic Leptosols	RNDLP	202.618	2.89
	Dystric Leptosol	DYSLP	1042.536	14.87
	Cambic Arenosols	CMBAR	211.732	3.02
	Dystric Cambisols	DYSCM	473.24	6.75
Slope Classes In %	0-5		910.729	12.99
	5-10		1339.101	19.10
	10-15		3117.792	44.47
	>15		1643.378	23.44

Importing Weather Data

Weather data to be used in a watershed simulation is imported in order to provide the moisture and energy inputs that control the water balance and determine the relative importance of the different components of the water cycle. The weather data required by SWAT consist of daily precipitation, maximum/minimum temperature, solar radiation, wind speed and relative humidity. Due to lack of data and quality related problems, in most of the stations daily precipitation and maximum/minimum temperature in dbase format were the climatic input variables imported together with their weather location. And as discussed above the Hargreaves method was used to determine the potential Evapotranspiration.

Sensitivity Analysis

SWAT is a complex model with many parameters that makes manual calibration difficult. Hence, sensitivity analysis was performed to limit the number of optimized parameters to obtain a good fit between the simulated and measured data. Sensitivity analysis helps to determine the relative ranking of which parameters most affect the output variance due to input variability which reduces uncertainty.

SWAT model has an embedded tool to perform sensitivity analysis and provides recommended ranges of parameter changes. SWAT2005 uses a combination of Latin Hypercube Sampling and One-At-a-Time sensitivity analysis methods (LH-OAT method). The concept of the Latin-Hypercube Simulation is based on the Monte Carlo Simulation to allow a robust analysis but uses a stratified sampling approach that allows efficient estimation of the output statistics while the One-Factor-At-a-Time is an integration of a local to a global sensitivity method. In local methods, each run has only one parameter changed per simulation which aides in the clarity of a change in outputs related directly to the change in the parameter altered (Green and van Griensven, 2007). For this study Sensitivity analysis was carried out for the calibration and warming up periods. A total of 27 parameters with ten intervals of LH sampling and 270 iterations were done to select the rank of these parameters. After sensitivity analysis, model calibrations have been done by selecting the most sensible parameters.

4.3.2 Model Calibration and Uncertainty Analysis

There are three calibration approaches widely used by the scientific community. These are the manual calibration, automatic calibration and a combination of the two. Manual calibration is the most widely used approach, but it is tedious, time consuming, and success of it depends on the experience of the modeler and knowledge of the watershed being modeled. Automatic calibration involves the use of a search algorithm to determine best-fit parameters and it is desirable as it is less subjective and due to extensive search of parameter possibilities can give results better than if done manually.

A base-flow filter program was used to determine the relative proportion of annual flow contribution from surface runoff or base-flow. The automated Web GIS based Hydrograph Analysis Tool (WHAT) was used to separate the surface runoff from the base-flow. WHAT, accessed from http://cobweb.ecn.purdue.edu/~what/ can also compute R^2 and Nash-Sutcliffe coefficient. After the base flow and surface runoff were separated, the surface runoff was calibrated by adjusting the sensitive parameters which affect surface runoff like CN2 (Initial SCS runoff curve number for moisture condition II), Ch_N2 (Manning’s ‘’n’’ value for the main channel) and Esco (Soil evaporation compensation factor).

The simulated versus observed values for each adjustment were evaluated with coefficient of determination (R^2) and Nash-Sutcliffe efficiency (E_{NS}) and when the values of R^2 was greater than 0.6 and E_{NS} was above 0.5, calibration of base-flow was followed. Base-flow calibration was performed by adjusting the sensitive parameters which affects groundwater contribution. The most sensitive base-flow parameters which were adjusted were GW_REVAP (Groundwater ''revap'' coefficient), REVAPMN (threshold depth of water in the shallow aquifer for ''revap'' or percolation to occur), and GWQMN (depth of water in the shallow aquifer required for return flow to occur). Like surface runoff calibration, the simulated versus observed values were evaluated with R^2 and E_{NS}. The parameters were adjusted until the R^2 values greater than 0.6 and E_{NS} results was above 0.5. However, after adjustments of base-flow parameters were done the surface runoff was checked because the adjustments of the base-flow parameters will affect the surface runoff in some way. Once the water balance was calibrated temporal flow calibration was performed at each step by adjusting parameters which affects the shape of the hydrograph. The parameters adjusted were Ch_K (effective hydraulic conductivity in main channel alluvium), ALPHA_BF (base flow alpha factor), Surlag (Surface runoff lag coefficient) and GW-DELAY (Groundwater delay time).

When the manual calibration of the model evaluation parameters reached to an unchanged level, the model was run automatically. Auto calibration was done using an extension tool implemented in SWAT which uses Parameter Solution Methods (PARASOL). Using the results in auto calibration uncertainty analysis was done by SWAT-CUP linked to GLUE. GLUE (Abbaspour et al., 2007) was used on a combined calibration and uncertainty analysis. The parameter aggregation leads to estimated uncertainty in the output; quantified by the 95% prediction uncertainty band calculated at the 2.5% and the 97.5% levels of the distribution. In order to evaluate model output related to the runoff component, simulated river discharge is compared to the measured stream flow using indices such as the root mean square error (R^2), and the Nash-Sutcliffe (E_{NS}) coefficient of efficiency (Nash and Sutcliffe, 1970). The R^2 value is an indicator of strength of relationship between the observed and simulated values. The E_{NS} indicates how well the plot of observed versus simulated value fits the 1:1 line. If the measured value is the same as all predictions, E_{NS} is 1. If the E_{NS} is between 0 and 1, it indicates deviations between measured and predicted values. If E_{NS} is negative, predictions are very poor, and the average value of observed value is a better estimate than the model prediction.

The R^2 and E_{NS} values are explained in equations below respectively.

$$R^2 = \frac{\left(\sum_{i=1}^{n}\left(Q_O - \bar{Q}_O\right)\left(Q_P - \bar{Q}_P\right)\right)^2}{\sum_{i=1}^{n}\left(Q_O - \bar{Q}_O\right)^2 \sum_{i=1}^{n}\left(Q_P - \bar{Q}_O\right)^2} \quad .... \; .... \; .... \; .Eqn\ 7$$

$$E_{NS} = \frac{\sum_{i-1}^{n}\left(Q_O - \bar{Q}_O\right)^2 - \sum_{i=1}^{n}\left(Q_P - Q_O\right)^2}{\sum_{i=1}^{n}\left(Q_O - \bar{Q}_O\right)^2} \quad .... \; .... \; .... \; .Eqn\ 8$$

Where: n is the number of observations during the simulation period

Q_P and Q_O are the predicted and observed values at each comparison point i

$\bar{Q}_P$ and $\bar{Q}_O$ are arthimetic mean of the predicted and observed values

Additionally, the *P-factor* and the *R-factor* are two indices commonly used to compare predicted output by uncertainty bands and evaluate the strength of the calibration and uncertainty analysis. *P-factor* gauges the degree to which measured data are bracketed in the 95% band of the predicted uncertainty (95PPU). The larger the *P- factor*, the more measured data are contained in the range (maximum *P-factor* = 1 implies all measured data are within the 95% bracket). The *R-factor* is a ratio between the thickness of the 95PPU band and the standard deviation of the measured data, indicating the width of the uncertainty interval. *R-factor* indicates the strength of the calibration and should be close to or smaller than a practical value of 1.

Model Validation

Model validation was performed after model calibration at the four gauged stations similar to that of the calibration. This involved running the calibrated model using independent data without changing the model parameters. As the model predictive capability was demonstrated as being reasonable in both the calibration and validation phases, the model was used for future predictions under different management scenarios.

5 RESULTS AND DISCUSSION

5.1 Climate Projection

5.1.1 Predictor Variables Selection

The best correlated predictor variables selected for minimum temperature, maximum temperature and precipitation for Gedo and Tikur Inch meteorological stations are listed in Table 5.

Table 5 Selected predictor variables for the predictands for Gedo and Tikur Inch station

Station Name	Predictor	Symbol	Predictand		
			TMAX	TMIN	PRCP
Gedo	Surface vorticity	ncepp_zaf		√	
	Surface wind direction	ncep_thaf	√		
	Surface divergence	ncep_zhaf	√		
	500hpa zonal velocity	ncepp5_uaf		√	
	850hpa divergence	ncepp8zhaf	√		
	500hpa geopotential height	ncepp500af	√	√	√
	850hpa meridional velocity	ncepp8_vaf			√
	850hpa geopotential height	ncepp850af			√
	Surface specific humidity	ncepshumaf	√	√	√
	Mean temperature at 2m	ncep tempaf	√		√
Tikur Inch	Mean sea level pressure	Ncepmaslpaf	√	√	
	Surface airflow strength	ncepp_faf	√		
	Surface zonal velocity	ncepp_uaf		√	√
	Surface vorticity	ncepp_zaf	√		√
	Surface wind direction	ncep_thaf	√		√
	Surface divergence	ncep_zhaf		√	√
	500hpa geopotential height	ncepp500af	√	√	√
	850hpa meridional velocity	ncepp8_vaf	√		√
	relative humidity at 850hpa	ncepp850af	√	√	√
	Mean temperature at 2m	ncep tempaf	√		√

For Gedo meteorological station the strongest correlation was obtained between the predictands and each predictor for each month. The correlation between minimum temperature and ncepp8_zaf was strongly correlated for all months except June, July and August. Ncepshumaf also showed good correlation with the minimum temperature for all months except September and October. The correlation of maximum temperature with the predictor variables was exceptionally strong for all the selected predictors. Ncepshumaf and ncep tempaf predictors gave better correlation from March to October except June. Ncepp850af also showed a good correlation in October and November. The precipitation showed a better correlation with ncepshumaf in the months of January, May, August, September and October.

For Tikur Inch meteorological station the strongest correlation was obtained between the predictands and each predictor for each month. The correlation of minimum temperature with the predictor variables was exceptionally strong for all the selected predictors. The correlation between maximum temperature and the predictors such as ncepmaslpaf, ncepp500af and ncepp850af are better correlation except September. The precipitation showed a better correlation with ncepp_uaf in the months of April, July and October.

5.1.2 Calibration and Validation of SDSM

For both Gedo and Tikur Inch the calibration was carried out from 1980-1990 for eleven years and the withheld data from 1991-2000 were used for model verification. Twenty ensembles of synthetic daily weather series generated using NCEP-reanalysis data for the verification of the calibrated model. The mean of the 20 ensembles of maximum temperature and minimum temperature values gave a better R^2 values, inferring that future projections would also be well replicated. The model develops a better multiple regression equation parameters for the maximum and minimum temperature than the precipitation. This is mainly due to the conditional nature of precipitation. In conditional models, there is an intermediate process between regional forcing and local weather (e.g., local precipitation amounts depend on wet–/dry–day occurrence, which in turn depend on regional–scale predictors such as humidity and atmospheric pressure) (Wilby and Dawson 2004).

5.1.3 Downscaling the GCM for the Baseline Period

5.1.3.1 Base line Scenario developed for Gedo station

Minimum temperature

The monthly minimum temperature downscaled for A2a and B2a emission scenarios in the baseline period shows a reasonably good agreement with the observed minimum temperature for all months as shown in Figure 10.

The variability of monthly minimum temperature of observed values is well preserved in the downscaled value from January to May and September to December. From May to August the variance of observed value is slightly higher than the downscaled values but the general trend of both observed and downscaled values shows a similar pattern as shows Figure 11.

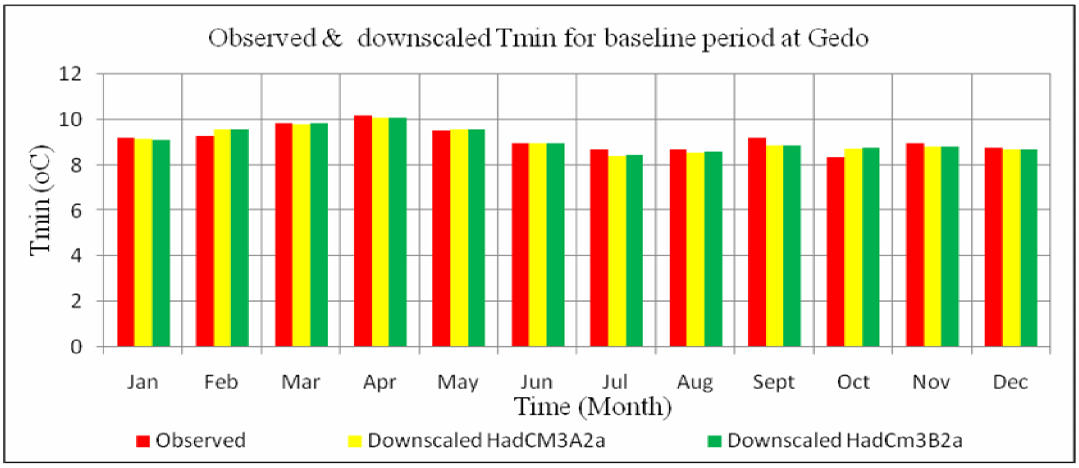

Figure 10 Observed and downscaled monthly mean Tmin for the baseline period

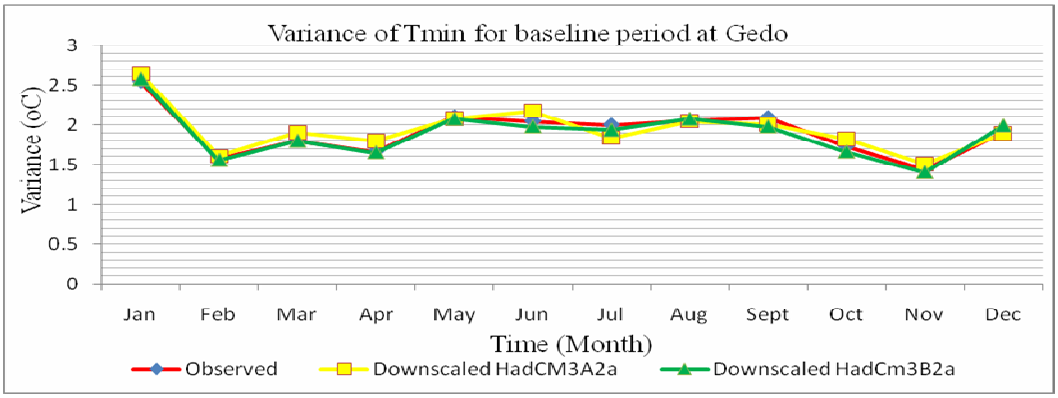

Figure 11 Variance of observed and downscaled Tmin for baseline period

Maximum Temperature

The downscaled monthly mean maximum temperature reveals strong relations with the observed temperature for the baseline period (1980-2000) of both in A2a and B2a emission scenarios as shown Figure 12.

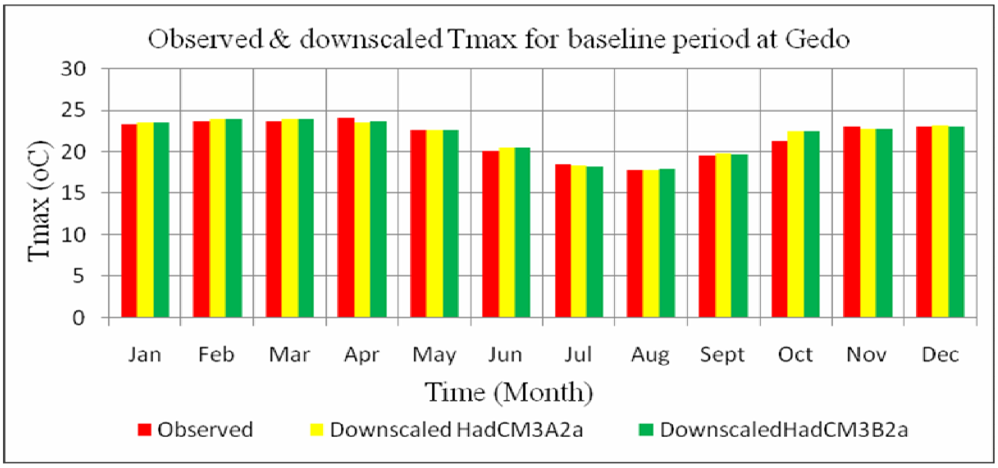

Figure 12 Observed and downscaled monthly Tmax for the baseline period

The variability of monthly maximum temperature of observed values is well preserved in the downscaled value from January to June. In July the variance of observed value is slightly higher than the downscaled values and from August to September the variance of observed value is slightly lower than the down scaled values but the general trend of both observed and downscaled values shows a similar pattern.

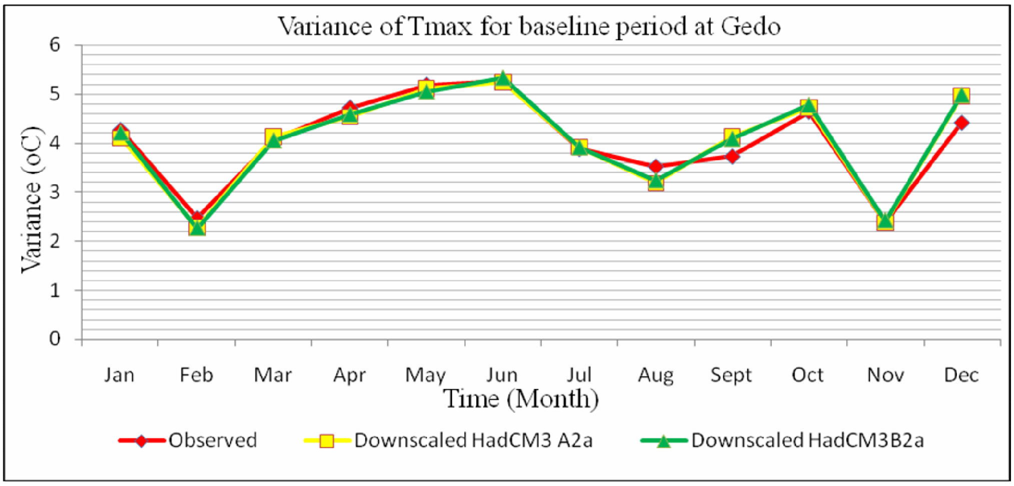

Figure 13 Variance of observed and downscaled Tmax baseline period

Precipitation

The SDSM model performs reasonably well in estimating the mean monthly precipitation in many months but there is a relatively model error in the month of July and September. The result, however, can be taken as satisfactory given the fact that precipitation downscaling is necessarily more problematic than temperature. The monthly precipitation downscaled for the baseline period is shown in Figure 14.

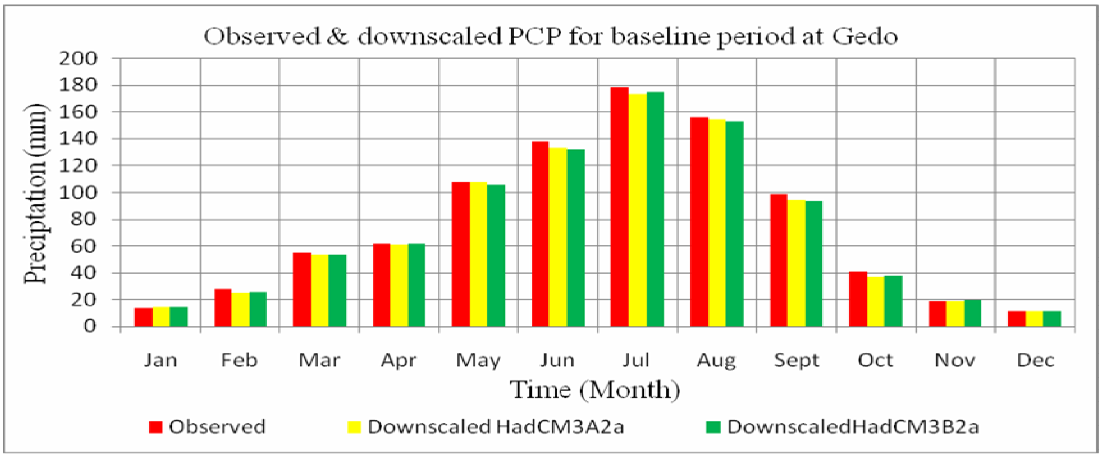

Figure 14 Mean monthly observed and downscaled precipitation for the baseline period

The variability of observed and downscaled precipitation shows good agreement in many months. Generally speaking the variance of observed and downscaled precipitation exhibits a similar pattern.

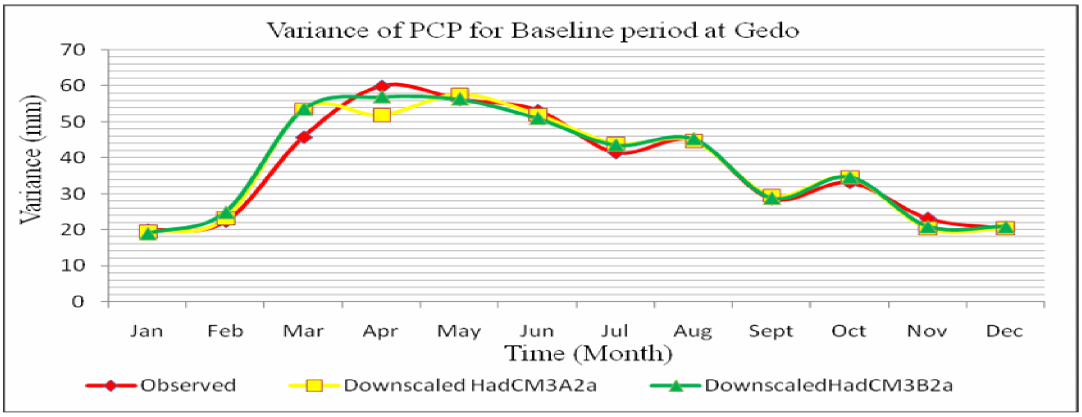

Figure 15 Variance of observed and downscaled precipitation for the baseline period

5.1.3.2 Base line Scenario developed for Tikur Inch station

Minimum temperature

The monthly minimum temperature downscaled for A2a and B2a emission scenarios at Tikur Inch station in the baseline period shows a reasonably good agreement with the observed minimum temperature for all months as shown in Figure 16.

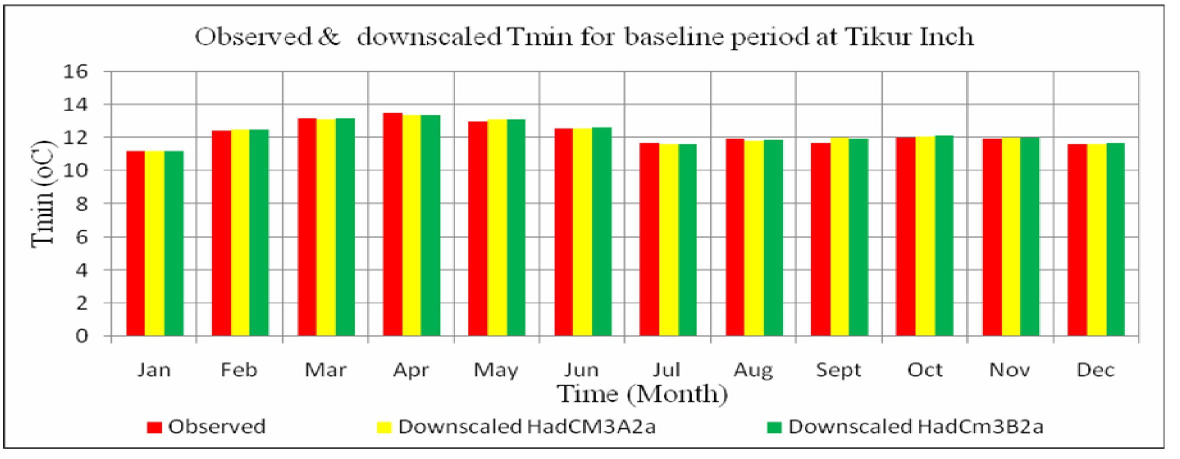

Figure 16 Observed and downscaled monthly mean Tmin for the baseline period

The variability of monthly minimum temperature of observed values is well preserved in the downscaled value for all months. For the months April, May, August and September the variance of observed value is slightly lower than the downscaled values but the general trend of both observed and downscaled values shows a similar pattern.

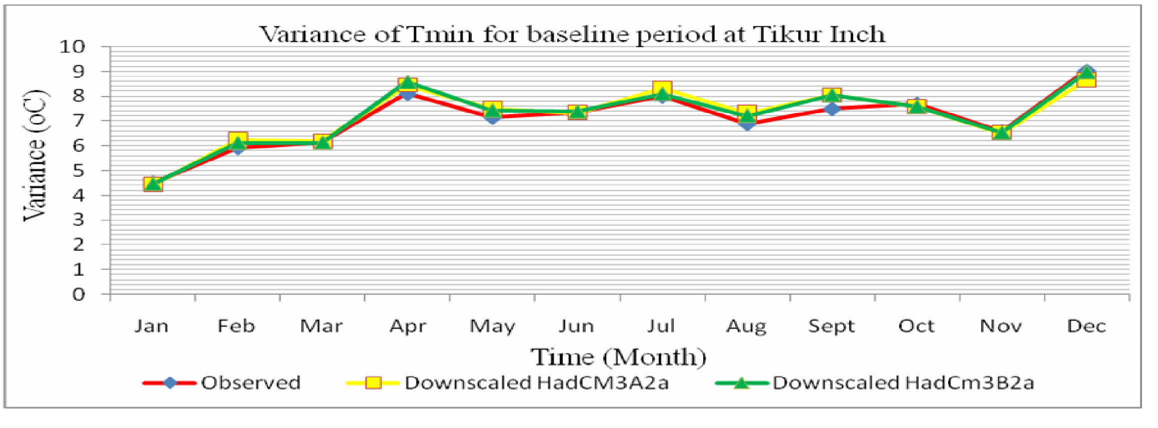

Figure 17 Variance of observed and downscaled Tmin for the baseline period

Maximum Temperature

The downscaled monthly mean maximum temperature reveals good quality relations with the observed temperature for the baseline period of both in A2a and B2a emission scenarios as shown Figure 18.

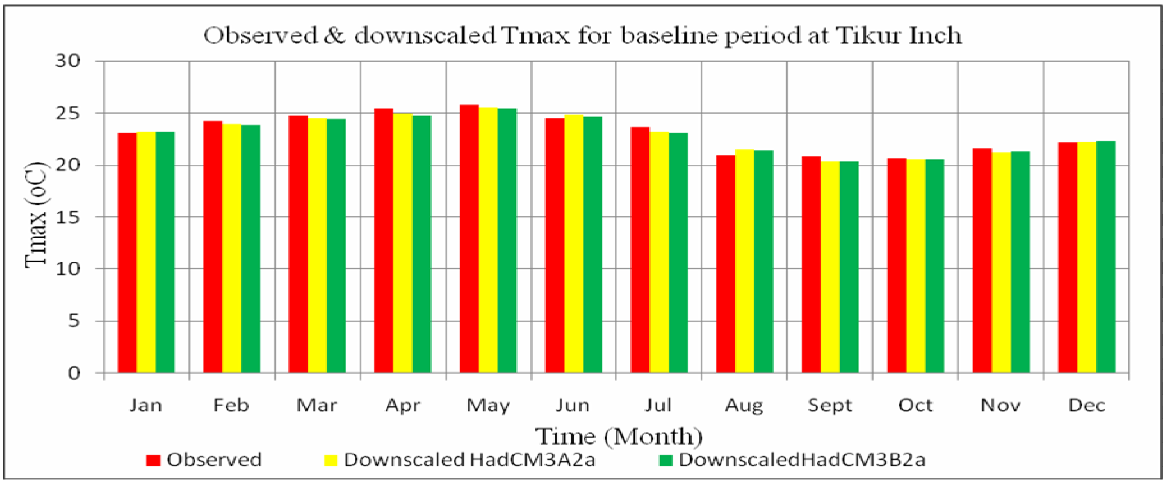

Figure 18 Observed and downscaled monthly mean Tmax for the baseline period

The variability of monthly maximum temperature of observed values is well preserved in the downscaled value but the variance of observed value is slightly lower than the down scaled values from August to November. The general trend of both observed and downscaled values shows a similar pattern.

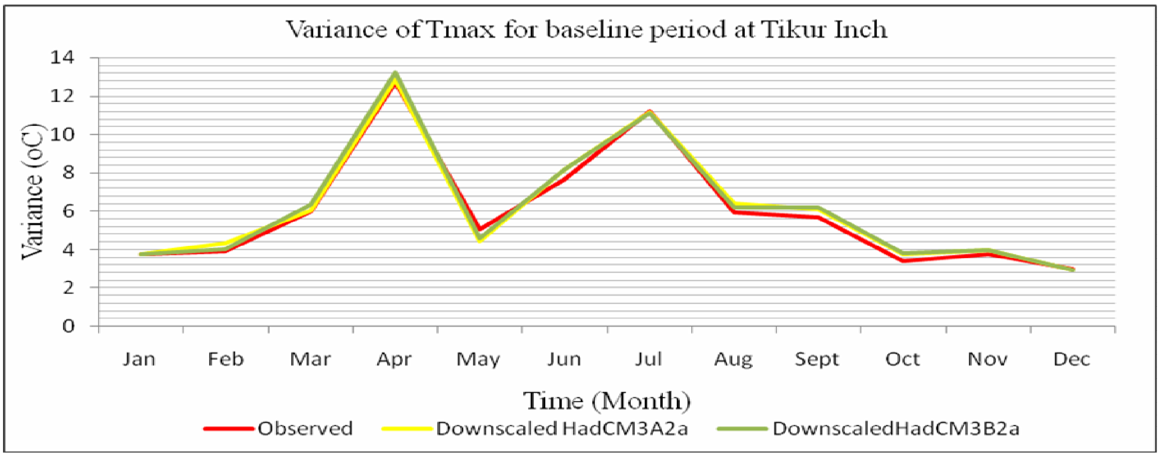

Figure 19 Variance of observed and downscaled Tmax for the base line period

Precipitation

The SDSM model performs reasonably well in estimating the mean monthly precipitation in many months but there is a relatively large model error in the month of February and September. The result, however, can be taken as satisfactory given the fact that precipitation downscaling is necessarily more problematic than temperature. The monthly precipitation downscaled for the baseline period is shown in Figure 20.

The variability of observed and downscaled precipitation shows good agreement in many months however, the variance of observed precipitation is higher than the downscaled value from September to November. Generally speaking the variance of observed and downscaled precipitation exhibits a similar pattern.

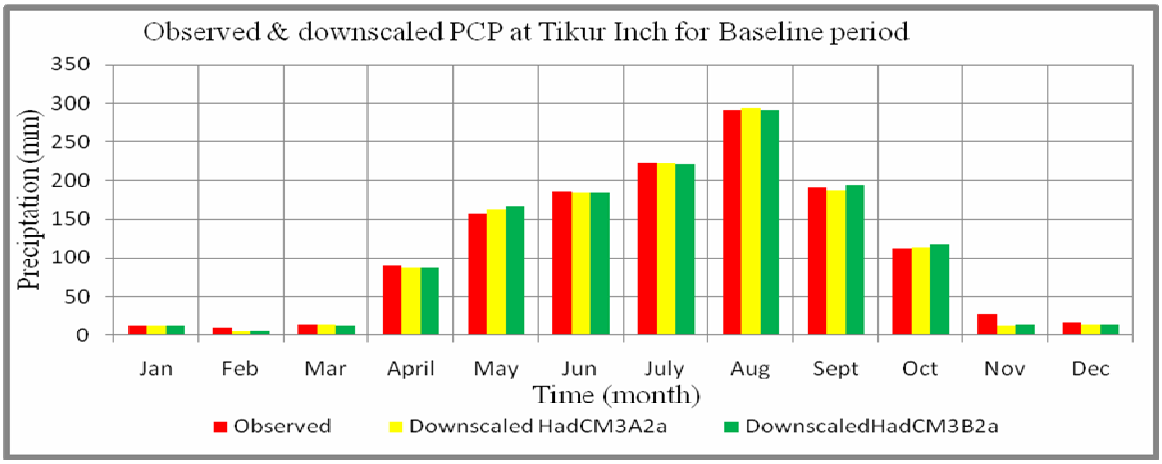

Figure 20 Mean monthly observed and downscaled precipitation for the baseline period

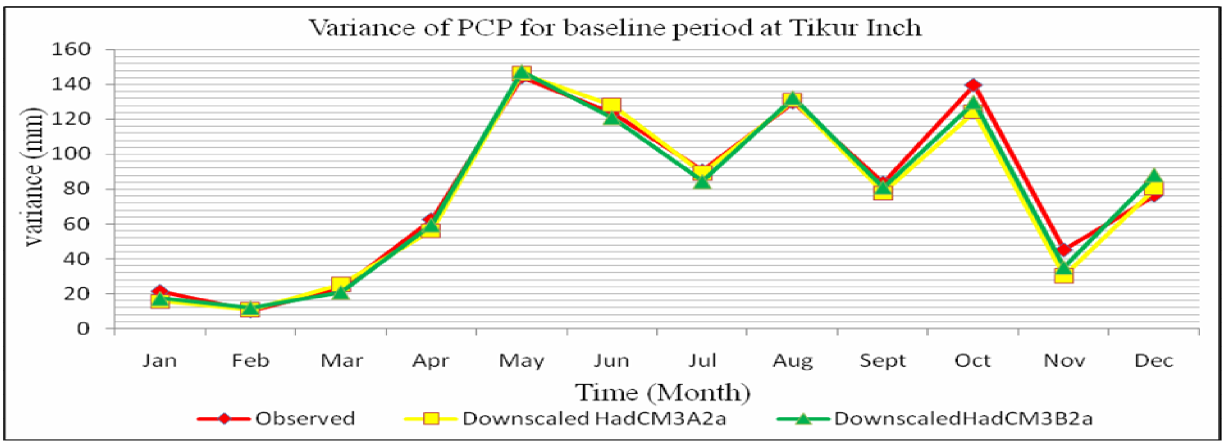

Figure 21 Variance of observed and downscaled precipitation for the baseline period

5.1.4 Downscaling the GCM for Future Scenario

The climate scenario for future period was developed from statistical downscaling using the GCM predictor variables for the two SRES emission scenarios (HadCM3A2a and HadCM3B2a) for 90 years based on the mean of 20 ensembles and the analysis was done based on three 30-year periods centered on the 2020s (2011-2040), 2050s (2041-2070) and 2080s (2071-2099). All the comparisons in the following analysis were done with respect to the baseline period (1980-2000) data at Gedo and Tikur Inch meteorological station.

Minimum temperature

For Gedo station the downscaled minimum temperature shows an increasing trend for all months in all future time horizons for both A2a and B2a emission scenarios. The average annual minimum temperature in 2020s will be increased by 1.5^{o}C and 1.35^{o}C for A2a and B2a emission scenario respectively. For the 2050s periods the average annual minimum temperature will be increased by 2.43^{o}C and 2.5^{o}C for A2a and B2a emission scenario respectively. For the 2080s periods the average annual minimum temperature will be increased by 3.9^{o}C and 3.8^{o}C for A2a and B2a emission scenario respectively.

Increasing minimum temperature showed more variation at the monthly time step with arrange from 0.5^{o}C to 2.6^{o}C in 2020s, 1.2^{o}C to 4.3^{o}C in 2050s and 2.4^{o}C to 5.5^{o}C in 2080s for both A2a and B2a emission scenario As comparing A2a and B2a emission scenarios the variations of minimum temperature for A2a emission scenario has more variation than the B2a emission scenario.

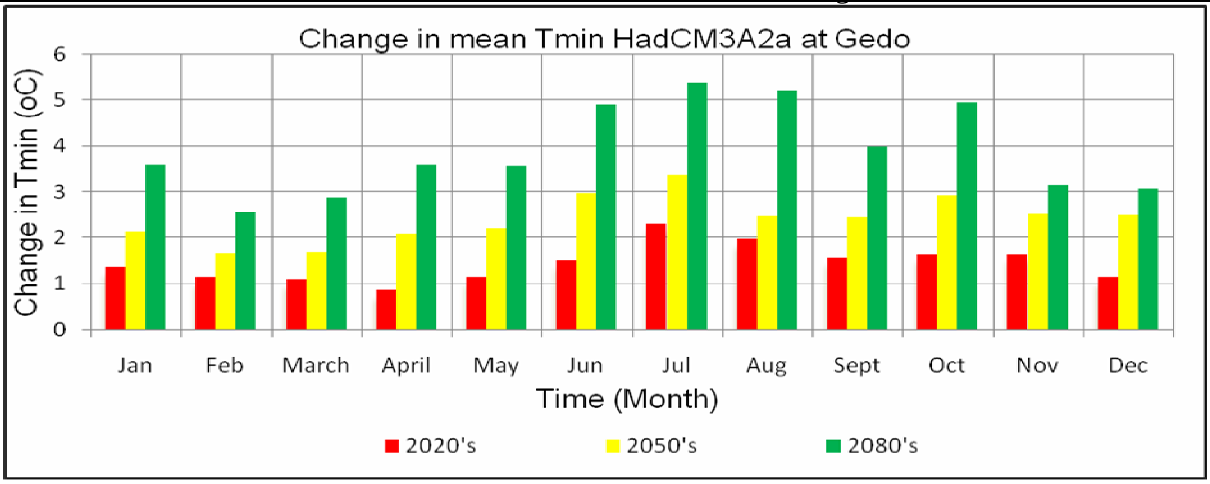

(a)

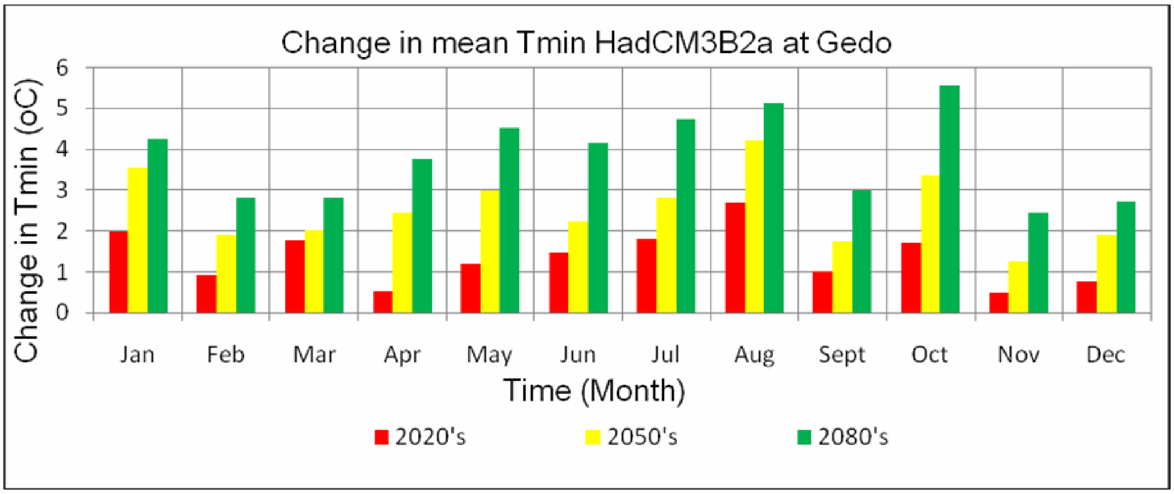

(b)

Figure 22 Change in Tmin(2011-2099) at Gedo, (a) & (b) for both scenarios

For Tikur Inch station the downscaled minimum temperature shows an increasing trend in all future time horizons for both A2a and B2a emission scenarios and the increase in A2a is higher than B2a emission scenarios. The average annual minimum temperature in 2020s will be increased by 1.28^{o}C and 1.17^{o}C for A2a and B2a emission scenario respectively. For the 2050s periods the average annual minimum temperature will be increased by 2.51^{o}C and 2.42^{o}C for A2a and B2a emission scenario respectively. For the 2080s periods the average annual minimum temperature will be increased by 3.52^{o}C and 3.43^{o}C for A2a and B2a emission scenario respectively.

Like Gedo the increasing minimum temperature at Tikur Inch shows more variation at the monthly time step with arrange from 0.6°C to 1.8°C in 2020s, 1.4°C to 3.5°C in 2050s and 2.4°C to 4.3°C in 2080s for both A2a and B2a emission scenario.

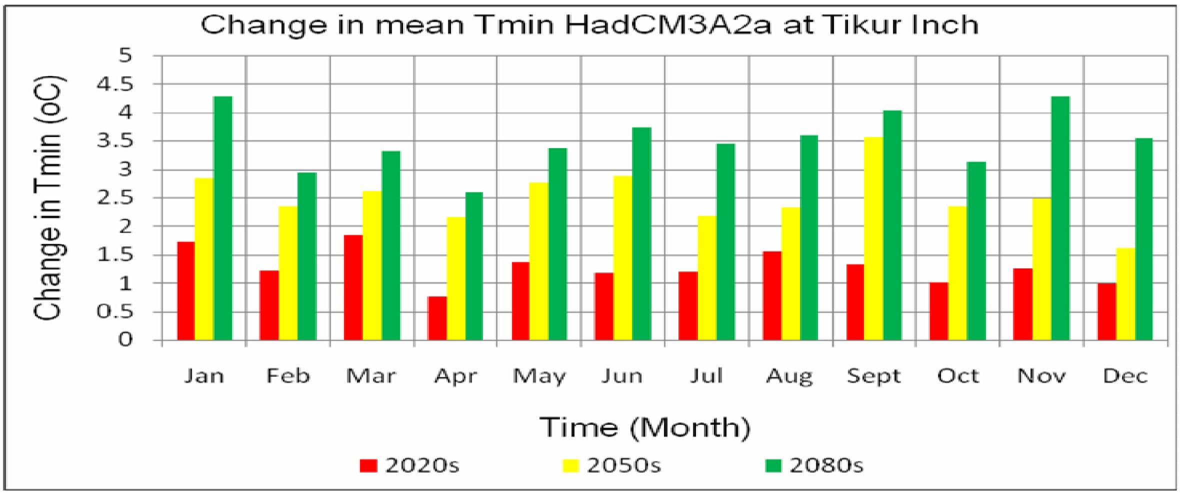

(a)

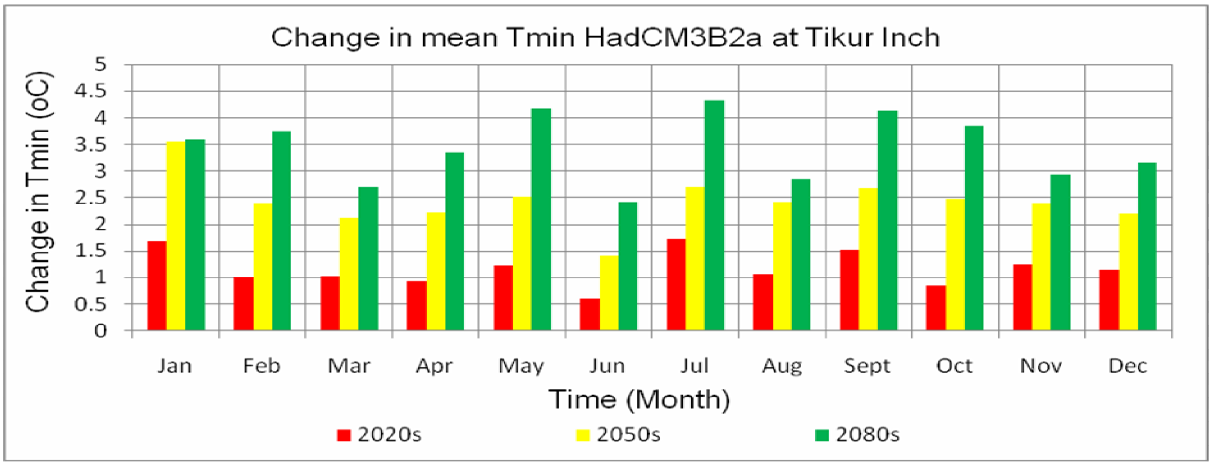

(b)

Figure 23 Change in Tmin(2011-2099) at Tikur Inch, (a) & (b) for both scenarios

Table 6 Monthly and Annual Tmin changes (^oC) under various scenarios

Gedo Tmin	Months with change in Tmin (^oC)												
Scenario	Jan	Feb	Mar	Apr	May	Jun	Jul	Aug	Sept	Oct	Nov	Dec	Annual
H3A2a 2020s	1.37	1.14	1.11	0.86	1.16	1.52	2.32	1.98	1.58	1.66	1.66	1.15	1.46
H3B2a2020s	1.99	0.91	1.77	0.53	1.19	1.45	1.79	2.67	1.02	1.70	0.47	0.76	1.35
H3A2a2050s	2.15	1.68	1.71	2.11	2.22	2.97	3.38	2.48	2.46	2.94	2.53	2.50	2.43
H3B2a2050s	3.55	1.90	2.01	2.43	3.00	2.22	2.81	4.19	1.75	3.36	1.24	1.88	2.53
H3A2a 2080s	3.59	2.57	2.89	3.59	3.56	4.92	5.38	5.23	4.00	4.96	3.17	3.06	3.91
H3B2a2080s	4.25	2.81	2.79	3.76	4.50	4.14	4.72	5.11	2.99	5.56	2.45	2.72	3.82
Tikur Inch Tmin	Months with change in Tmin (oC)												
Scenario	Jan	Feb	Mar	Apr	May	Jun	Jul	Aug	Sept	Oct	Nov	Dec	Annual
H3A2a 2020s	1.72	1.21	1.83	0.75	1.37	1.17	1.20	1.56	1.32	1.01	1.24	0.99	1.28
H3B2a2020s	1.68	1.01	1.04	0.94	1.23	0.61	1.72	1.07	1.52	0.86	1.26	1.16	1.17
H3A2a2050s	2.84	2.35	2.62	2.17	2.76	2.88	2.18	2.33	3.55	2.35	2.48	1.62	2.51
H3B2a2050s	3.56	2.40	2.12	2.22	2.52	1.41	2.69	2.42	2.67	2.48	2.41	2.21	2.43
H3A2a 2080s	4.29	2.94	3.31	2.59	3.37	3.73	3.44	3.60	4.03	3.13	4.28	3.53	3.52
H3B2a2080s	3.60	3.74	2.69	3.36	4.17	2.41	4.33	2.85	4.13	3.84	2.93	3.16	3.44

Maximum Temperature

For Gedo station the overall analysis (2011-2099) of maximum temperature showed that there may be increasing trends in both emission scenarios (A2a and B2a). The average annual maximum temperature in 2020s will be increased by 1.55^{o}C and 1.45^{o}C for A2a and B2a emission scenario respectively. For the 2050s periods the average annual maximum temperature will be increased by 2.76^{o}C and 2.63^{o}C for A2a and B2a emission scenario respectively. For the 2080s periods the average annual maximum temperature will be increased by 4.22^{o}C and 3.94^{o}C for A2a and B2a emission scenario respectively. Increasing maximum temperature showed more variation at the monthly time step with arrange from 0.8^{o}C to 2.2^{o}C in 2020s, 2.1^{o}C to 3.9^{o}C in 2050s and 2.9^{o}C to 5.1^{o}C in 2080s for both A2a and B2a emissions scenarios.

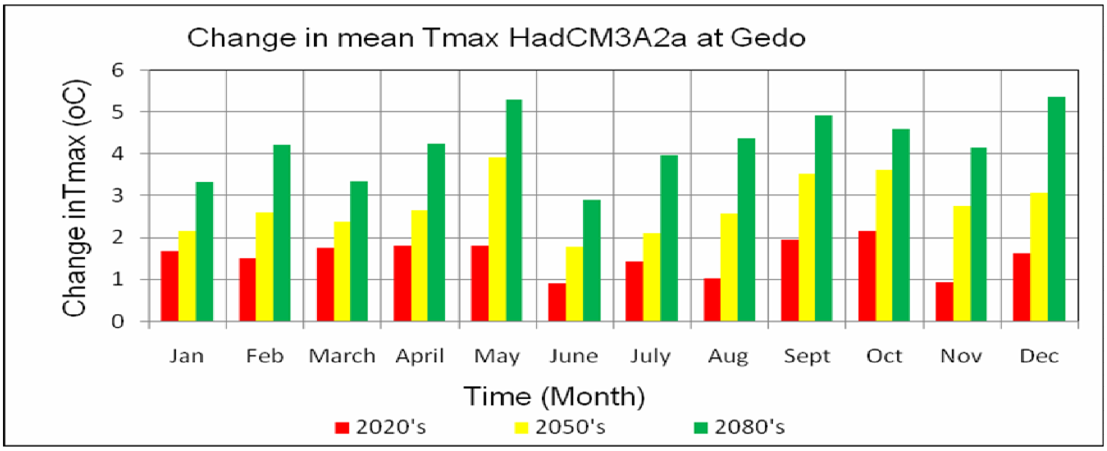

(a)

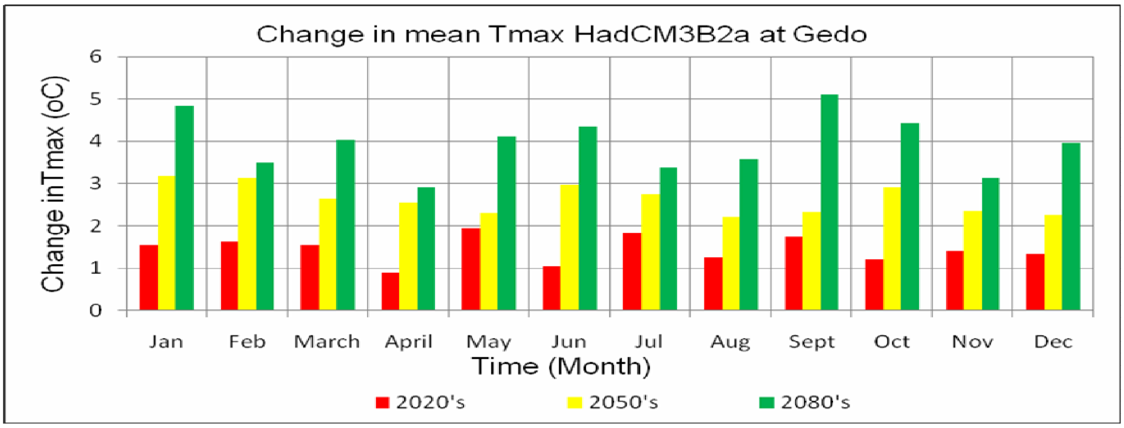

(b)

Figure 24 Change in Tmax (2011-2099) at Gedo, (a) & (b) for both scenarios

For Tikur inch station the overall analysis (2011-2099) of maximum temperature showed that there may be an increasing trend for both emission scenarios (A2a and B2a). The average annual maximum temperature in 2020s will be increased by 1.565^{o}C and 1.416^{o}C for A2a and B2a emission scenario respectively. For the 2050s periods the average annual maximum temperature will be increased by 2.71^{o}C and 2.63^{o}C for A2a and B2a emission scenario respectively. For the 2080s periods the average annual maximum temperature will be increased by 4.1^{o}C and 3.8^{o}C for A2a and B2a emission scenario respectively. Increasing maximum temperature showed more variation at the monthly time step with a range from 0.9^{o}C to 2.06^{o}C in 2020s, 2.4^{o}C to 3.3^{o}C in 2050s and 2.9^{o}C to 4.7^{o}C in 2080s for both A2a and B2a emission scenario.

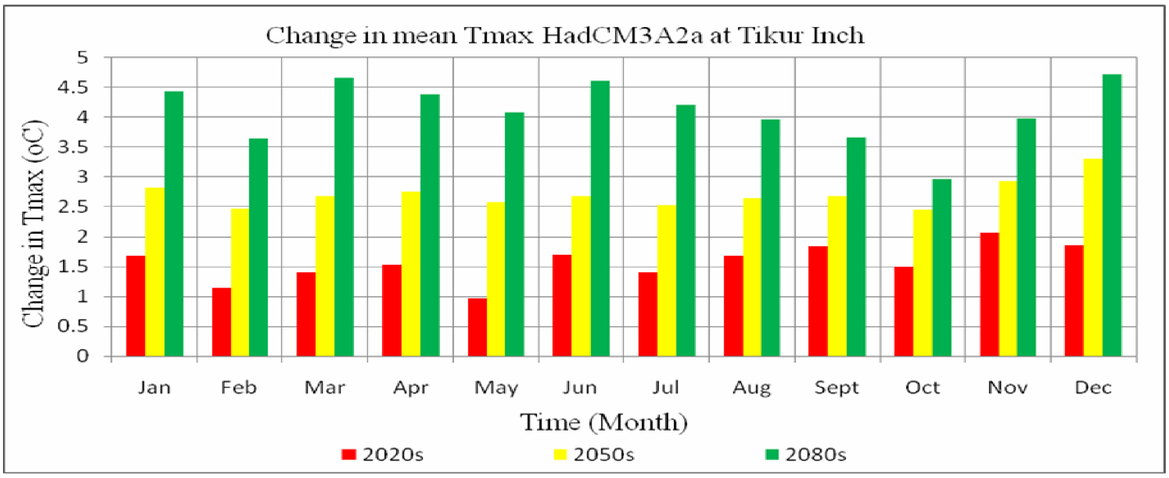

(a)

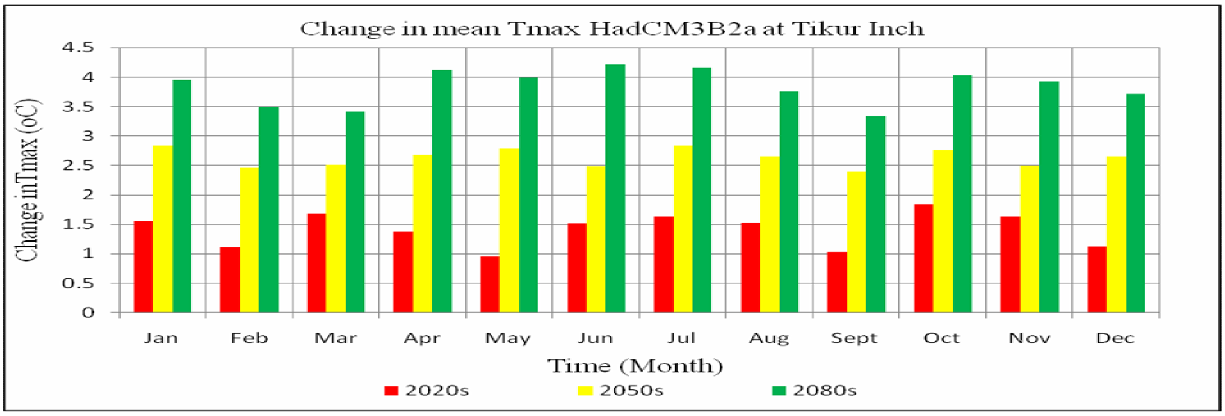

(b)

Figure 25 Change in Tmax (2011-2099) at Tikur Inch, (a) & (b) for both scenarios

Generally as compared for both Gedo and Tikur Inch minimum and maximum temperature downscaling, the increment for A2a scenario is greater than B2a scenario because A2a scenario represents a medium high emission scenario which produces more CO_2 concentration than the B2a emission scenario which represents a medium low emission scenario.

Table 7 Monthly and Annual Tmax changes (°C) under various scenarios

Gedo Tmax	Months with change in Tmax (°C)												
Scenario	Jan	Feb	Mar	Apr	May	Jun	Jul	Aug	Sept	Oct	Nov	Dec	Annual
H3A2a 2020s	1.69	1.52	1.75	1.81	1.80	0.92	1.43	1.03	1.96	2.17	0.93	1.64	1.55
H3B2a2020s	1.54	1.63	1.55	0.89	1.95	1.06	1.84	1.25	1.75	1.20	1.42	1.34	1.45
H3A2a2050s	2.15	2.60	2.38	2.65	3.91	1.79	2.10	2.58	3.53	3.61	2.74	3.08	2.76
H3B2a2050s	3.18	3.14	2.64	2.55	2.31	2.97	2.76	2.22	2.32	2.91	2.34	2.26	2.63
H3A2a 2080s	3.33	4.21	3.35	4.25	5.29	2.90	3.97	4.38	4.91	4.60	4.13	5.35	4.22
H3B2a2080s	4.84	3.49	4.02	2.92	4.12	4.34	3.39	3.58	5.11	4.44	3.15	3.96	3.95
Tikur Inch Tmax	Months with change in Tmax (°C)												
Scenario	Jan	Feb	Mar	Apr	May	Jun	Jul	Aug	Sept	Oct	Nov	Dec	Annual
H3A2a 2020s	1.67	1.14	1.41	1.53	0.98	1.70	1.41	1.68	1.84	1.50	2.07	1.86	1.57
H3B2a2020s	1.56	1.12	1.69	1.37	0.96	1.51	1.64	1.53	1.03	1.84	1.63	1.13	1.42
H3A2a2050s	2.82	2.46	2.67	2.76	2.58	2.68	2.53	2.64	2.67	2.46	2.94	3.31	2.71
H3B2a2050s	2.84	2.45	2.52	2.68	2.78	2.49	2.83	2.66	2.40	2.75	2.50	2.65	2.63
H3A2a 2080s	4.43	3.65	4.66	4.38	4.08	4.61	4.21	3.97	3.66	2.97	3.99	4.73	4.11
H3B2a2080s	3.95	3.49	3.41	4.12	3.99	4.22	4.16	3.76	3.33	4.03	3.93	3.71	3.84

Precipitation

For Gedo station the precipitation projection exhibited an increase in average mean precipitation in periods (2020s, 2050s and 2080s). As can be shown in Figure 26 (a) and (b) below, in all periods there may be a decrease in precipitation for months September & October and increase in all other months for both emission scenarios (A2a and B2a). The overall effect in 2020s may be an increase of average annual precipitation by 15.35% in the A2a scenario and 18.11% in the B2a scenario. In 2020s, the maximum monthly average precipitation observed in December which is increase up to 3.058% & 4.87% in both A2a & B2a emission scenarios respectively. The overall effect in 2050s may be an increase of average annual precipitation by 18.067% in the A2a scenario and 23.995% in the B2a scenario. In 2050s, the increase in monthly average precipitation may reach up to 5.369% for December in the A2a scenario and 7.701% for November in the B2a scenario.

In 2080s the A2a and B2a scenarios showed an increase in average annual precipitation amount by 16.414% and 23.063% respectively. In the 2080s, the decrease in monthly average precipitation may reach up to 1.995% for October in the A2a scenario and 3.23% for September in the B2a scenario.

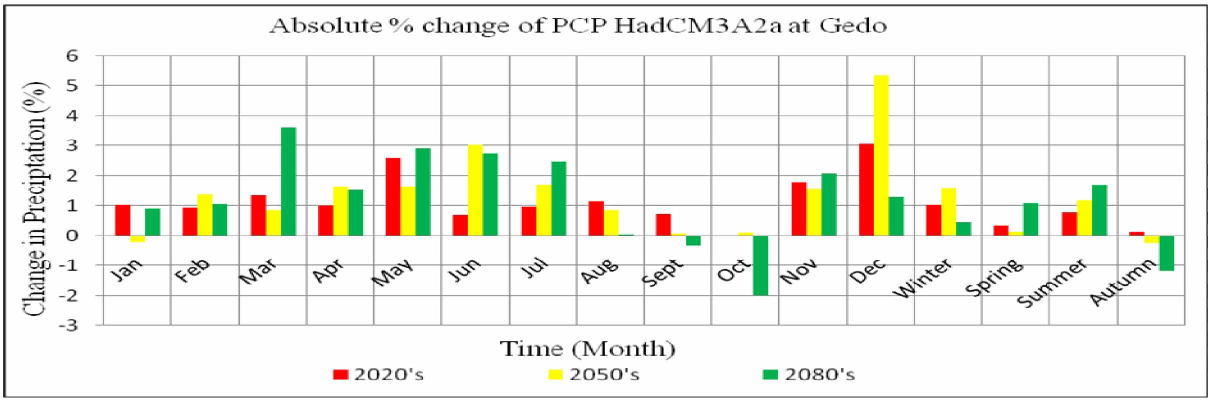

(a)

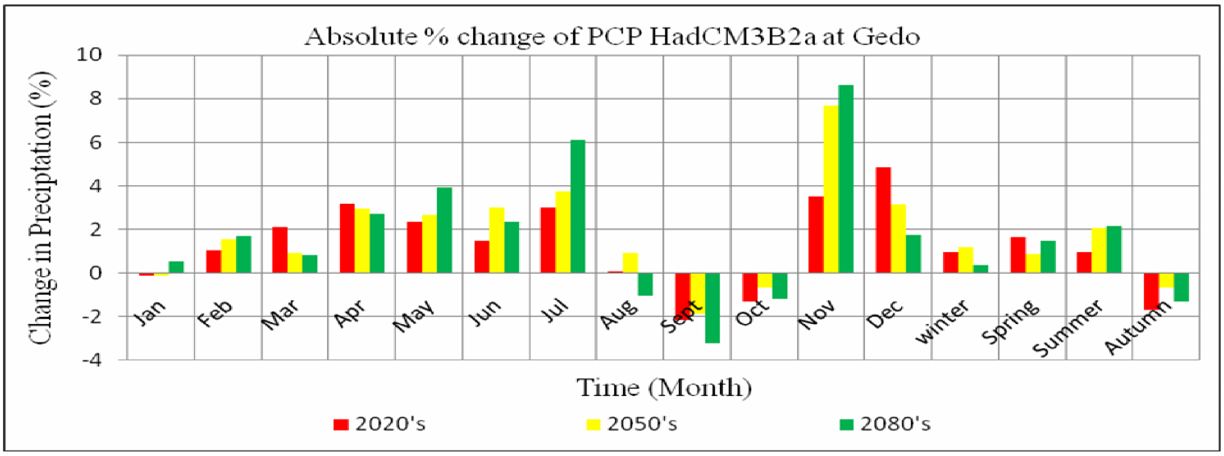

(b)

Figure 26 Absolute percentage change of precipitation at Gedo, (a) & (b) for both scenarios

For Tikur Inch the precipitation projection exhibited an increase in annual average precipitation in all periods (2020s, 2050s and 2080s). In 2020s, the A2a scenario showed average monthly precipitation increase up to 37.296% in the month of November and B2a showed an increase up to 15.813% in the month of January. The overall effect in 2050s may be an increase of average annual precipitation by 11.995% in the A2a scenario and 20.643% in the B2a scenario. In 2050s, the increase in monthly average precipitation may reach up to 42.529% for January in the A2a scenario and 24.204% for November in the B2a scenario.

In 2080s the A2a and B2a scenarios showed an increase in average annual precipitation amount by 17.302% and 20.103% respectively. In the 2080s, the increase in monthly average precipitation may reach up to 68.916% for January in the A2a scenario and 27.686% for September in the B2a scenario.

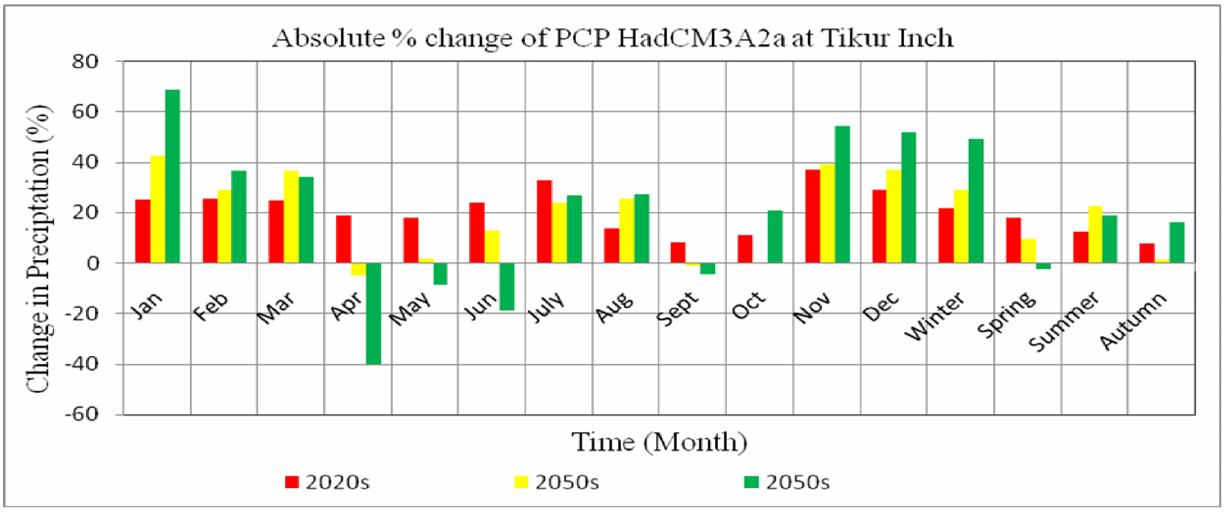

(a)

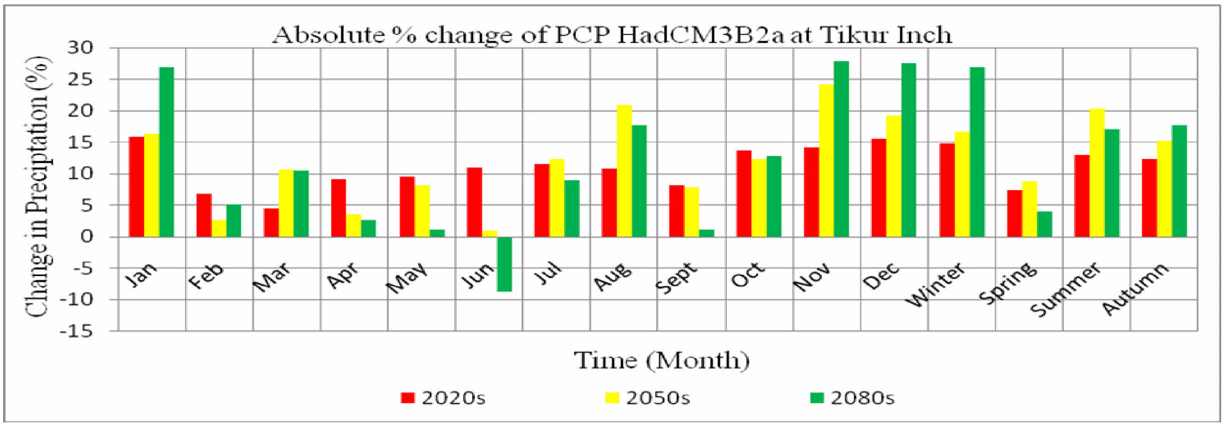

(b)

Figure 27 Absolute percentage change of precipitation at Tikur Inch, (a) & (b) for both Scenarios

For Gedo the variation of projected precipitation using A2a and B2a emission scenarios is not clearly identifiable. At Tikur Inch the variation of precipitation is higher in A2a emission scenario as compared with B2a emission scenario for all time horizons.

Table 8 Annual and monthly precipitation changes (%) under various scenarios

Gedo PCP	Months with change in PCP (%)												
Scenario	Jan	Feb	Mar	Apr	May	Jun	Jul	Aug	Sept	Oct	Nov	Dec	Annual
H3A2a 2020s	1.03	0.94	1.35	0.99	2.61	0.70	0.99	1.15	0.71	0.02	1.78	3.06	15.35
H3B2a2020s	-0.10	1.05	2.14	3.21	2.35	1.47	3.01	0.08	-2.15	-1.33	3.53	4.87	18.11
H3A2a2050s	-0.20	1.40	0.86	1.66	1.66	3.03	1.71	0.87	0.07	0.10	1.56	5.37	18.67
H3B2a2050s	-0.09	1.58	0.91	2.98	2.66	2.99	3.74	0.92	-1.87	-0.67	7.70	3.15	24.00
H3A2a 2080s	0.53	1.70	0.82	2.74	3.92	2.37	6.11	-1.05	-3.23	-1.17	8.59	1.73	16.40
H3B2a2080s	0.53	1.70	0.82	2.74	3.92	2.37	6.11	-1.05	-3.23	-1.17	8.59	1.73	23.06
Tikur Inch PCP	Months with change in PCP (%)												
Scenario	Jan	Feb	Mar	Apr	May	Jun	Jul	Aug	Sept	Oct	Nov	Dec	Annual
H3A2a 2020s	25.20	25.88	24.77	18.94	17.99	23.86	33.02	13.68	8.20	11.20	37.30	28.94	16.65
H3B2a2020s	15.81	6.88	4.48	9.16	9.51	10.99	11.63	10.75	8.13	13.80	14.26	15.59	14.00
H3A2a2050s	42.53	29.19	36.58	-4.64	1.87	13.11	23.81	25.76	-0.94	0.26	39.41	37.19	12.00
H3B2a2050s	16.27	2.68	10.58	3.64	8.15	1.00	12.31	20.91	7.82	12.29	24.20	19.18	20.60
H3A2a 2080s	68.92	36.67	34.11	-39.86	-8.57	-18.85	26.89	27.41	-4.61	20.89	54.60	52.18	17.30
H3B2a2080s	26.91	5.09	10.45	2.71	1.13	-8.76	8.89	17.76	1.20	12.81	27.87	27.61	20.10

5.2 SWAT Model Results

5.2.1 Calibration and Uncertainty Analysis

The SWAT model was calibrated (manually and automatically) and validated using measured daily stream flow data collected at the four gauged stations. The total available historical stream flow data (1990-2000) were divided into two sets: 6years (1991-1996) for calibration (1990 was assumed to be an initialization year) and 4 years for validation (1997-2000) for all stations. The sub-basin watersheds characteristics, including land use, and soil properties were held constant throughout the simulation period. The initial values of each calibration parameter were generated by Arc SWAT during sensitivity analysis.

Sensitivity analysis was carried out for the calibration and warming up periods for all the four hydrological gauged stations. A total of 27 parameters with 270 iterations were done at each gauged station to select the rank of these parameters. Van Griensven *et al*., (2006), characterize Global rank 1 as "very important", rank 2 to 6 as 'important", rank 7 to 19 as "slightly important" and rank 27 as "not important". Appendix C shows the relative sensitivity (rank) of parameters with respect to the four gauged stations.

The parameters were allowed to vary during the calibration process within acceptable ranges across the basin until an acceptable fit between the measured and simulated values was obtained at each watershed outlet; no changes were made to the calibrated parameters during the 4-year validation simulation. Hydrologic calibration parameters and their values for the four Guder Sub-basin gauged stations are shown in Table 9.

Table 9 Hydrologic calibration parameters values with their global average

S.No	Hydrological parameters	Calibrated parameter values for gauged stations			
		Guder	Indris	Debis	Fatto
1	GWQMN	30.00	90.00	90.00	30.00
2	CN2	35.00	35.00	40.00	45.00
3	ALPHA_BF	0.15	1.00	0.90	0.30
4	Esco	0.10	0.02	0.15	0.08
5	REVAPMN	0.50	60.00	60.00	10.00
6	Sol-Awc	0.26	0.16	0.38	0.09
7	GW_REVAP	0.16	0.18	0.02	0.20
8	CH_K2	100.00	80.00	110.00	50.00
9	GW_DELAY	10.00	10.00	20.00	80.00
10	Surlag	1.01	1.16	1.15	1.04

The calibration and validation results for all gauged stations in Table 10 show that there is a good agreement between the daily simulated and observed flows. The calibration and validation is demonstrated by the coefficient of determination (R^2) and Nash-Sutcliffe simulation efficiency (E_{NS}) values. Both values for the four gauged stations fulfilled the requirement of $R^2 > 0.6$ and $E_{NS} > 0.5$, which is recommended by (Santhi et al., 2001).

S.NO	Station Name	During Calibration		During Validation		Uncertainty Analysis	
		R^2	E_{NS}	R^2	E_{NS}	P-factor	R-factor
1	Guder	0.73	0.73	0.80	0.79	0.90	1.2
2	Indris	0.69	0.68	0.74	0.73	0.87	1.4
3	Debis	0.71	0.69	0.76	0.74	0.83	1.56
4	Fatto	0.65	0.65	0.76	0.75	0.88	1.3

Table 10 *Calibration & validation with uncertainty analysis results* for *Guder gauged station*

Uncertainty analysis was done using SWAT-CUP linked to GLUE on measured stream flow data. The degree to which all uncertainties are accounted for is quantified by a measure referred to as the *P-factor*, which is the percentage of measured data bracketed by the 95% prediction uncertainty (95PPU) and another measure quantifying the strength of a calibration/uncertainty analysis is the *R-factor*, which is the average thickness of the 95PPU band divided by the standard deviation of the measured data. The results of the four hydrological gauged stations of P-factor and R-factor for daily discharge are shown in Table 10.

For example Guder @ Guder gauging stations daily discharge, 90% of the observed data is bracketed by the 95PPU (*P-factor*) and the thickness of the 95PPU (R-factor) had a value of 1.2, which is a good result. The smaller R-factor value, the smaller the uncertainties and the better is the calibration work. A value close to 1 is highly desirable for *R-factor* with a *P-factor* also close to 1.

As seen from the calibration and the validation results, it is deduced that the model represented the hydrological characteristics of the watershed at each gauging stations and used for as a base line for further analysis.

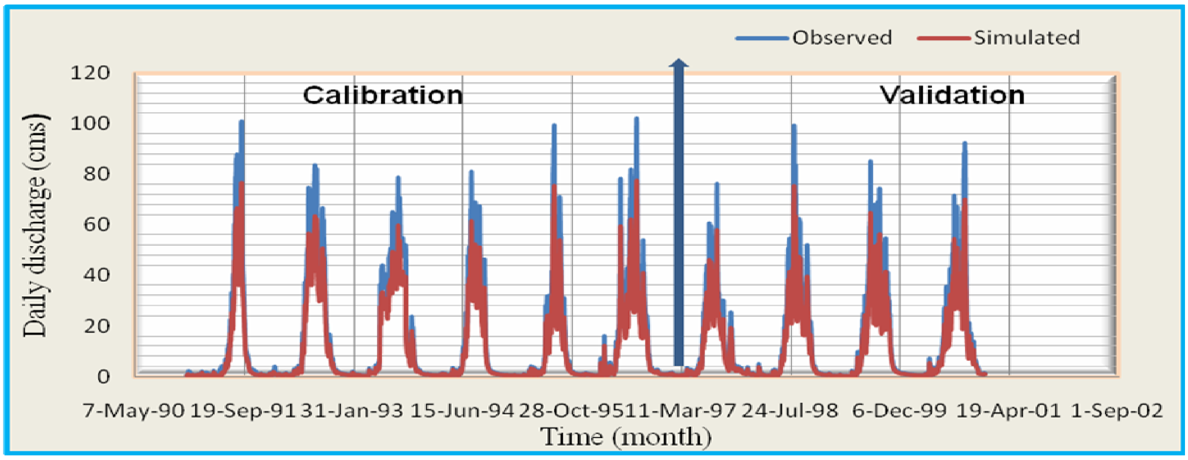

Figure 28 Observed and simulated flow hydrograph for calibration & validation at Guder

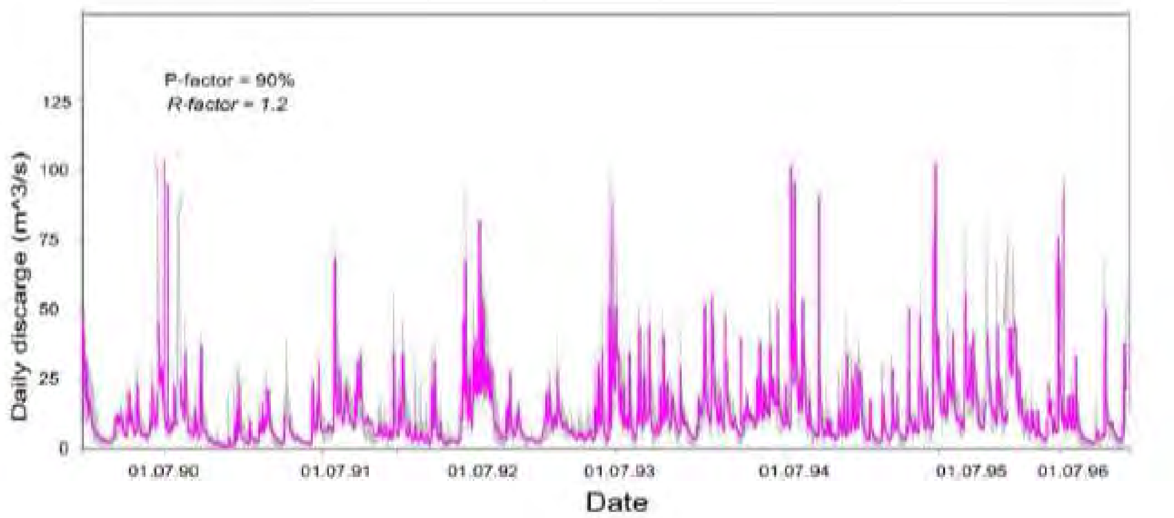

Figure 29 Simulated and observed daily discharge Guder @ Guder during calibration

5.2.2 Climate Change Impact on the Flow Volume

5.2.2.1 Climate Change Impact on Monthly Flow Volume

Climate change impact on monthly flow volume was analyzed by comparing baseline river flow with the future flows for the 2020s, 2050s and 2080s. In the 2020s for the A2a scenario, the flow volume may show an increase for all the months. In this period an increase up to 55% in monthly flow volume may be expected. Increase in flow volume may be observed in months which showed an increase in monthly precipitation. In the 2020s for B2a scenario, the same effect as the A2a scenario of 2020s may be observed. But the increase in monthly flow volume is expected to reach up to 56%.

In 2050s for both A2a & B2a scenarios, the increase in precipitation is reflected in an increase in flow volume. For A2a scenario the monthly variation of change in precipitation is between 5% and 49%. And also for B2a emission scenario the monthly variation of change in precipitation is between 2% and 57%.

In 2080s for the A2a and B2a emissions scenarios an increase in flow volume observed in all months. For A2a scenario the monthly variation of change in precipitation is between 2% and 58%. And also for B2a emission scenario the monthly variation of change in precipitation is between 4% and 59%.

Table 11 Monthly flow volume changes (%) under various scenarios

Scenario	Change in monthly flow volume (%)											
	Jan	Feb	Mar	Apr	May	Jun	Jul	Aug	Sept	Oct	Nov	Dec
H3A2a2020s	24	13	7	12	10	43	19	24	55	44	6	21
H3B2a2020s	25	14	8	13	13	41	23	30	56	47	20	17
H3A2a2050s	41	46	17	42	42	33	22	49	44	5	26	29
H3B2a2050s	48	40	15	52	57	26	6	26	38	2	31	43
H3A2a2080s	58	50	2	18	53	21	32	38	16	23	12	44
H3B2a2080s	59	57	4	15	46	18	27	49	16	24	6	40

As shown from Table 11 the percentage change in monthly flow volume at Upper Guder Catchment there is no much significant variation as comparing A2a and B2a SRES emission scenarios.

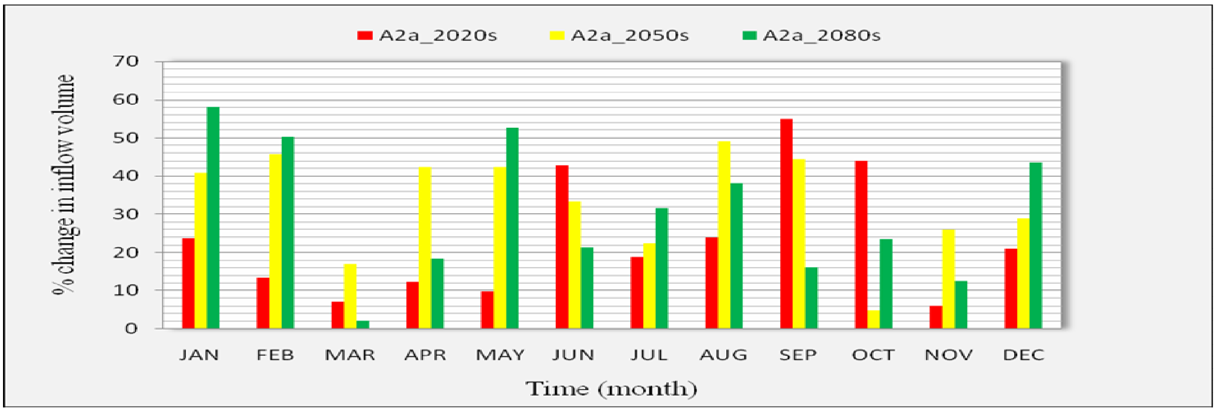

Figure 30 Monthly percentage change in flow volume for the A2a scenario

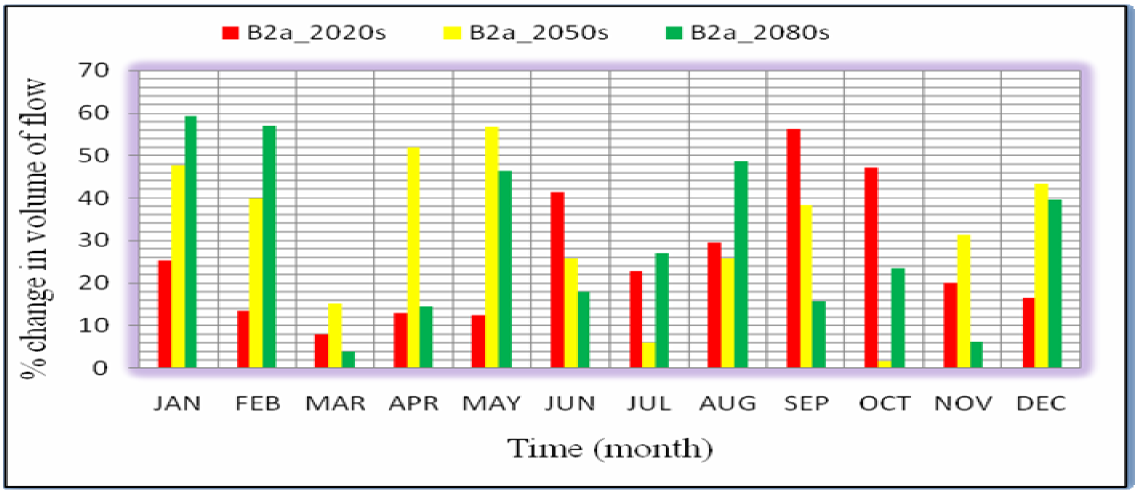

Figure 31 Monthly percentage change in flow volume for the B2a scenario

5.2.2.2 Climate Change Impact on Seasonal and Annual Flow Volume

The impacts of climate change on the seasonal and annual flow volume are discussed so as to foresee its consequence on the socio-economic condition on Upper Guder Catchment. As discussed in the previous chapter, there are four seasons in the study area: Kiremt (June to August), Belg (March to May), Tsedey (September to November) and Bega (December to February).

For both A2a and B2a scenarios, there may be average annual increase in flow volume for the next 90 years up to 35%. Kiremt season shows an increase in flow volume, the increasing ranges from 19% to 51% for the A2a scenario and 18% to 52% for the B2a scenario .In Belg and Tsedey seasons the flow volume may increases for both scenarios up to 41%. In the Kiremt season the flow volume may increase in both scenarios for all time horizons up to 35%. Also in Bega season both scenarios show that there might be an increase in flow volume up to 52%. Table 12 and Figure 31 & 32 show that Annual and Seasonal percentage change of flow volume under various scenarios.

Table 12 Annual and Seasonal flow volume changes (%) under various scenarios

Scenario	Change in Annual and Seasonal flow volume (%)				
	Bega	Belg	Kiremt	Tsedey	Annual
H3A2a 2020s	19	10	28	35	23
H3B2a2020s	18	11	31	41	26
H3A2a2050s	38	34	35	25	33
H3B2a2050s	44	41	19	24	32
H3A2a2080s	51	24	30	17	35
H3B2a2080s	52	22	31	15	30

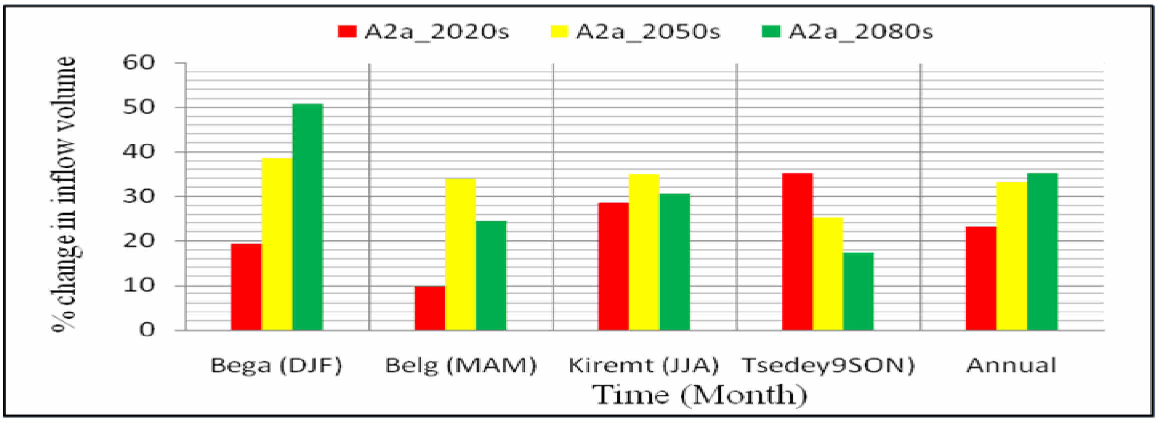

Figure 32 Percentage change in seasonal and annual flow volume for A2a scenario

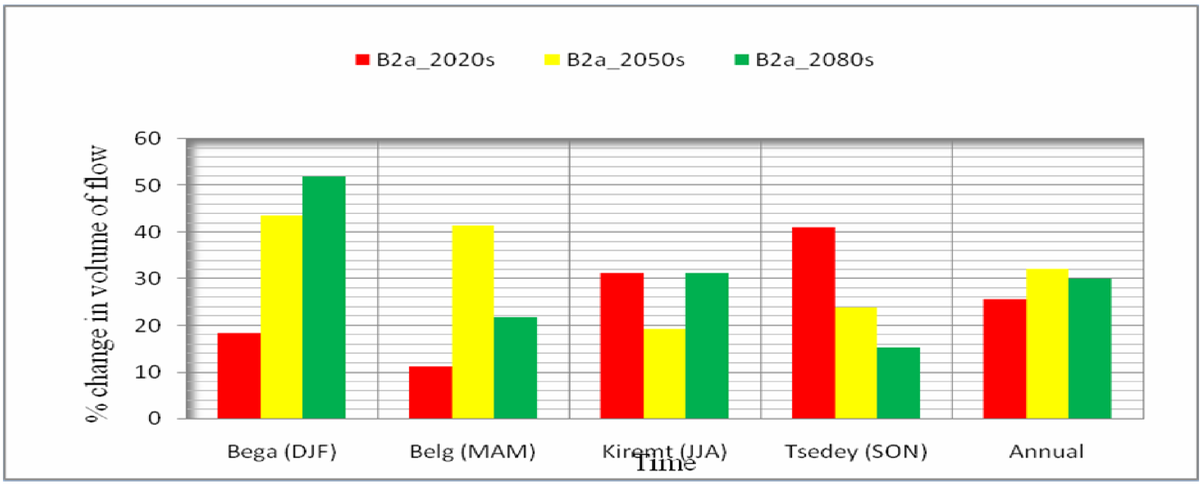

Figure 33 Percentage change in seasonal and annual flow volume B2a scenario

5.2.3 Sensitivity of Evapotranspiration to Climate Change

Evapotranspiration rates are controlled by several variables including the available water and energy. A temperature increase leads to higher energy available for evapotranspiration. Although a warmer atmosphere can hold more water, the actual changes in evapotranspiration will depend on the humidity levels and the wind patterns. Due to data limitations the Hargreaves method is used in this study to calculate potential evapotranspiration that depends on minimum and maximum temperatures. Daily baseline temperature (1990-2000) and future temperature simulated by GCM out of SRES A2a and B2a emission scenarios downscaled with SDSM was used to obtain potential evapotranspiration using SWAT Hydrological model. The simulations for the Upper Guder catchment suggest that annual estimates of potential evapotranspiration are predicted to increase with increase in temperature. The projected on average annual increase in potential evapotranspiration is 3 - 15% for the 2020s and 7 - 25% for the 2050s and 2080s for both A2a and B2a emissions scenarios with respect to the baseline period (1990-2000).

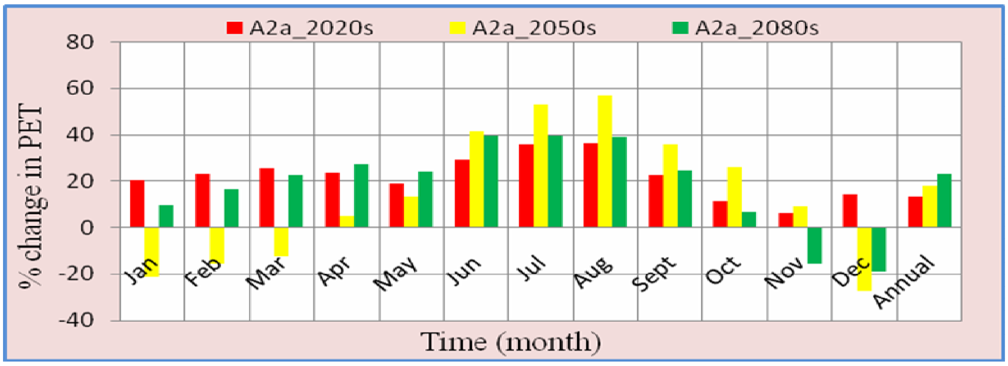

(a)

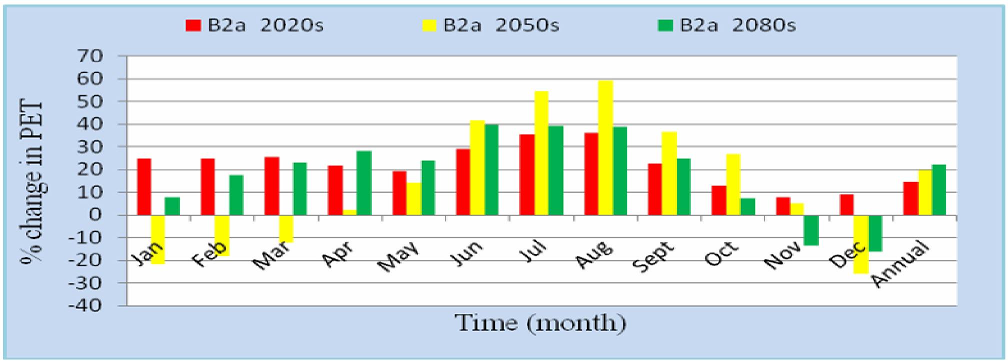

(b)

Figure 34 Percentage change in monthly and annual Potential Evapotranspiration (a&b)

5.2.4 Uncertainties in the Study

There are various sources of uncertainties in hydrological climate change impact assessment works. The uncertainties for this study results from GCM outputs, as a result of the downscaling approach and hydrological model development.

For estimates based on downscaling of General Circulation Models (GCMs) outputs, different levels of uncertainties occurred due to: scenario uncertainty and their conversion into atmospheric concentrations (IPCC 2007; IPCC-TGICA 2007). Climate scenarios have many unknowns and uncertainties originate in the assumptions, the methodology and the understanding underlying the scenarios. Insufficient knowledge, a lack of understanding of the scientific principles and processes involved, and difficulties in reproducing these physical processes through simulations with computer-based tools, all add to the uncertainty inherent in the scenarios. Other uncertainties in the future projections of climate generally stem from uncertainties in defining the factors (e.g. population growth, economic growth and development, energy use, control measures, transfer of clean technology to developing countries) that affect future emissions scenarios. Converting these emissions to atmospheric concentrations of the relevant greenhouse gases is also problematic.

There are uncertainties related to the data used for downscaling model. Despite appropriate data checking and filling missing values was done using the weather generator component of the SDSM before the analysis, certain level of error was introduced at this stage. Besides the SDSM model prediction assumes that the relationship developed between the predictands and predictors at recorded climatic conditions will hold the same in the future. However, this assumption may not be true. The SDSM technique used in this study needed the screening of weather parameters (predictors). Finding good predictors-predictand correlation was a core part of the downscaling process. However, even after several trial and errors, the correlation coefficients found were very small especially for the precipitation predictand variable as precipitation is problematic due to its conditional nature. So precipitation is one of the main inputs of the SWAT model it will result in uncertainty in the estimations of flow volumes in the future. The assumptions involved in the hydrologic model simulation for future are also a portion of the uncertainty.
Any or all of the above uncertainties may cause the results to deviate from reality. Hence great care should be taken in interpreting the result by taking into account all these uncertainties.

6 CONCLUSION AND RECOMMENDATION

6.1 Conclusion

In this study, the impact of climate change on the hydrology of Guder sub-basin were assessed based on projected climate conditions by using GCM out puts of HadCM3 SRES A2a and B2a emissions scenarios with Statistical Downscaling (SDSM) modeling approach, a complex physically based semi distributed hydrologic model (SWAT) and SWAT-CUP linked to GLUE.

For both Gedo and Tikur Inch stations the downscaled minimum temperature shows an increasing trend for all future time horizons for both A2a and B2a emission scenarios. At Gedo the average annual minimum temperature will be increased in 2020s by 1.5^{o}C and 1.35^{o}C, in 2050s by 2.43^{o}C and 2.5^{o}C and in 2080s by 3.9^{o}C and 3.8^{o}C for A2a and B2a emission scenario respectively. Also at Tikur Inch the average annual minimum temperature will be increased in 2020s by 1.28^{o}C and 1.17^{o}C, in 2050s by 2.51^{o}C and 2.42^{o}C and in 2080s by 3.52^{o}C and 3.43^{o}C for A2a and B2a emission scenario respectively.

For both Gedo and Tikur Inch stations the downscaled maximum temperature showed that there may be increasing trends in both emission scenarios (A2a and B2a). At Gedo the average annual maximum temperature will be increased in 2020s by 1.55^{o}C and 1.45^{o}C, in 2050s by 2.76^{o}C and 2.63^{o}C and in 2080s by 4.22^{o}C and 3.94^{o}C for A2a and B2a emission scenario respectively. Also at Tikur Inch the average annual maximum temperature will be increased in 2020s by 1.565^{o}C and 1.416^{o}C, in 2050s by 2.71^{o}C and 2.63^{o}C and in 2080s by 4.1^{o}C and 3.8^{o}C for A2a and B2a emission scenario respectively.

Precipitation projection exhibited an increase in annual average precipitation for both stations in all time horizons. At Gedo there may be an increase in precipitation in summer, winter and spring seasons in the next 90 years, but there may be a decrease in precipitation during autumn for both A2a and B2a emission scenarios. In Tikur Inch there may be an increase in precipitation for all seasons in the next 90 years for both A2a and B2a emission scenarios. The maximum increase in average annual precipitation observed in 2080s for A2a and B2a emission scenarios in the stations of Gedo by 16.414% & 23.063% and for Tikur inch by 17.302% & 20.103% respectively.

The projected annual temperature and precipitation changes showed that the climate in the study area will generally become warmer and wetter in each scenario. The possible range of climate change conditions were translated into a possible range of stream flow using SWAT model.

Sensitivity analysis of the SWAT model was done at four gauged stations within the watershed of the study area. Model calibration has been performed by manual calibration followed by automatic calibration at the four gauged stations using the sensitivity rank. In all the gauged stations R^2 values greater than 0.6 and E_{NS} values greater than 0.5 has been obtained during calibration and validation period. Uncertainty analysis was done and shows that most of the stream flow data at the four gauged stations are bracketed in 95PPU. Based on these results the model was used to assess the impact of climate change on the hydrological conditions of the study area.

Climate change impact on flow volume of Guder River was analyzed on a monthly, seasonal and annual basis. For both A2a and B2a emissions scenarios, there may be an average annual increase in flow volume for the next 90 years up to 35%. And also all seasons show an increase in flow volume for both scenarios. The projected increase in annual Potential Evapotranspiration in the Sub-basin will vary on annual average from 3 - 15% for the 2020s and 7 - 25% for the 2050s and 2080s for both A2a and B2a emissions scenarios.

6.2 Recommendation

As this study was done in a limited time and resource, the results should be taken as a starting point for further studies in the Guder sub-basin.

The outcome of this study is based on single GCMs and two emission scenarios. However, it is often recommended to apply different GCMs and emission scenarios so as to make comparison between different models as well as to explore a wide range of climate change scenarios that would result in different hydrological impacts. Hence this work should be extended in the future by including different GCMs and emission scenarios.

In this study, downscaling of the large scale variables was done at Gedo and Tikur Inch meteorological stations, and it was assumed that this change will be applicable to other stations as well. However, it is recommendable if climate change assessment will be done downscaling large scale variables at each station found in the study area.

In addition to fluctuations on temperature and precipitation, deforestation and population growth are among current trends over the sub- basin. Hence, it is good to see the impacts of climate and land use changes over the Guder sub-basin.

REFERENCES

Abbaspour K.C., J. Yang, I. Maximov, R. Siber, K. Bogner, J. Mieleitner, J. Zobrist, R.Srinivasan, 2007: Modeling hydrology and water quality in the pre-alpine/alpine Thur watershed using SWAT. *Journal of Hydrology,* 333:413-430.

Awulachew S.B., M. McCartney T.S. Steenhuis & A.A. Ahmed, 2008a: *A Review of Hydrology, Sediment and Water Resource Use in the Blue Nile Basin*, IWMI WP 131

Bader D.C., 2008: Climate Models: An Assessment of Strengths and Limitations. A Report by the U.S. Climate Change Science Program and the Subcommittee on Global Change Research [Bader D.C., C. Covey, W.J. Gutowski Jr., I.M. Held, K.E. Kunkel, R.L. Miller, R.T. Tokmakian and M.H. Zhang (Authors)], Department of Energy, Office of Biological and Environmental Research, Washington D.C, USA, 124 pp

BCEOM, 1998: Abbay River Basin Integrated Development Master Plan Project: phase 2 data Collection-site Investigation Survey and Analysis for land use and land cover. Addis Ababa, Ministry of Water Resources

BCEOM, 1999: Abbay River Basin Integrated Development Master Plan Project: phase 2 data Collection-site Investigation Survey and Analysis for soil, Addis Ababa, Ministry of Water Resources

Carter, T.R., 2007: General Guidelines on the use of scenario data for Climate Impact and Adaptation Assessment, Finnish Environmental Institute, Helsinki, Finland

Chow, V.T., 1964: *Handbook of Applied Hydrology*: McGraw-Hill Book Company.

Conway, D., 2005: From headwater tributaries to international river: Observing and adapting to Climate variability and change in the Nile basin. Global Environmental Change, 15, 99–114.

Cunderlik, M. J. 2003: *Hydrologic model selection fort the CFCAS project: Assessment of Water Resources Risk and Vulnerability to Changing Climatic Conditions, Project Report I* University of Western Ontario, Canada.

Dibike, Y. B. and Coulibaly, P., 2005: Hydrologic impact of climate change in the Saguenay Watershed, comparison of downscaling methods and hydrologic models, J. Hydrol., 307(1–4)

IPCC (R.T.Watson .R.T, M.C.Zinyowera, R.H.Moss) 1997: The Regional Impacts of Climate Change: An Assessment of Vulnerability. Cambridge University Press, UK. pp 517

IPCC (2001a): *Climate Change, 2001: The Scientific Basis*. Contribution of Working Group I to the Third Assessment Report of the Intergovernmental Panel on Climate Change

IPCC (2001b): *Climate Change, 2001: Impacts, Adaptation, and Vulnerability* Contribution of Working Group II to the Third Assessment Report of the Intergovernmental Panel on Climate Change

IPCC (Intergovernmental Panel on Climate Change), 2007: Climate Change 2007: Impacts, Adaptation, and Vulnerability—Contribution of Working Group II to the Third Assessment Report of the Intergovernmental Panel on Climate Change, edited by M. L. Parry et al *Cambridge Univ. Press*, Cambridge, U. K

IPCC (Intergovernmental Panel on Climate Change), 1999: J.E.Penner, D.H.Lister, D.J.Griggs, D.J.Dokken, M.McFarland (Eds.) Prepared in collaboration with the Scientific Assessment Panel to the Montreal Protocol on Substances that Deplete the Ozone Layer *Cambridge University Press*, UK. pp 373

IPCC-TGICA, 2007: *General Guidelines on the Use of Scenario Data for Climate Impact and Adaptation Assessment*, Version 2, Prepared by T.R. Carter on behalf of the Intergovernmental Panel on Climate Change Task Group on Data and Scenario Support for Impact and Climate Assessment, pp66

Kim U, J.J Kaluarachchi, & V.U Smakhtin, 2008: *Climate Change Impacts on Hydrology and Water Resources of the Upper Blue Nile Basin, Ethiopia*, IWMI RR 126

Kim, U., and J.J. Kaluarachchi 2009, Climate Change Impacts on Water Resources in the Upper Blue Nile River Basin, Ethiopia. Journal of the American Water Resources Association (JAWRA) 45(6), 1361-1378.

Lahmer.W.B, Pfutzner and A.Becker, 2001: Assessment of land use and climate change impacts on The Mesoscale, Physchem, Earth 26(7-8) pp. 565-57.

Mohamed E. Elshamy, Robert Baligira, Eman Abdel-Ghaffar and Semu A. Moges; 2009: Investigating the Climate Sensitivity of different Nile Sub-Basins, *Thirteenth International Water Technology Conference, IWTC 13 2009, Hurghada, Egypt*

MoWR, 2002: Water Sector Development Program, 2002-2016. Main Report Volume II, Addis Ababa, 2002

Muluneh B., 2008: Evaluation of Impact of Climate Change on Water Resource Availability in the Catchments of Blue Nile Basin, MSc. Thesis at Arba Minch University, Ethiopia

Neitsch S.L., J.G. Arnold, J.R. Kiniry, J.R. Williams, 2005: Soil and Water Assessment Tool (SWAT) Theoretical Documentation, Version 2005, Grassland Soil and Water Research Laboratory, Agricultural Research Service, Blackland Research Center, Texas Agricultural Experiment Station

Neitsch S.L., J.G. Arnold, J.R. Kiniry, J.R. Williams, 2005: Soil and Water Assessment Tool (SWAT) Input/output File Documentation, Version 2005, Grassland Soil and Water Research Laboratory, Agricultural Research Service, Blackland Research Center, Texas Agricultural Experiment Station

NMSA 2001: Initial National Communication of Ethiopia to the United Nations Framework Convention on Climate Change (UNFCCC), National Meteorological Services Agency, Addis Ababa, Ethiopia

Rizwan Nawaz, Timothy Bellerby, Mohamed Sayed and Mohamed Elshamy; 2010: Blue Nile Runoff Sensitivity to Climate Change, *the Open Hydrology Journal*, 2010, *4*, 137-151

Robert.L and Christian W.Dawson, 2007: Statistical Downscaling Model (SDSM) version 4.2, A decision support tool for the assessment of regional climate change impacts, user manual, Department of Geography, Lancaster University, UK

Santhi S., Arnold J.G., Williams J.R., Dugas W.A., Srinivasan, R. and L.M. Hauck, 2001: Validation Of SWAT model on a large river basin with point and nonpoint sources. Journal of the American Water Resources Association 37:1169-1188.

Van Griensven, A., Green C.H., 2007. Auto-calibration in Hydrological Modeling: Using SWAT2005 In small-scale watersheds, Science Direct, Environmental Modeling & Software 23 (2008), 422-434, available at: www.sciencedirect.com.

Van Griensven A., Meixner T., Grunwald S. Bishop, T. Diluzio, M., Srinivasan R., 2006: A global Sensitivity analysis tool for the parameters of multi-variable catchment models, *Unpublished Paper obtained from Dr. Van Griensven of UNSECO-IHE.* Environmental Sciences, University of California; Backland Research and Extension Center, Texas A &M University; and Spatial Sciences Laboratory, Texas A & M University

Vogel, R.M., 2006: Regional Calibration of Watershed Models. In *Watershed Models*; Singh, V.P, Frevert, D.K., Eds.; CRC Press: Boca Raton, USA; Chapter 3, pp. 47-71.

Willems, P. 2000. *Probabilistic modeling of the emission receiving surface waters,* Phthesis, Faculty of Engineering, Katholieke Universiteit, Leuven, Belgium

Winchell.M, Srinivasan.R Di Luvizio.M, Arnold.J, 2009: ArcSWAT2.3.4 Interface for SWAT2005, User's Guide, Blackland Research Center Texas Agricultural Experimentation Station; Soil and Water Research laboratory; USDA Agricultural Research Service

Xu, C. Y., 1999: From GCMs to river flow: a review of downscaling techniques and hydrological Modeling approaches, Progress in Physical Geography, 23, pp. 229–249.

Xu, C.Y., 2000: Modeling the effect of climate change on water resources in central Seweden, Water resources Mngt. 14(3) pp. 177-189

Yihun D., 2009: Hydrological Modeling to Assess Climate Change Impact at Gilgel Abbay River, Lake Tana Basin, Ethiopia. MSc. thesis at Lund University, Division of Water Resources Engineering

Zheng Y., Keller A.A, 2007: Uncertainty assessment in watershed-scale water quality modeling and Management: 1. Framework and application of generalized likelihood uncertainty estimation (GLUE) approach. Water Resources Research 43: 1-13

Website References:

Lierch, S., 2003: Dew02 Users" Manual, Berlin, pp5. PDF Manual available from http://www.brc.tamus.edu/swat/soft_links.htl [accessed on 15 January, 2011]

The HadCM3 predictor variables for the A2a and B2a experiments, available at: http://www.cccsn.ca/Download_Data/HadCM3_Predictors-e.html [accessed on 10 Dec., 2010]

SWAT Official Web Site [Online]: Available at: http://www.brc.tamus.edu/swat/ [Accessed on January, 2011]

WHAT: Web Based Hydrograph Analysis Tool. [Online] Available at: http://cobweb. ecn.purdue.edu/~what/ [Accessed on 12 March 2011]

ANNEXES

Appendix A: Meteorological variables used for modeling work

Table 13 Summary of Average Monthly Meteorological Variables from 1990-2000 for Stations Considered in the SWAT Modeling Work

1. Monthly Precipitation in mm

1.Gedo Station			Latitude 9.05^{O}			Longitude 37.433^{O}			Elevation 2500masl			
YEAR	JAN	FEB	MAR	APR	MAY	JUN	JULY	AUG	SEP	OCT	NOV	DEC
1990	18.0	57.7	88.4	25.6	127.2	149.8	114.6	181.1	55.4	17.6	0.0	3.9
1991	23.0	40.5	33.6	9.5	51.7	217.1	209.5	223.6	105.4	1.8	2.3	12.7
1992	48.1	47.9	67.5	44.7	66.2	202.3	199.3	205.6	121.4	72.5	42.1	8.3
1993	14.4	24.3	31.0	115.0	177.5	146.3	218.9	99.1	55.6	7.8	0.0	0.0
1994	8.2	2.8	40.6	62.3	89.3	102.5	187.3	103.2	157.7	8.1	6.0	0.0
1995	0.0	6.2	12.2	102.4	89.2	82.6	99.6	95.8	83.9	15.9	15.9	31.9
1996	10.5	0.0	46.4	60.1	129.0	42.6	69.3	102.0	35.1	0.0	73.5	3.0
1997	29.3	2.2	12.4	26.3	55.8	48.4	53.6	100.6	19.7	60.8	82.5	7.2
1998	17.0	22.1	41.7	41.9	63.7	113.1	181.1	98.5	42.8	63.9	11.6	1.5
1999	0.0	0.0	10.0	29.3	57.5	82.2	175.9	64.7	59.8	53.5	10.9	2.8
2000	0.0	0.0	5.8	36.7	64.2	67.9	174.6	210.1	75.6	82.6	26.7	8.5
AVG	**15.3**	**18.5**	**35.4**	**50.3**	**88.3**	**114.1**	**153.1**	**134.9**	**73.9**	**35.0**	**24.7**	**7.3**

2.Kachisie Station			Latitude 9.35^{O}			Longitude 37.2^{O}			Elevation 2520masl			
YEAR	JAN	FEB	MAR	APR	MAY	JUN	JULY	AUG	SEP	OCT	NOV	DEC
1990	7.2	24.7	92.4	34.4	92.4	127.5	427.6	507.0	374.7	16.3	0.0	1.0
1991	13.7	32.7	97.8	36.4	33.1	246.2	345.3	465.4	240.9	6.5	0.5	17.6
1992	48.4	77.5	52.6	132.7	118.5	292.6	386.3	393.3	248.3	217.9	26.7	8.1
1993	7.0	41.0	43.7	196.8	282.2	211.7	458.9	514.3	310.1	98.7	15.4	2.3
1994	7.8	4.2	32.4	62.4	124.6	341.9	396.5	478.2	176.9	52.3	9.0	5.1
1995	0.0	7.9	80.6	106.9	204.1	140.0	361.1	250.8	225.2	35.2	12.3	4.2
1996	35.2	18.4	124.3	104.9	218.7	265.5	474.5	319.2	169.0	90.9	35.9	4.4
1997	30.5	54.6	62.0	119.3	148.8	202.6	354.1	304.1	168.1	314.5	186.6	3.1
1998	41.2	0.0	82.8	8.1	151.5	268.7	297.6	427.5	307.9	202.6	9.2	0.0
1999	11.1	0.0	0.9	38.5	112.0	333.9	390.3	556.3	223.7	271.0	8.4	6.8
2000	0.0	0.0	18.5	109.1	114.0	335.9	365.3	499.2	353.4	143.1	64.3	40.7
AVG	**18.4**	**23.7**	**62.5**	**86.3**	**145.4**	**251.5**	**387.0**	**428.7**	**254.4**	**131.7**	**33.5**	**8.5**

3.Tikur Inch Station			Latitude 8.783^{O}			Longitude 37.633^{O}			Elevation 2480masl			
YEAR	JAN	FEB	MAR	APR	MAY	JUN	JULY	AUG	SEP	OCT	NOV	DEC
1990	22.0	121.0	78.6	94.5	136.5	382.3	411.4	532.3	288.0	15.8	22.7	10.0
1991	27.3	47.6	50.3	46.0	67.8	223.2	315.6	357.8	201.9	12.8	0.0	6.6
1992	50.9	78.3	23.9	90.8	68.9	218.0	387.6	323.3	167.4	84.2	16.6	33.0
1993	13.6	35.8	31.9	201.2	234.5	444.3	407.1	451.5	312.7	315.5	17.6	0.0
1994	0.0	11.2	46.7	68.2	137.0	264.2	381.3	172.8	199.4	0.2	13.2	0.0
1995	0.0	5.5	112.5	80.7	106.9	210.4	543.3	457.7	208.5	19.9	6.0	28.1
1996	44.7	45.3	270.5	120.0	229.1	220.9	396.7	514.6	328.7	52.4	62.0	36.8
1997	77.2	1.6	32.7	204.3	144.7	295.8	318.6	307.4	176.9	70.9	94.8	28.3
1998	58.5	67.4	76.4	30.3	141.6	221.6	314.5	436.0	272.3	283.6	23.0	0.0
1999	6.9	7.6	3.0	18.8	136.2	183.2	309.3	314.0	346.9	169.2	0.0	3.3
2000	0.0	0.0	17.4	146.9	204.9	255.3	224.6	346.0	259.6	123.6	43.4	21.4
AVG	**27.4**	**38.3**	**67.6**	**100.2**	**146.2**	**265.4**	**364.5**	**383.0**	**251.1**	**104.4**	**27.2**	**15.2**

2. Average monthly maximum temperature

1.Gedo Station			Latitude 9.05^{O}			Longitude 37.433^{O}			Elevation 2500masl			
YEAR	JAN	FEB	MAR	APR	MAY	JUN	JULY	AUG	SEP	OCT	NOV	DEC
1990	23.4	23.1	23.0	23.2	23.1	19.6	17.9	16.9	17.5	22.4	24.7	24.9
1991	24.5	24.8	24.7	25.7	24.4	20.8	18.2	19.5	21.9	24.6	24.3	24.6
1992	23.2	23.8	24.5	24.9	24.1	21.6	17.0	16.3	19.4	21.3	22.1	21.6
1993	24.2	23.6	24.7	21.1	21.3	20.5	17.2	17.3	17.3	22.9	24.0	24.9
1994	24.6	24.8	24.4	24.5	24.2	22.6	20.8	19.4	21.7	24.1	23.7	25.0
1995	25.3	25.2	25.6	25.0	23.1	22.8	20.0	18.6	20.3	22.7	24.0	23.7
1996	23.2	24.9	23.0	22.7	21.4	18.8	17.8	18.6	19.9	23.6	22.7	24.0
1997	23.0	24.2	24.1	22.8	22.5	21.3	20.7	18.0	21.0	21.6	21.7	23.3
1998	23.6	24.2	21.9	22.4	21.4	20.0	18.2	19.2	18.2	20.6	21.4	22.9
1999	23.1	24.5	23.6	23.3	22.6	18.2	17.1	18.5	20.8	20.9	23.6	23.8
2000	24.8	25.1	24.7	21.7	22.3	22.0	17.2	18.5	18.3	19.9	23.3	23.6
AVG	**23.9**	**24.4**	**24.0**	**23.4**	**22.8**	**20.7**	**18.4**	**18.3**	**19.7**	**22.2**	**23.2**	**23.8**

2.Kachisie Station			Latitude 9.35^{O}			Longitude 37.2^{O}			Elevation 2520masl			
YEAR	JAN	FEB	MAR	APR	MAY	JUN	JULY	AUG	SEP	OCT	NOV	DEC
1990	22.0	21.7	22.3	23.1	23.2	21.5	18.3	18.2	18.0	20.1	21.2	21.6
1991	22.8	23.7	23.4	24.8	25.7	23.0	19.6	19.2	20.0	21.0	21.8	21.0
1992	21.8	22.3	25.0	25.0	24.3	22.3	19.8	17.8	19.5	19.8	20.0	20.8
1993	21.6	22.2	23.6	20.8	20.9	19.9	16.5	17.8	18.3	19.3	20.1	20.9
1994	22.2	23.5	23.4	23.9	22.4	19.5	16.2	17.5	19.5	17.6	20.1	21.2
1995	22.0	23.6	23.6	22.4	21.1	21.4	16.8	17.7	18.4	19.3	20.5	21.6
1996	20.1	22.9	23.0	21.5	20.1	18.6	17.6	17.3	18.6	19.7	19.9	20.3
1997	21.3	23.4	24.0	21.9	22.1	19.7	18.0	18.2	19.9	20.2	19.6	20.8
1998	21.3	24.5	23.6	24.4	23.2	20.9	16.9	17.2	18.6	18.9	19.2	20.1
1999	21.5	23.9	23.7	22.6	23.1	20.8	17.2	18.4	18.3	19.4	19.4	20.3
2000	21.9	23.4	24.8	21.9	22.7	20.7	18.1	17.3	18.7	19.8	19.6	20.2
AVG	**21.7**	**23.2**	**23.7**	**22.9**	**22.6**	**20.8**	**17.7**	**17.9**	**18.9**	**19.6**	**20.1**	**20.8**

3.Tikur Inch Station			Latitude 8.783^{O}			Longitude 37.633^{O}			Elevation 24800masl			
YEAR	JAN	FEB	MAR	APR	MAY	JUN	JULY	AUG	SEP	OCT	NOV	DEC
1990	23.2	22.3	23.4	23.9	24.2	21.2	20.1	20.3	20.3	22.6	23.3	24.2
1991	24.8	24.6	23.7	24.9	25.2	21.8	18.7	19.7	21.4	22.7	23.4	23.3
1992	22.4	22.9	24.5	23.9	24.0	21.0	19.2	18.6	20.1	21.8	22.9	23.7
1993	23.6	23.7	25.2	22.7	22.7	21.2	20.4	19.9	20.0	22.4	23.6	24.0
1994	25.0	25.1	24.9	24.8	23.5	21.1	19.7	19.1	21.3	23.7	24.3	25.2
1995	25.3	26.1	26.1	24.1	24.0	21.3	19.5	20.6	22.0	24.9	24.5	23.1
1996	22.9	25.3	24.4	23.9	23.3	19.6	18.7	18.6	20.4	23.5	24.5	24.0
1997	23.4	23.6	24.5	24.8	25.2	20.3	19.0	20.4	22.4	23.2	24.5	24.4
1998	24.3	24.6	24.5	26.4	24.7	22.7	19.6	19.3	21.5	22.8	24.5	25.1
1999	24.7	26.7	24.9	26.1	23.9	21.6	20.4	20.4	21.3	22.1	24.5	24.8
2000	24.8	27.0	27.6	24.8	23.9	21.1	20.5	19.9	21.3	22.9	24.5	24.2
AVG	**24.0**	**24.7**	**24.9**	**24.6**	**24.1**	**21.2**	**19.6**	**19.7**	**21.1**	**23.0**	24.5	**24.2**

3. Average monthly minimum temperature

1.Gedo Station			Latitude 9.05^{O}			Longitude 37.433^{O}			Elevation 2500masl			
YEAR	JAN	FEB	MAR	APR	MAY	JUN	JULY	AUG	SEP	OCT	NOV	DEC
1990	9.6	9.1	8.8	9.1	7.8	7.5	7.1	6.8	6.7	6.8	8.2	8.1
1991	9.4	8.9	10.6	11.1	11.2	10.7	9.5	10.0	10.2	8.5	7.6	8.7
1992	8.0	9.0	9.3	9.9	9.7	9.8	7.6	7.6	7.7	7.8	7.9	9.5
1993	10.8	10.4	9.7	9.6	9.3	8.4	7.0	7.3	7.2	9.8	9.1	10.1
1994	10.2	10.5	10.2	10.3	10.3	10.1	10.0	9.5	9.4	8.4	8.6	7.8
1995	8.8	9.3	9.9	9.8	10.3	9.4	9.2	8.4	10.2	9.3	9.6	9.2
1996	9.5	10.0	9.6	9.2	8.7	7.7	7.8	7.5	7.8	9.5	8.7	8.1
1997	8.5	8.8	9.0	9.0	8.7	8.4	8.2	7.4	8.5	8.2	8.4	8.9
1998	9.1	9.4	9.3	9.4	8.7	7.7	7.5	7.8	8.3	8.4	7.6	7.6
1999	8.6	8.2	8.5	9.2	9.4	8.2	7.3	7.9	8.8	9.2	7.4	8.9
2000	8.2	8.7	9.5	9.1	9.3	8.6	7.6	7.8	7.4	8.7	10.0	9.5
AVG	**9.2**	**9.3**	**9.5**	**9.6**	**9.4**	**8.8**	**8.1**	**8.0**	**8.4**	**8.6**	**8.5**	**8.8**

2.Kachisie Station			Latitude 9.35^{O}			Longitude 37.2^{O}			Elevation 2520masl			
YEAR	JAN	FEB	MAR	APR	MAY	JUN	JULY	AUG	SEP	OCT	NOV	DEC
1990	10.2	11.4	11.5	12.3	12.0	10.3	8.5	9.1	9.2	8.9	10.5	10.2
1991	11.7	12.0	11.7	10.7	10.9	9.1	8.6	8.4	8.5	8.1	7.6	7.9
1992	8.8	9.4	9.8	10.0	9.8	9.4	9.2	8.5	7.7	6.9	6.7	6.8
1993	10.2	9.6	10.7	11.0	11.4	10.6	8.9	8.4	9.3	9.5	8.9	9.7
1994	10.2	10.8	11.0	11.5	10.7	9.6	8.4	8.2	9.6	9.2	9.5	9.1
1995	10.1	11.2	10.9	11.5	10.9	10.7	10.3	9.9	10.3	9.8	10.2	8.9
1996	10.1	10.6	11.3	11.3	10.6	10.0	9.6	9.4	9.7	9.5	9.1	9.3
1997	10.4	10.7	11.4	10.9	10.5	10.2	9.5	9.4	9.7	9.5	9.5	9.7
1998	9.9	10.7	11.5	12.3	11.6	9.4	9.0	9.1	8.8	8.9	7.4	7.2
1999	8.4	9.2	9.6	12.3	12.2	10.9	10.2	9.9	10.4	10.0	9.0	10.0
2000	10.4	11.1	12.2	11.6	12.1	11.0	10.2	10.0	10.4	10.2	10.0	10.4
AVG	**10.0**	**10.6**	**11.1**	**11.4**	**11.2**	**10.1**	**9.3**	**9.1**	**9.4**	**9.1**	**8.9**	**9.0**

3.Tikur Inch Station			Latitude 8.783^{O}			Longitude 37.633^{O}			Elevation 2480masl			
YEAR	JAN	FEB	MAR	APR	MAY	JUN	JULY	AUG	SEP	OCT	NOV	DEC
1990	5.6	7.6	8.1	7.2	7.7	7.7	7.4	8.5	7.3	5.3	5.4	3.5
1991	5.5	6.1	8.1	8.5	7.4	7.9	8.4	7.9	6.9	4.3	3.6	2.8
1992	4.9	7.2	6.5	7.1	7.0	7.2	7.1	6.8	5.1	5.0	3.3	3.0
1993	3.3	4.7	3.9	6.3	6.2	5.5	5.7	5.1	4.5	5.3	1.9	1.5
1994	1.1	1.9	5.4	5.8	5.2	5.7	5.9	5.7	4.1	2.0	1.5	0.7
1995	0.6	2.3	2.8	6.5	5.4	5.8	4.7	5.0	3.2	0.8	0.7	2.0
1996	2.8	1.9	4.9	4.4	3.9	5.0	4.2	4.7	3.8	1.5	0.9	0.3
1997	2.8	-2.3	3.1	4.2	3.8	4.3	8.8	9.8	9.3	8.1	7.9	6.5
1998	7.6	8.2	9.9	9.6	10.4	10.2	9.8	9.6	8.7	8.9	4.2	2.7
1999	4.4	4.2	5.9	8.2	9.2	8.8	8.9	8.1	6.9	7.8	3.9	3.6
2000	4.8	4.2	6.7	9.6	9.5	9.4	9.6	9.2	8.3	8.1	6.6	4.7
AVG	**3.9**	**4.2**	**5.9**	**7.0**	**6.9**	**7.0**	**7.3**	**7.3**	**6.2**	**5.2**	**3.6**	**2.8**

Appendix B: List of Coupled Atmospheric General Circulation Models

Table 14 Coupled Atmospheric General Circulation Models for which climate change simulations held (Carter, 2007)

Modeling center	Country	Model(s)
Commonwealth Scientific and Industrial Research Organization (CSIRO)	Australia	CSIRO-Mk2
Max Plank Institute for Meteorology (formerly Deutsches Klimarechenzentrum, DKRZ)	Germany	ECHAM4/OPYC and ECHAM3/LSG
Hadley Centre for Climate Prediction and Research	UK	UKHadCM2 and HadCM3
Canadian Centre for Climate modeling and Analysis(CCCMA)	Canada	CGCM1 and CGCM2
Geophysical Fluid Dynamics Laboratory (GFDL)	USA	GFDL-R15 and GFDL-R30
National Centre for Atmospheric Research (NCAR)	USA	NCAR DOE-PCM
Centre for Climate Research Studies (CCSR) and National Institute for Environmental Studies (NIES)	Japan	CCSR-NIES

Appendix C: SWAT model results

Table 15 Sensitivity analysis results for 7 simulation years (1990-1996) at the 4 gauged stations

Hydrological Parameters		Sensitivity rank at			
Name	Description	Guder	Indris	Debis	Fatto
Sol_K	Saturated hydraulic conductivity	1	11	10	6
Sol_Awc	Available water capacity	2	2	7	10
Sol_Z	Soil depth	3	3	6	5
Surlag	Surface runoff lag time	4	1	18	15
Esco	Soil evaporation compensation Factor	5	10	3	4
GWQMN	Threshold depth of water in the shallow aquifer required for return flow to occur	6	12	1	2
ALPH_BF	Base flow alpha factor [days]	7	8	4	1
Slope	Average slope steepness	8	14	9	9
CH_K2	Channel effective hydraulic conductivity	9	7	16	14
REVAPMN	Threshold water depth in the shallow aquifer for “revap”	10	9	2	3
Canmx	Maximum canopy storage	11	5	11	7
Blai	Maximum potential leaf area index	12	4	8	11
CN2	SCS runoff curve number	13	6	13	12
GW_DELAY	Groundwater delay [days]	14	15	12	13
GW_REVAP	Groundwater ‘’revap’’ coefficient	15	13	5	8
Epco	Plant uptake compensation factor	16	16	15	27
CH_N2	Manning’s ‘’n’’ value for the main channel	17	18	17	18
SLSUBBSN	Average slope length	18	19	27	16
Biomix	Biological mixing efficiency	19	17	14	17
Sol_Alb	Moisture soil albedo	27	27	27	19
Smfmn	Melt factor for snow on December 21	27	27	27	27
Smfmx	Melt factor for snow on June 21	27	27	27	27
Smtmp	Snow melt base temperature	27	27	27	27
Timp	Snow pack temperature	27	27	27	27
Tlaps	Temperature lapse rate	27	27	27	27
Sftmp	Snowfall temperature	27	27	27	27

Table 16 SWAT model results of average daily flows at the mouth of Guder River in a month (m3/s) at base line period (1990-2000)

Year	JAN	FEB	MAR	APR	MAY	JUN	JUL	AUG	SEP	OCT	NOV	DEC
1990	0.5	36.2	32.2	68.0	59.1	224.1	427.5	562.7	370.8	178.0	88.4	40.9
1991	20.4	20.6	42.4	22.6	46.7	266.9	390.8	579.7	391.3	175.9	89.4	43.8
1992	48.4	74.9	45.7	94.9	90.8	235.7	472.6	560.1	395.7	265.7	119.1	67.0
1993	35.5	104.4	29.7	210.7	238.9	285.1	469.6	515.7	380.2	245.9	98.1	45.2
1994	18.2	10.6	26.6	67.8	104.6	222.1	425.6	410.9	425.1	184.3	96.7	44.8
1995	18.2	14.0	45.2	111.8	126.7	172.0	387.8	460.5	361.4	178.4	94.0	62.1
1996	60.7	36.1	162.9	140.7	202.0	265.1	393.2	524.7	400.0	191.1	112.7	53.1
1997	33.7	33.1	29.4	100.0	81.4	193.5	299.6	347.9	226.4	204.1	160.7	74.7
1998	83.5	62.7	67.6	58.2	113.0	217.3	437.1	538.5	329.0	254.0	103.4	47.2
1999	25.3	10.5	23.2	12.8	50.8	189.6	374.7	421.2	345.8	277.9	110.2	56.0
2000	25.4	9.9	7.7	46.0	78.0	175.0	297.7	376.9	349.7	225.9	128.4	66.6

Appendix D: Types of predictor variables

Table 17 Types of predictor variables available for both NECP and HadCM3

No	Predictor Variable	Predictor description	No	Predictor Variable	Predictor description
1	Mslpaf	mean sea level pressure	14	P5zhaf	5000hpa divergence
2	P_faf	surface air flow strength	15	P8_faf	850 hpa air flow strength
3	P_uaf	surface zonal velocity	16	P8_uaf	850 hpa zonal velocity
4	P_vaf	surface meridional velocity	17	P8_vaf	850 hpa meridional velocity
5	P_zaf	surface vorticity	18	P8_zaf	850 hpa vorticity
6	P_thaf	surface wind direction	19	P850af	850 hpa geopotential height
7	P_zhaf	surface divergence	20	P8thaf	850 hpa wind direction
8	P5_faf	500 hpa air flow strength	21	P8zhaf	850 hpa divergence
9	P5_uaf	500 hpa zonal velocity	22	P500af	Relative humidity at 500hpa
10	P5_vaf	500 hpa meridional velocity	23	P850af	Relative humidity at 850hpa
11	P5_zaf	500 hpa vorticity	24	rhumaf	Near surface relative humidity
12	P500af	500 hpa geopotential height	25	Shumaf	Surface specific humidity
13	P5thaf	500 hpa wind direction	26	tempaf	Mean temperature at 2m